



# Status of the Standard Model Higgs boson searches with the ATLAS detector

**Andrea Gabrielli** *on behalf of the ATLAS Collaboration*



**Winter Institute LNF-2013-1, Frascati 22-24 January 2013**

# Outline

---

✓ Higgs @ LHC;

✓ LHC and ATLAS detector;

✓ Higgs discovery;

✓ Latest results;

✓ Higgs properties:

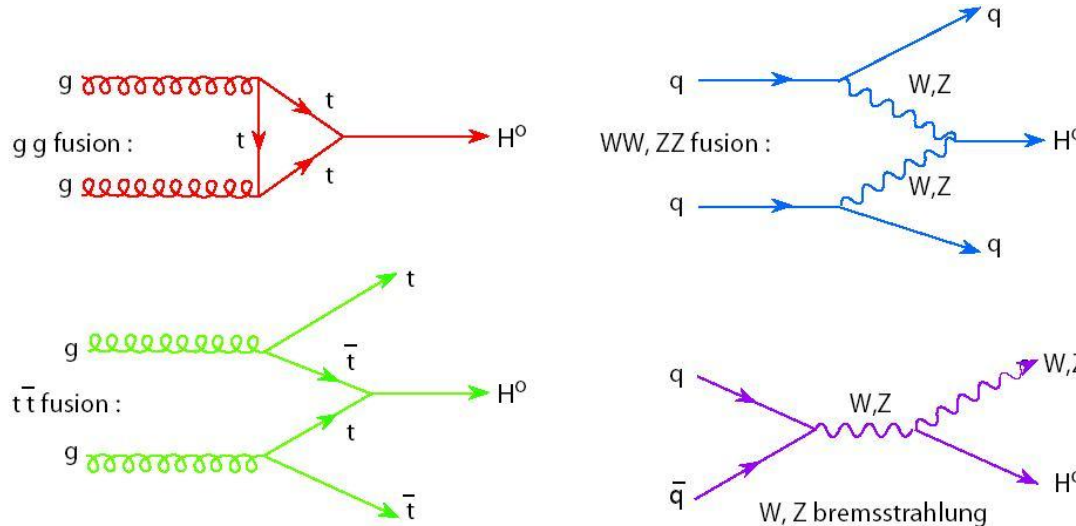
- Mass;

- Couplings;

- $J^P$ ;

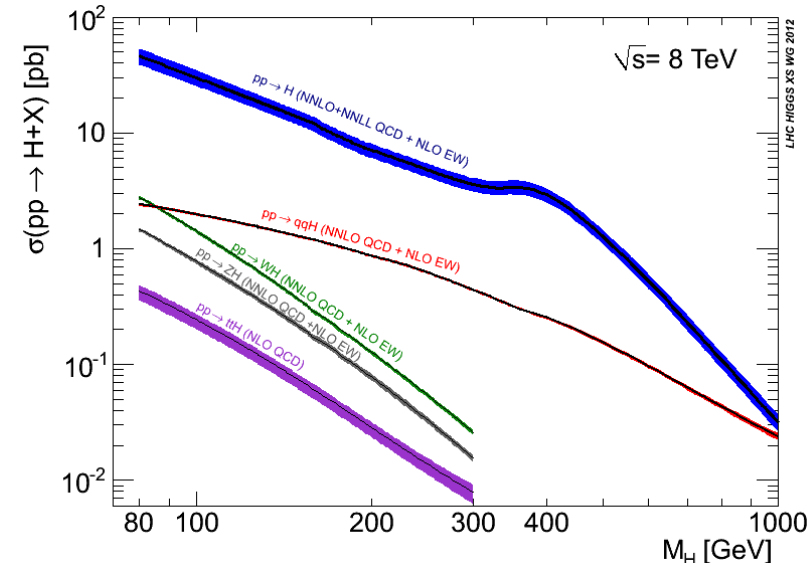
✓ Conclusions.

# Higgs @ LHC



SM Higgs production ( $m_H = 125 \text{ GeV } c^{-2}$  @ 8 TeV):

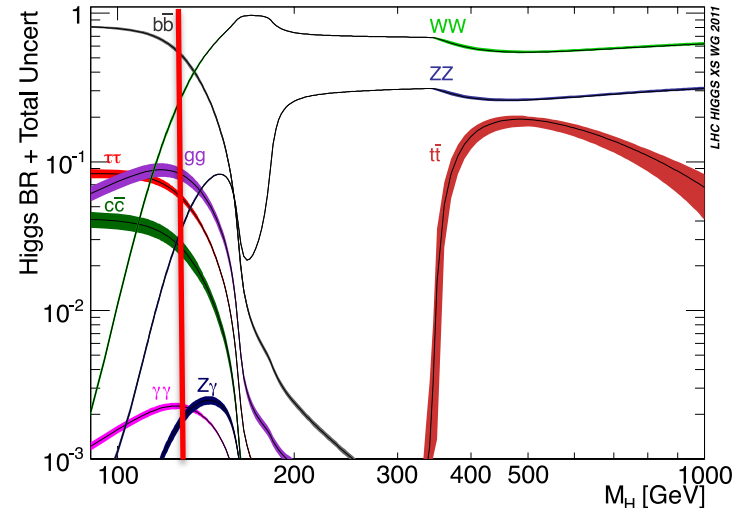
- **gluon-gluon Fusion (ggF):**  
19.52 pb (uncertainty 15-20%);
- **Vector Boson Fusion (VBF):**  
1.58 pb (uncertainty 5%);
- **Associated production with W/Z (VH):**  
0.7/0.4 pb (uncertainty 5%);
- **Associated production with ttbar (ttH):**  
0.13 pb (uncertainty 15%).



# Higgs @ LHC

## Standard Model Higgs decays:

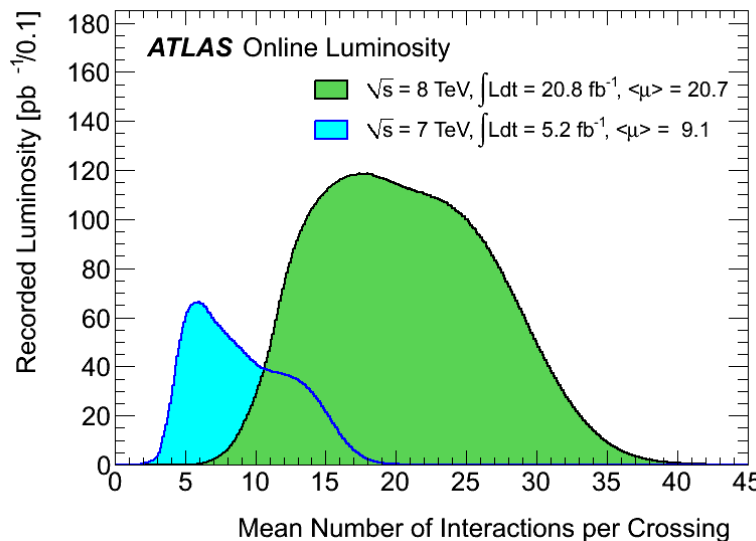
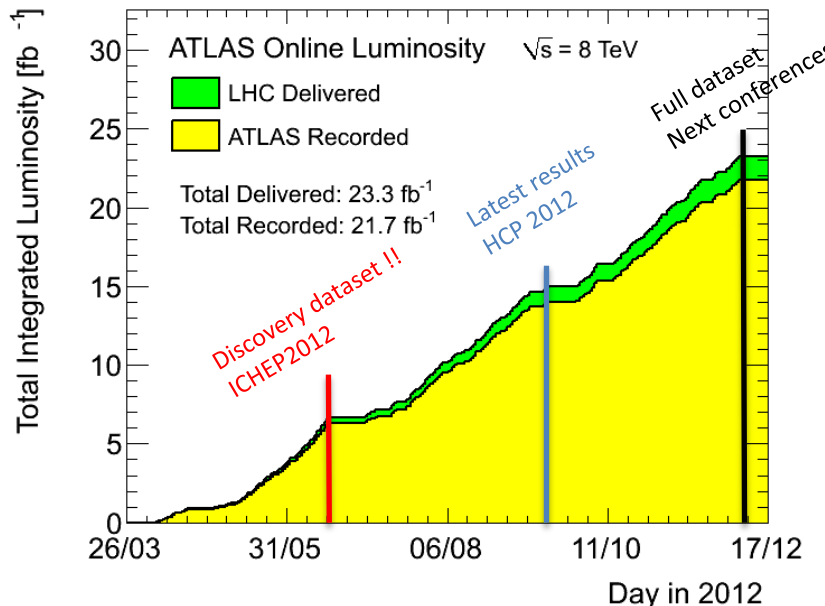
- $H \rightarrow \gamma\gamma$ :  
low mass, high bkg and mass resolution;
  - $H \rightarrow ZZ^{(*)} \rightarrow 4l$ :  
full mass range, low BR, high purity  
and mass resolution;
  - $H \rightarrow WW^{(*)} \rightarrow l\nu l\nu$ :  
full mass range, small mass resolution,  
high rate;
  - $H \rightarrow \tau\tau$ :  
low mass;
  - $VH \rightarrow V + bb$ :  
associated production VH, V= Z or W.
- High mass resolution
- High Branching Ratio



Expected events per  $\text{fb}^{-1}$ , BEFORE the selection:

	<b>125</b>	<b>300</b>
$\gamma\gamma$	53	-
$ZZ$	2.9	5.6
$WW$	59	32
$\tau\tau$	1500	-
$bb$ Only VH	600	-

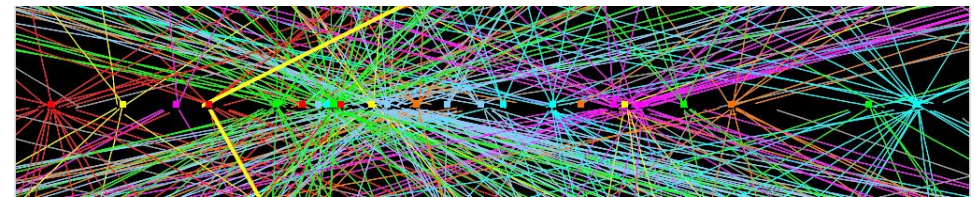
# Large Hadron Collider



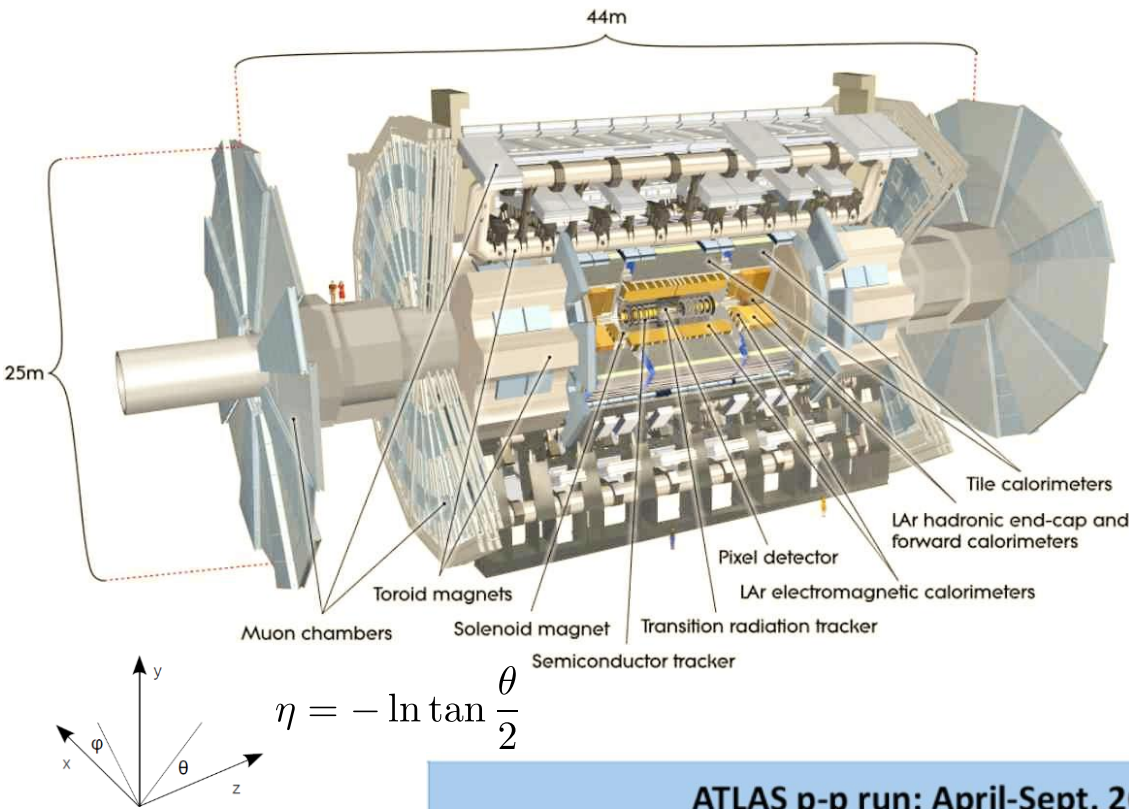
## Performance of LHC:

- Proton-proton collider @  $\sqrt{s} = 7$  (2011) and 8 (2012) TeV;
- Peak luminosity  $7.7 \cdot 10^{33} \text{ cm}^{-2} \text{ s}^{-1}$ ;
- Integrated lumi delivered:  
 $\sim 23 \text{ fb}^{-1}$  at 8 TeV and  $\sim 5 \text{ fb}^{-1}$  at 7 TeV;
- Bunch crossing 50 ns.

A candidate Z boson event in the dimuon decay with **25 reconstructed vertices**:



# A Toroidal Lhc ApparatuS



ATLAS p-p run: April-Sept. 2012										
Inner Tracker			Calorimeters			Muon Spectrometer			Magnets	
Pixel	SCT	TRT	LAr	Tile	MDT	RPC	CSC	TGC	Solenoid	Toroid
100	99.3	99.5	97.0	99.6	99.9	99.8	99.9	99.9	99.7	99.2
All good for physics: 93.7%										

Luminosity weighted relative detector uptime and good quality data delivery during 2012 stable beams in pp collisions at  $\sqrt{s}=8$  TeV between April 4<sup>th</sup> and September 17<sup>th</sup> (in %) – corresponding to  $14.0 \text{ fb}^{-1}$  of recorded data. The inefficiencies in the LAr calorimeter will partially be recovered in the future.

## Inner detector:

- ✓ Silicon;
- ✓ Transition radiation Tracker;
- ✓ Solenoid (2 T).

## EM calorimeter:

- ✓ Sampling LAr.

## HAD calorimiter:

- ✓ Plastic scintillator (barrel);
- ✓ LAr technology (endcap).

## Muon system:

- ✓ 3 air-core toroids;
- ✓ Reco and trigger chambers.

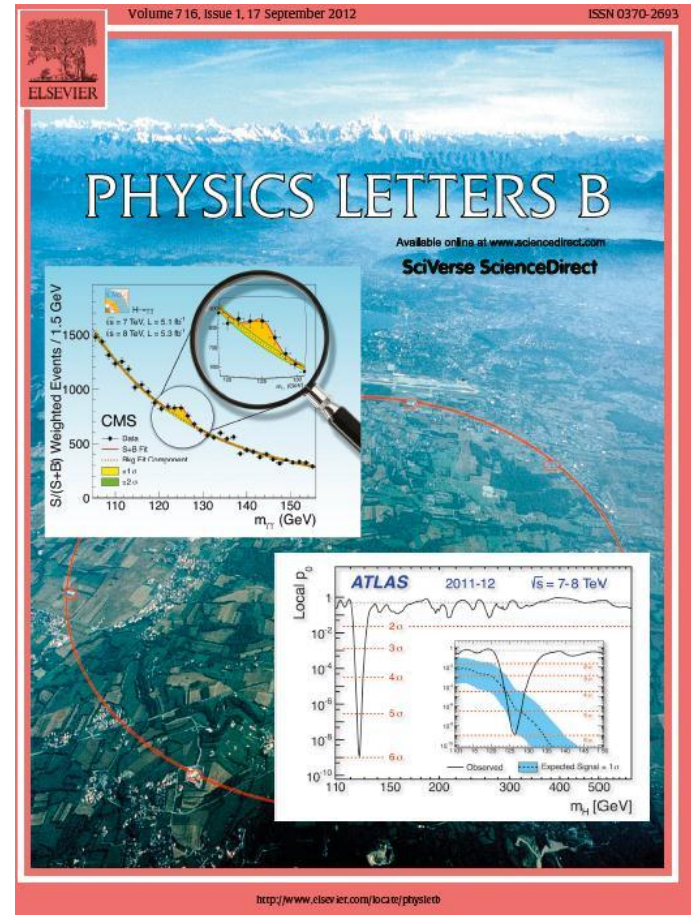
# Higgs discovery

4<sup>th</sup> July 2012, ATLAS [1] and CMS [2] collaborations announced the observation of a new particle.

**ATLAS channels 7 + 8 TeV**

( $4.8 \text{ fb}^{-1}$  7 TeV and  $5.8 \text{ fb}^{-1}$  8 TeV) :

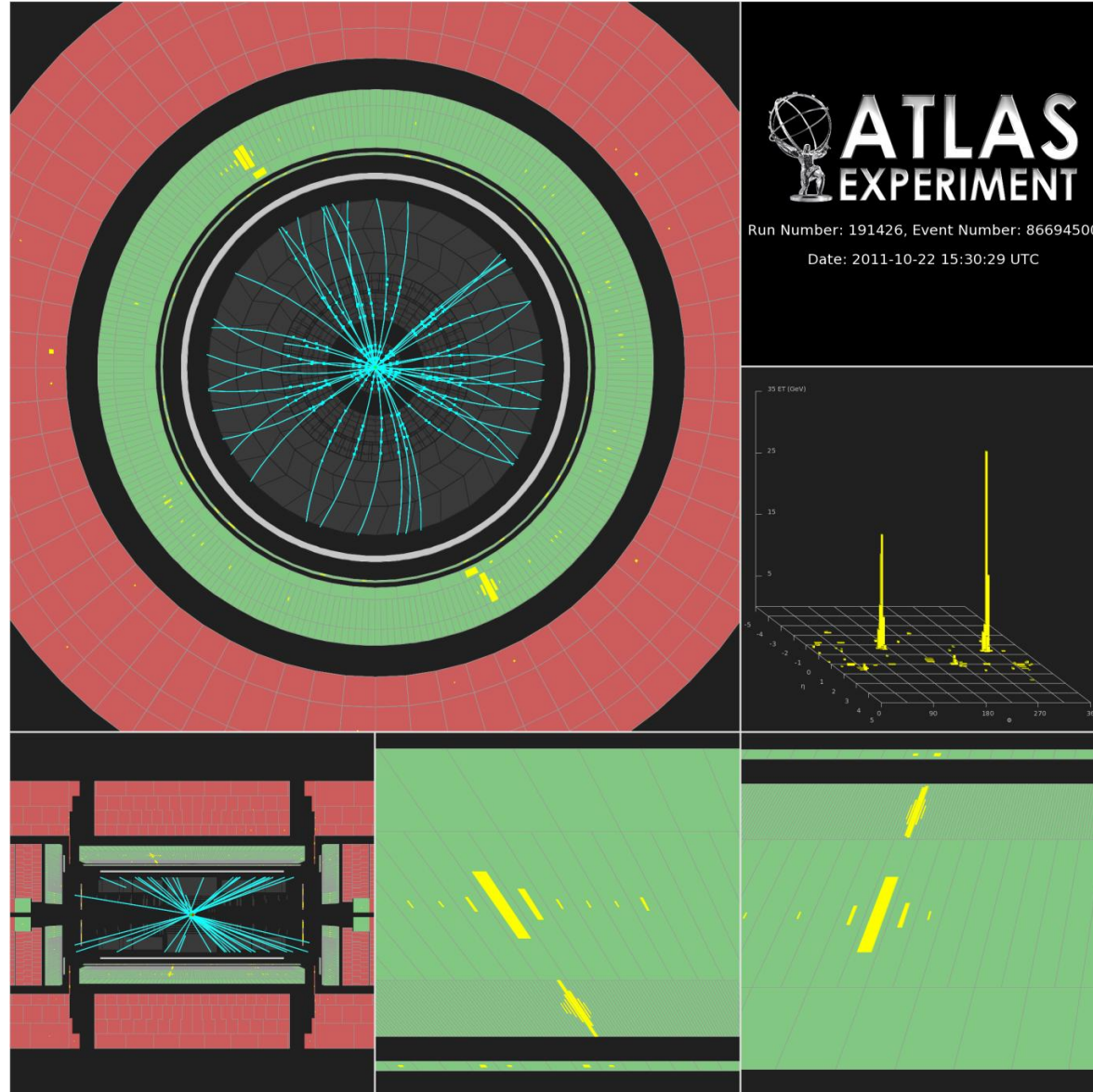
- $\text{H} \rightarrow \gamma\gamma$ ;
- $\text{H} \rightarrow \text{ZZ} \rightarrow 4l$ ;
- $\text{H} \rightarrow \text{WW} \rightarrow l\nu l\nu$ .



[1] ATLAS Collaboration, Observation of a new particle in the search for the Standard Model Higgs boson with the ATLAS detector at the LHC, Phys. Lett. B 716 (2012) 1–29, arXiv:1207.7214 [hep-ex].

[2] CMS Collaboration, Observation of a new boson at a mass of 125 GeV with the CMS experiment at the LHC, Phys. Lett. B 716 (2012) 30–61, arXiv:1207.7235 [hep-ex].

# $H \rightarrow \gamma\gamma$

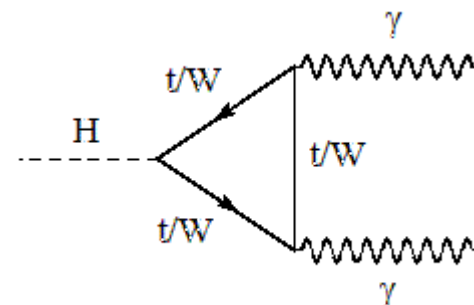


# $H \rightarrow \gamma\gamma$

## Higgs to gamma gamma:

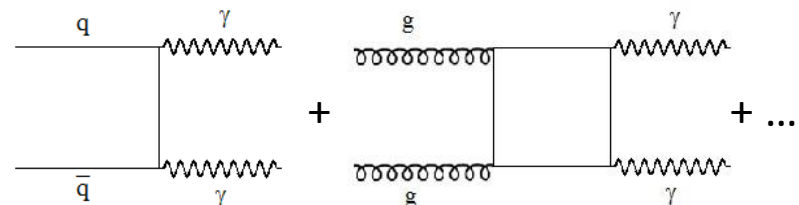
- BR:  $\sim 10^{-3}$  (@  $m_H = 125$  GeV c $^{-2}$ );
- Bkg:  $\gamma\gamma$ ,  $\gamma + \text{jets}$ , jet-jet;
- **Ten exclusive categories** (to increase sensitivity):
  - $\gamma$  converted (unconverted);
  - $\gamma$  pseudorapidity;
  - $P_T$  trust  $\gamma\gamma$ ;
  - VBF selection;
- Signal purity (S/B)  $\sim 2\%-20\%$ ;
- Strong jet rejection is needed;
- Lumi  $4.8 \text{ fb}^{-1}$  @ 7 TeV and  $5.8 \text{ fb}^{-1}$  @ 8 TeV (4<sup>th</sup> July 2012).

Signal:



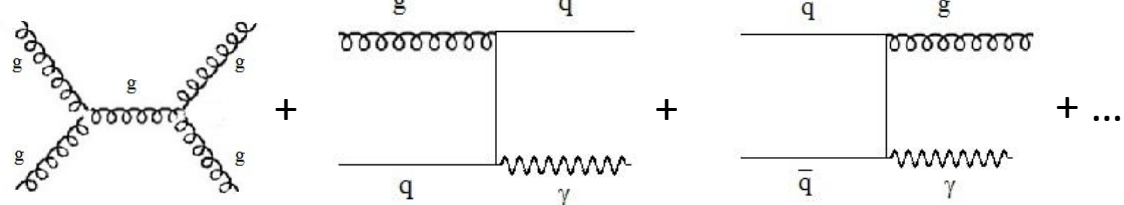
Irreducible bkg:  $\text{pp} \rightarrow \gamma\gamma + X$  ( $\sim 75\%$  total bkg)

Normalization and shape from MC + control region:

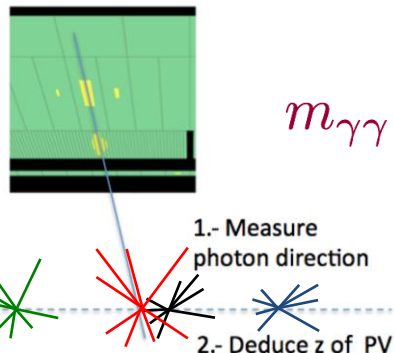


Reducible bkg:  $\text{pp} \rightarrow \gamma j, jj, D-Y$

Normalization and shape from MC + control region :



# $H \rightarrow \gamma\gamma$

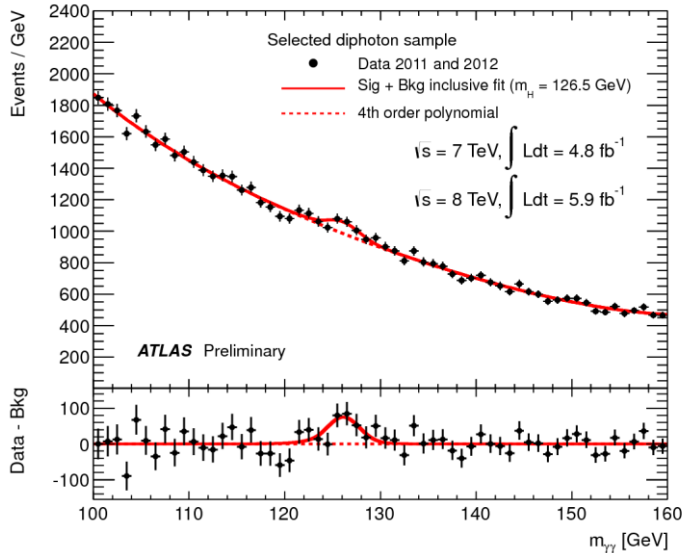


$$m_{\gamma\gamma} = 2E_1 E_2 (1 - \cos\theta)$$

## Tracking calorimeter:

measure the photon direction and the position of the primary vertex (small pileup dependence).

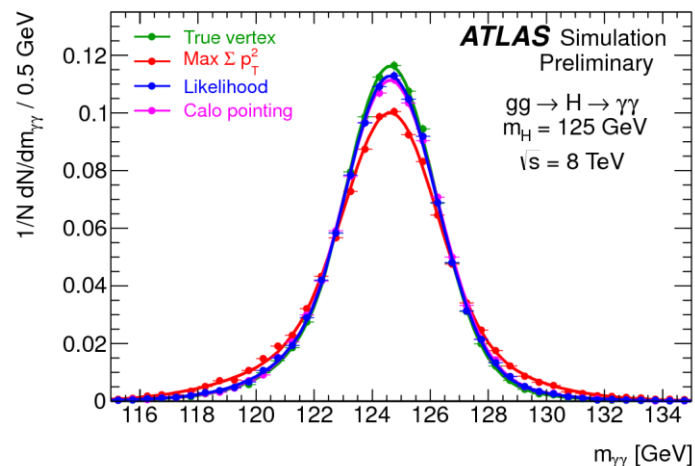
$m_{\gamma\gamma}$  distribution for the combined  $\sqrt{s} = 7$  TeV and  $\sqrt{s} = 8$  TeV data:



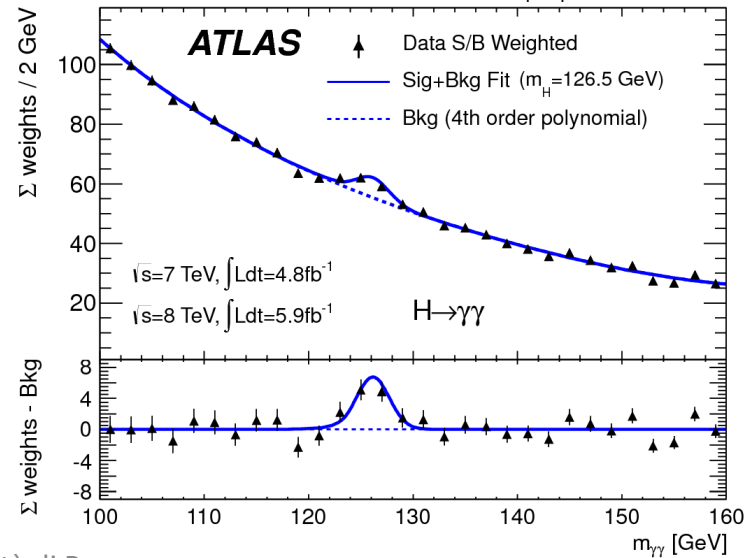
24/01/2013

A. Gabrielli - INFN - Università di Roma  
"Sapienza"

Distribution of expected  $m_{\gamma\gamma}$  for different algorithm used to determine the longitudinal vertex position:



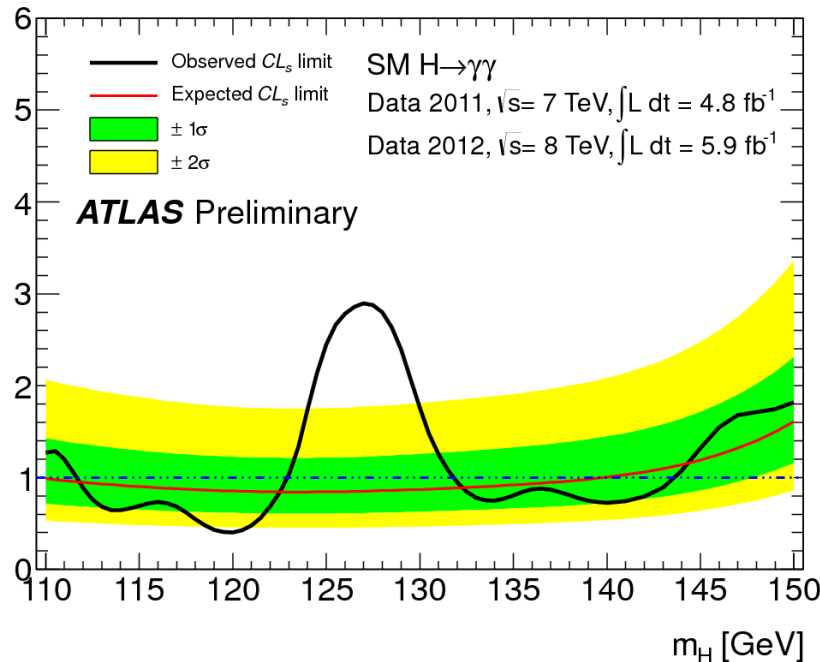
$m_{\gamma\gamma}$  distribution for the combined  $\sqrt{s} = 7$  TeV and  $\sqrt{s} = 8$  TeV data weighted ( $\ln(1 + S_i/B_i)$ ):



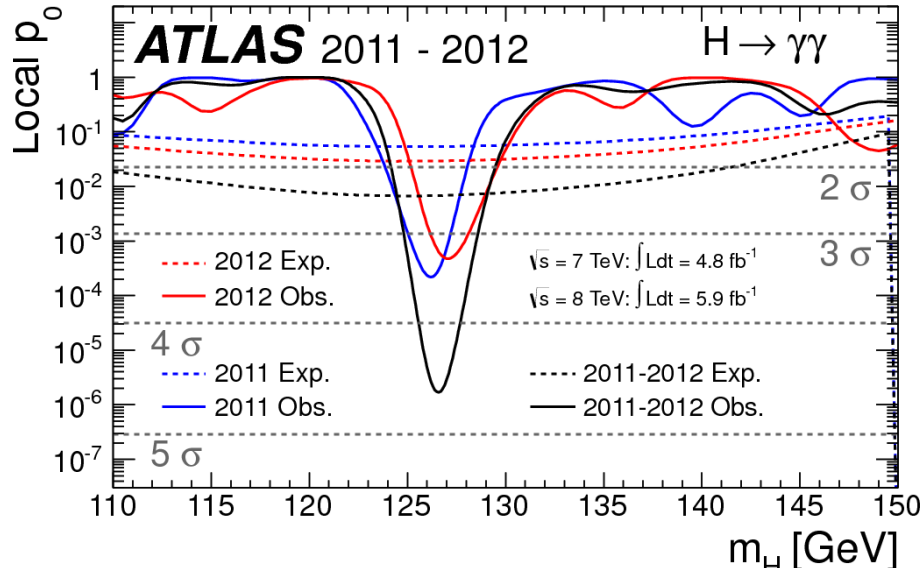
10

# H → γγ

Observed and expected CLs limit on the normalized signal strength vs Higgs mass:



Observed and expected p-value vs Higgs mass:



p-value = “probability” that result is as or less compatible with the background only hypothesis

## Higgs to gamma gamma (4<sup>th</sup> July 2012):

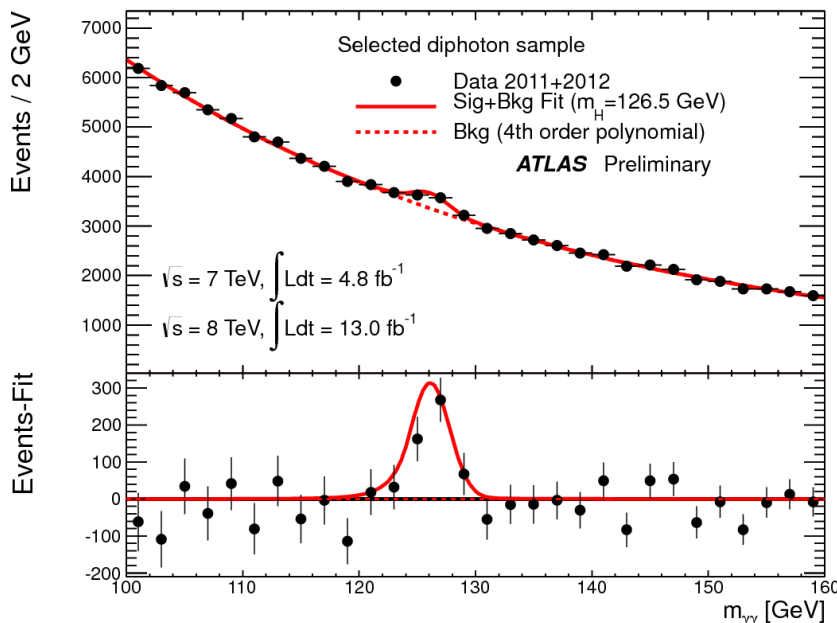
- The SM Higgs boson is excluded at 95% CL: **112-122.5** and **132-143** GeV c<sup>-2</sup> (exp. 110-139.5 GeV c<sup>-2</sup>);
- Observed  $p_0 \sim 4.5$  standard deviation (exp 2.5) @  $m_H = 126.5$  GeV c<sup>-2</sup>;
- Signal strength  $\mu = 1.9 \pm 0.5$ .

# H $\rightarrow$ $\gamma\gamma$ : latest results

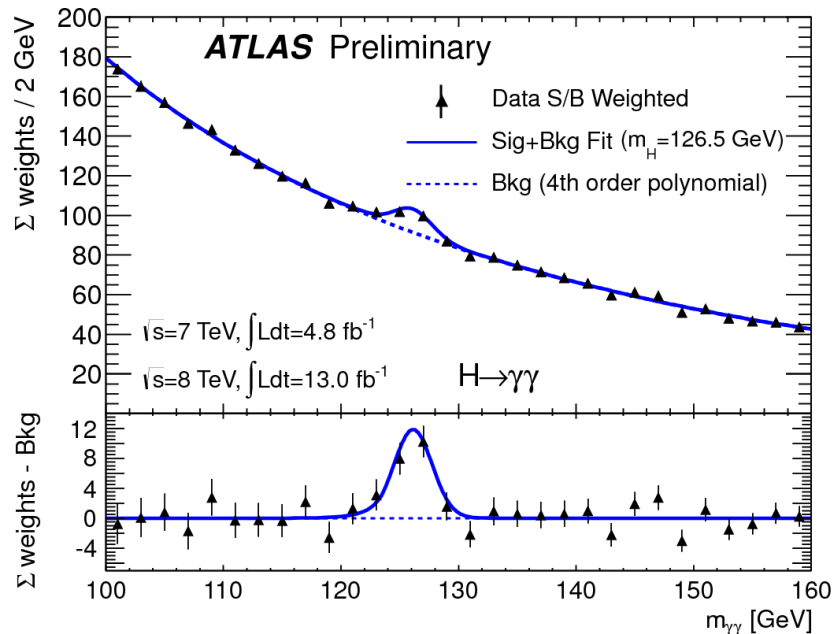
## Higgs to gamma gamma update:

- Lumi  $4.8 \text{ fb}^{-1}$  @ 7 TeV and  $13 \text{ fb}^{-1}$  @ 8 TeV (Council December 2012);
- Analysis has been re-optimized;
- Added two new categories for the VH production.

$m_{\gamma\gamma}$  distribution for the combined  $\sqrt{s} = 7 \text{ TeV}$  and  $\sqrt{s} = 8 \text{ TeV}$  data:

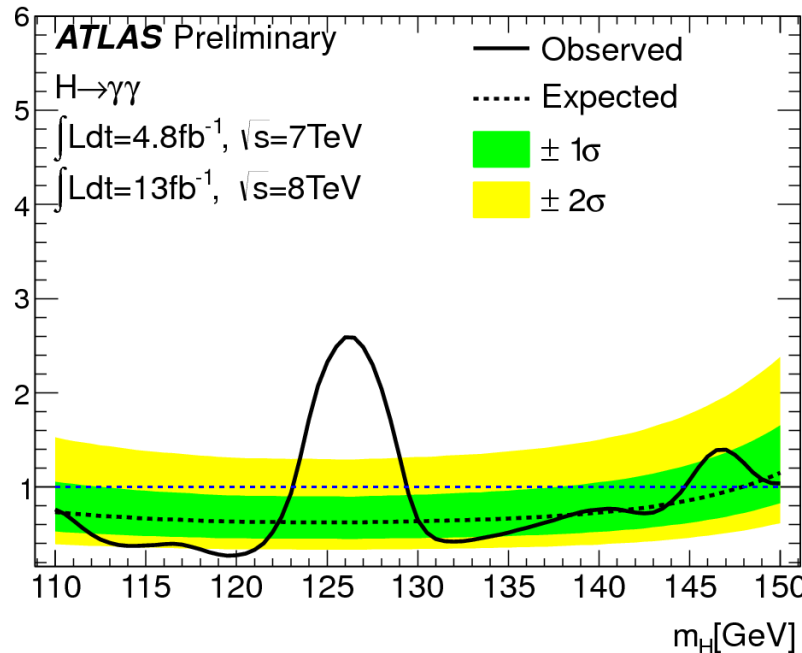


$m_{\gamma\gamma}$  distribution for the combined  $\sqrt{s} = 7 \text{ TeV}$  and  $\sqrt{s} = 8 \text{ TeV}$  data weighted ( $\ln(1 + S_i/B_i)$ ):



# $H \rightarrow \gamma\gamma$ : latest results

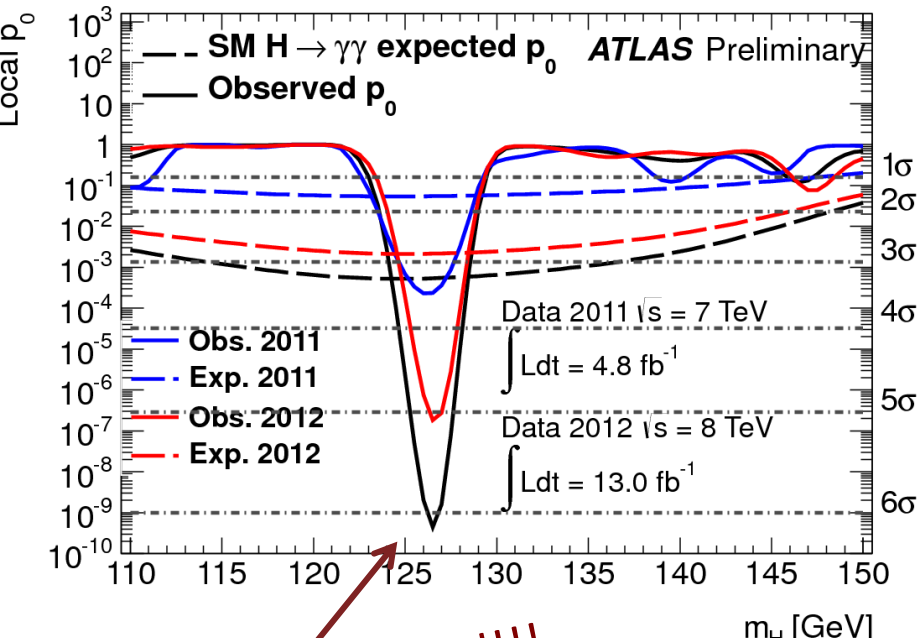
Observed and expected CLs limit on the normalized signal strength vs Higgs mass:



Higgs to gamma gamma (Council 2012):

- The SM Higgs boson is excluded at 95% CL:  $110\text{-}122.5$  and  $129.5\text{-}144.5 \text{ GeV c}^{-2}$  (exp.  $110\text{-}139.5 \text{ GeV c}^{-2}$ );
- Observed  $p_0 \sim 6.1$  standard deviation (exp 4.1) @  $m_H = 126.6 \text{ GeV c}^{-2}$ ;
- Signal strength  $\hat{\mu} = 1.8 \pm 0.3(\text{stat})^{+0.29}_{-0.21}(\text{syst})$

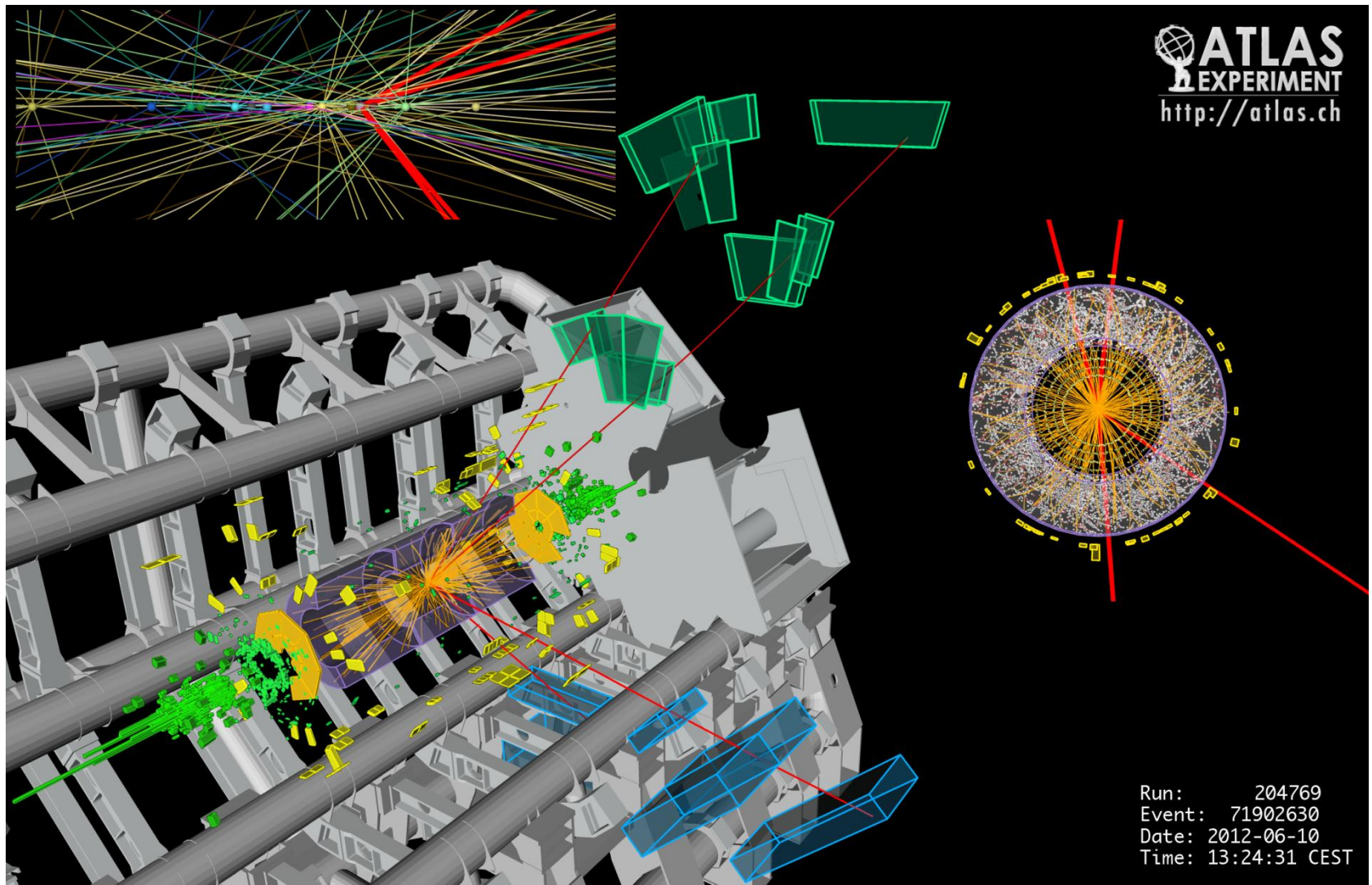
Observed and expected p-value vs Higgs mass:



Signal is confirmed!!!

The compatibility with the SM prediction is estimated to be at the  $2.4 \sigma$  level

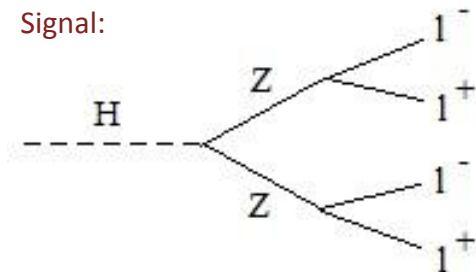
$H \rightarrow ZZ^{(*)} \rightarrow 4l$



# $H \rightarrow ZZ^{(*)} \rightarrow 4l$

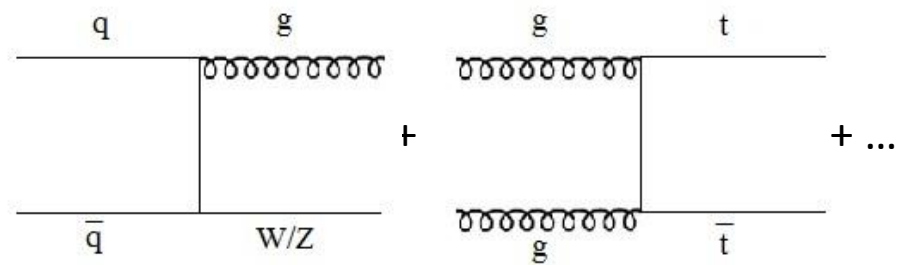
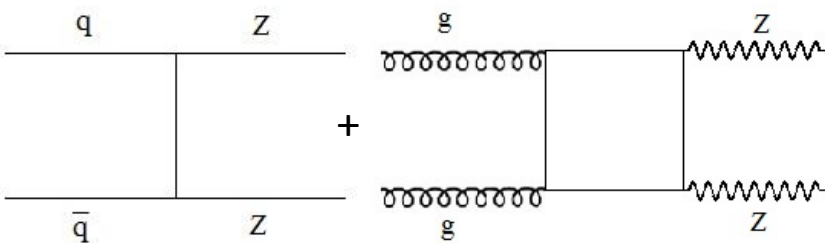
Higgs to four leptons (“golden channel”):

- BR:  $\sim 10^{-4}$  (@  $m_H = 125 \text{ GeV } c^{-2}$ );
- Bkg:  $ZZ$ ,  $Z+\text{jets}$ , top;
- **Signal purity (S/B)  $\sim 1$** ;
- Lumi  $4.8 \text{ fb}^{-1}$  @ 7 TeV and  $5.8 \text{ fb}^{-1}$  @ 8 TeV  
(4<sup>th</sup> July 2012).



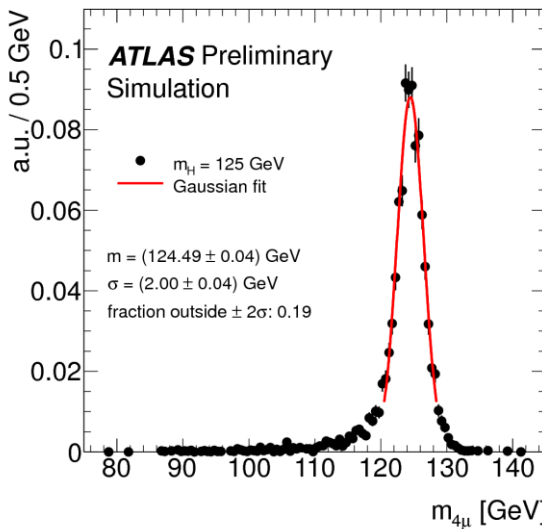
Irreducible bkg:  $pp \rightarrow ZZ$  ( $\sim 70\%$  total bkg)  
rejection: kinematic cuts e.g.  $m_{12}$  and  $m_{34}$   
Shape and normalization from MC:

Reducible bkg:  $pp \rightarrow Z+\text{jet}$ ,  $t\bar{t}$ ... rejection: isolation of leptons, ...  
 $Z+\text{jet}$  from control region,  $Zbb$  shape from MC and normalization from data:

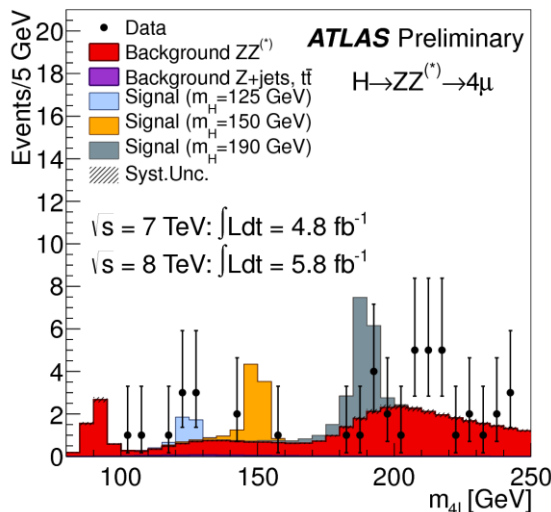


# $H \rightarrow ZZ^{(*)} \rightarrow 4l$

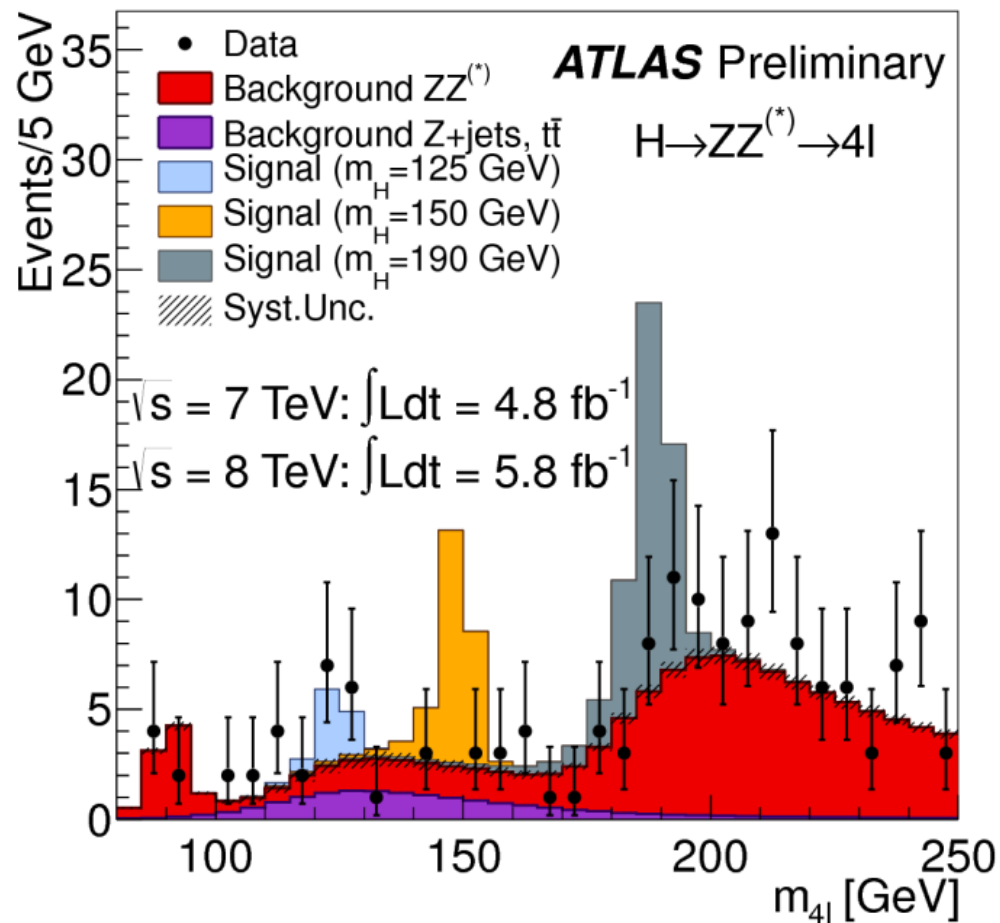
Invariant mass distribution for simulated  
 $H \rightarrow ZZ^{(*)} \rightarrow 4\mu$ :



$m_{4\mu}$  distribution for the combined  $\sqrt{s} = 7 \text{ TeV}$  and  $\sqrt{s} = 8 \text{ TeV}$  data:

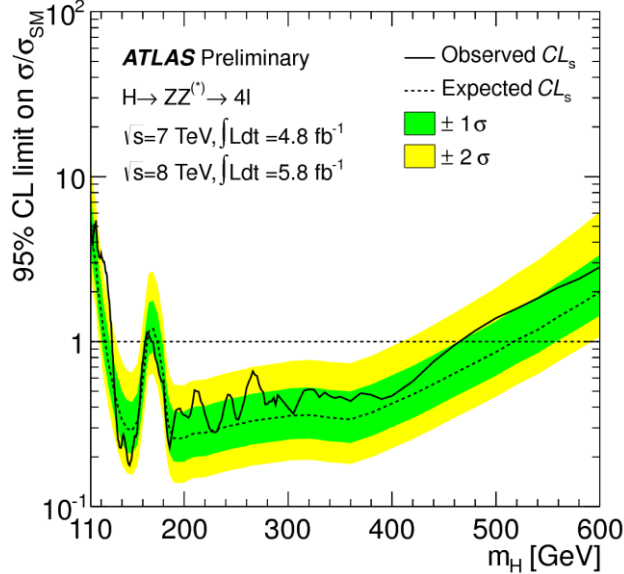


$m_{4l}$  distribution for the combined  $\sqrt{s} = 7 \text{ TeV}$  and  $\sqrt{s} = 8 \text{ TeV}$  data:



# $H \rightarrow ZZ^{(*)} \rightarrow 4l$

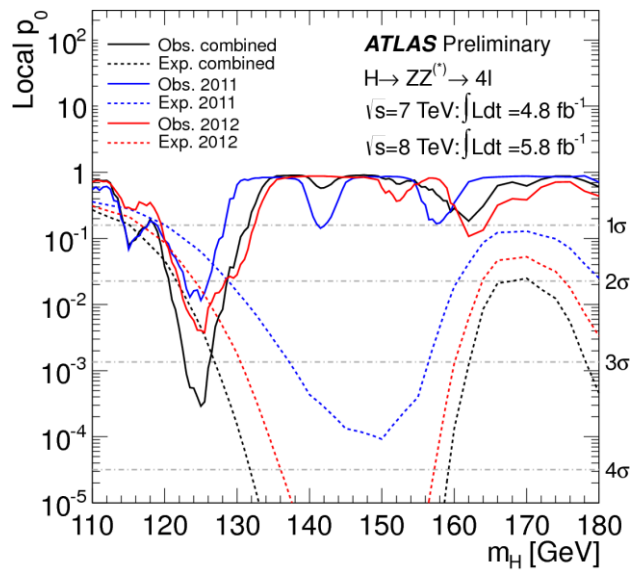
Observed and expected CLs limit on the normalized signal strength vs Higgs mass:



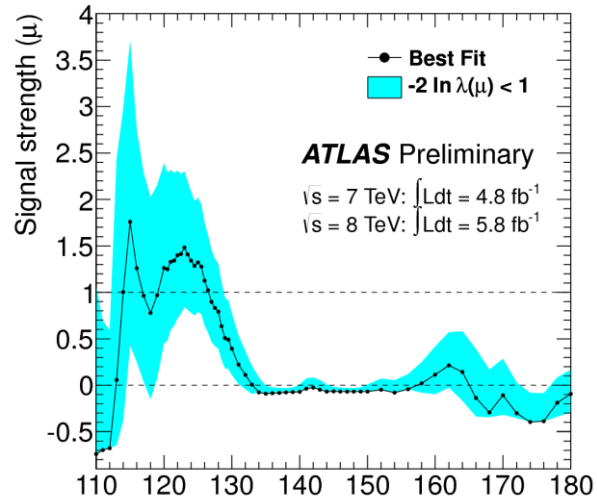
Higgs to four leptons (4<sup>th</sup> July 2012):

- The SM Higgs boson is excluded at 95% CL:  
131-162 and 170-460 GeV c<sup>-2</sup>  
(exp. 124-164 and 176-500 GeV c<sup>-2</sup>);
- Observed p<sub>0</sub> ~ 3.6 standard deviation (exp 2.7)  
@ m<sub>H</sub> = 125 GeV c<sup>-2</sup>;
- Signal strength μ = 1.2 +/- 0.6.

Observed and expected p-value vs Higgs mass:



Fitted signal strength parameter vs m<sub>H</sub>:

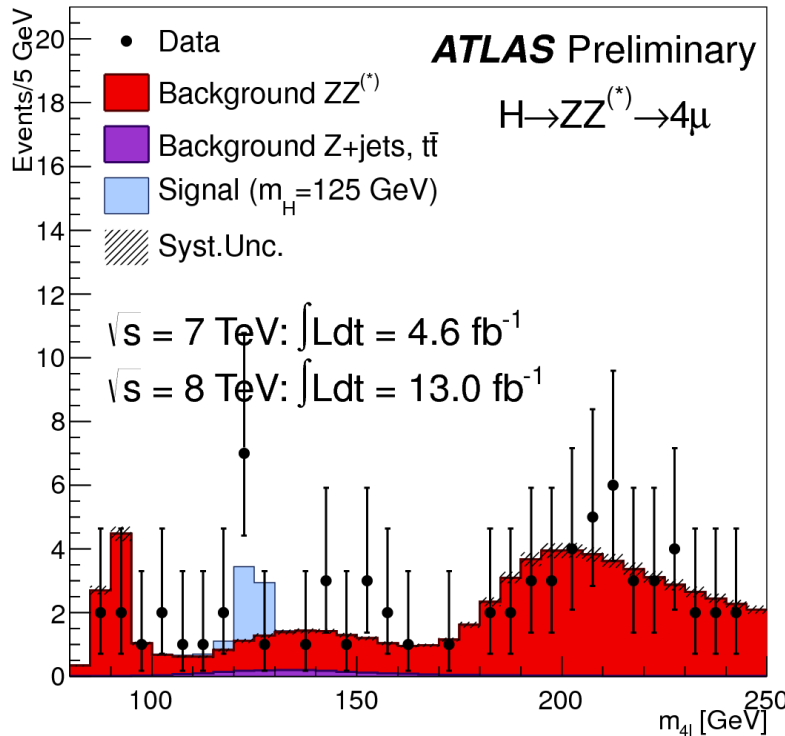


# $H \rightarrow ZZ^{(*)} \rightarrow 4l$ : latest results

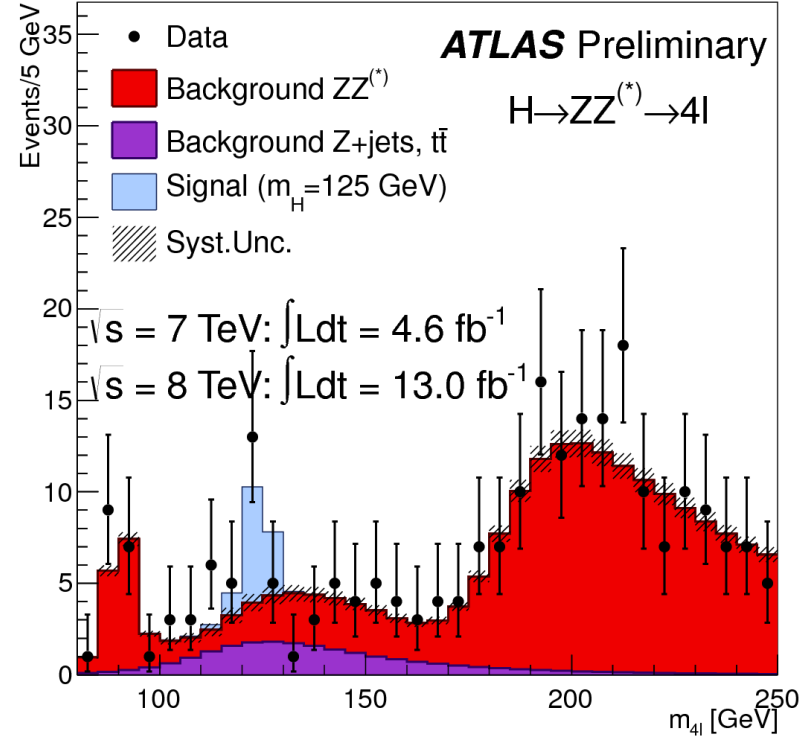
## Higgs to four leptons update:

- Lumi  $4.8 \text{ fb}^{-1}$  @ 7 TeV and  $13 \text{ fb}^{-1}$  @ 8 TeV (Council December 2012);
- Analysis has been re-optimized.

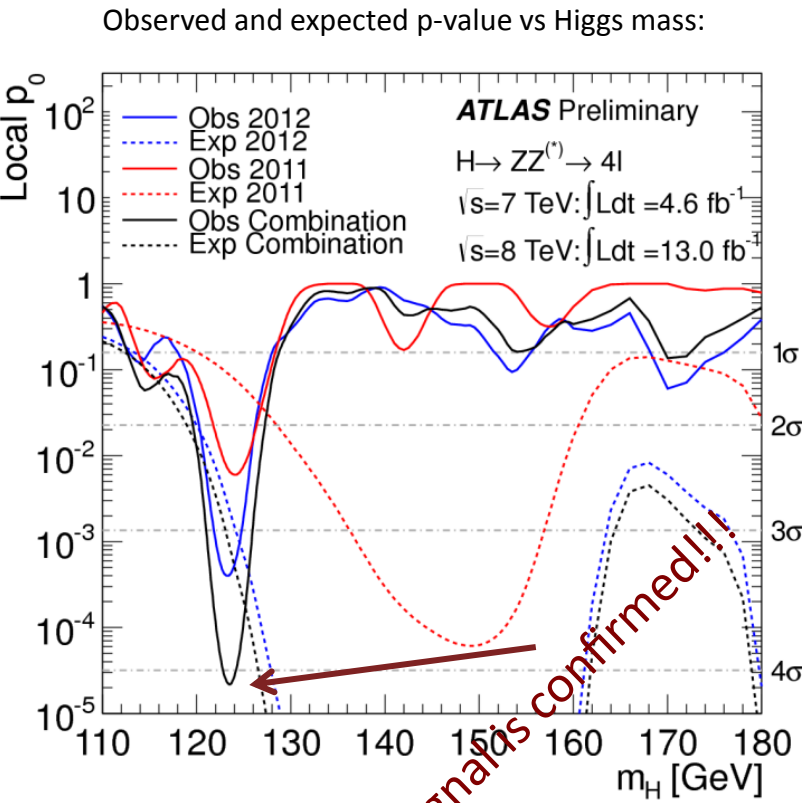
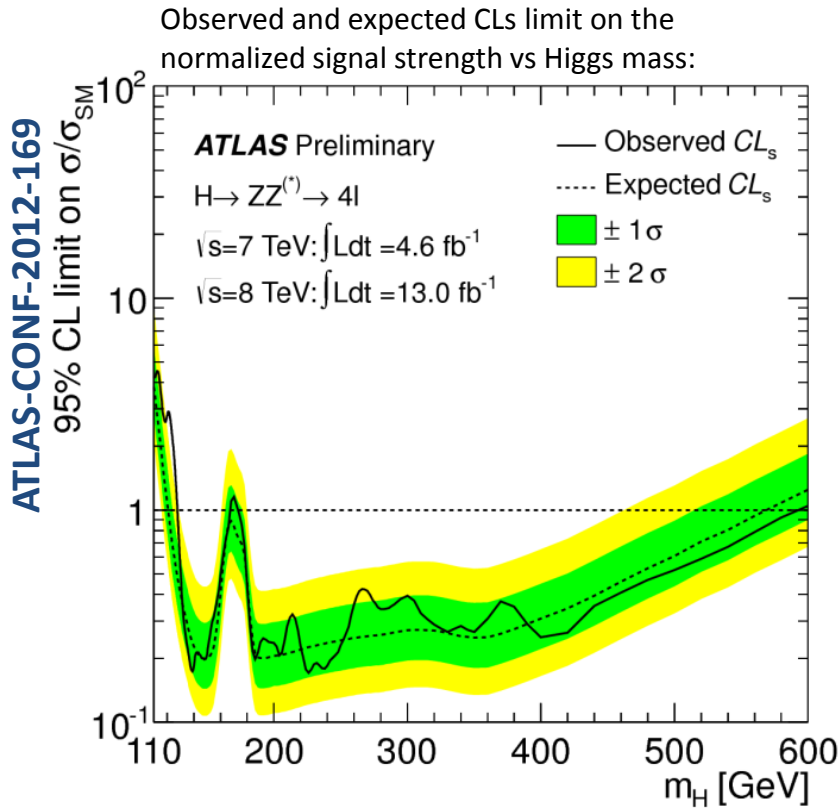
$m_{4\mu}$  distribution for the combined  $\sqrt{s} = 7 \text{ TeV}$  and  $\sqrt{s} = 8 \text{ TeV}$  data:



$m_{4l}$  distribution for the combined  $\sqrt{s} = 7 \text{ TeV}$  and  $\sqrt{s} = 8 \text{ TeV}$  data:



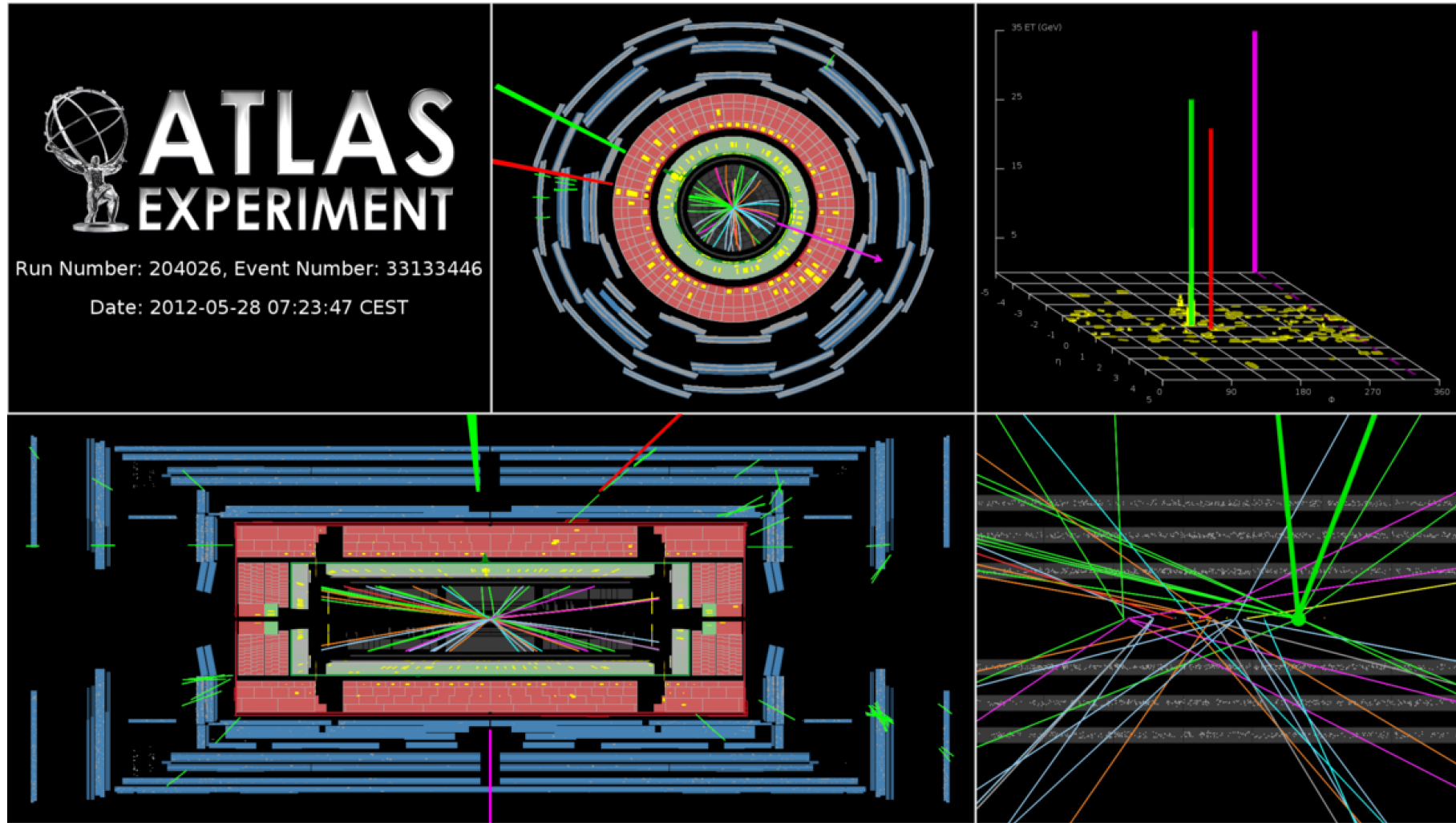
# $H \rightarrow ZZ^{(*)} \rightarrow 4l$ : latest results



Higgs to four leptons (Council 2012):

- The SM Higgs boson is excluded at 95% CL: **127.7-166** and **174-600**  $\text{GeV c}^{-2}$  (exp. 120-580  $\text{GeV c}^{-2}$ );
- Observed  $p_0 \sim 4.1$  standard deviation (exp 3.1) @  $m_H = 123.5 \text{ GeV c}^{-2}$ ;
- Signal strength  $\hat{\mu} = 1.3 \pm 0.4$

# $H \rightarrow WW^{(*)} \rightarrow l\nu l\nu$

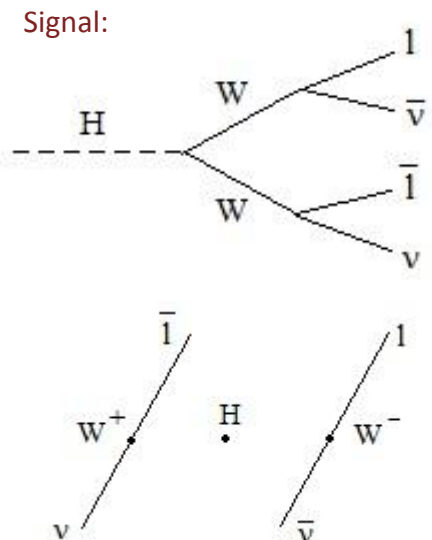
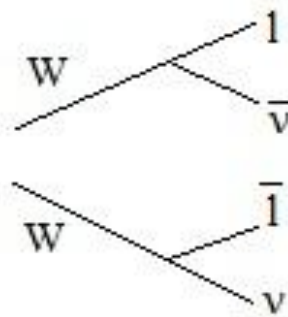


# $H \rightarrow WW^{(*)} \rightarrow l\nu l\nu$

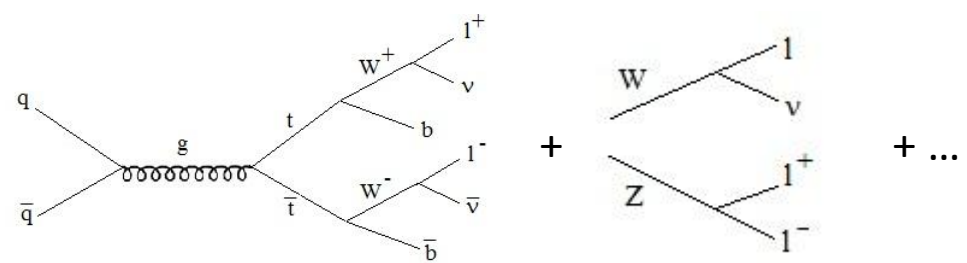
Higgs to WW:

- BR:  $\sim 2.5 \times 10^{-3}$  (@  $m_H = 125$  GeV c $^{-2}$ );
- Bkg: WW, W+jets, jet-jet, top;
- **Different-flavour e/ $\mu$  (D-Y rejection);**
- Signal purity (S/B)  $\sim 10\%$ ;
- Discriminant variables:  $m_{||}$ ,  $\Delta\phi_{||}$ ,  $m_T$ ;
- Lumi  $4.8 \text{ fb}^{-1}$  @ 7 TeV and  $13 \text{ fb}^{-1}$  @ 8 TeV  
(HCP 2012).

Irreducible bkg:  $pp \rightarrow WW$ , rejection:  $\Delta\phi_{||} H$  has spin 0, WW bkg from simulation + control region:

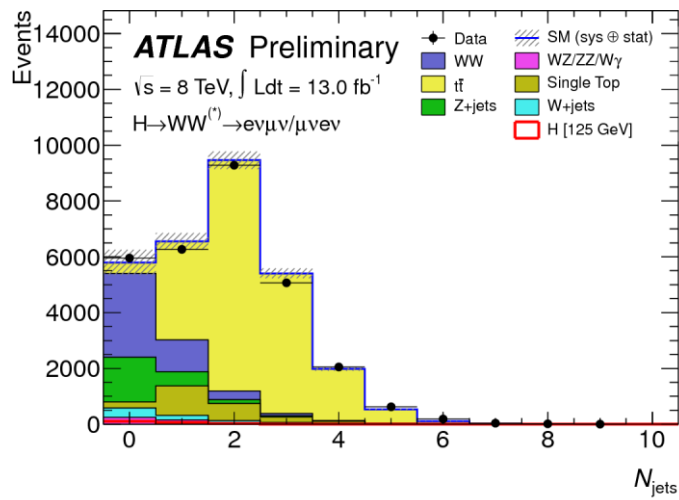


Reducible bkg:  $pp \rightarrow WZ, Z/W+jet, tt$ . rejection: isolation of leptons , ..., W+jets from data, other simulation + control region:

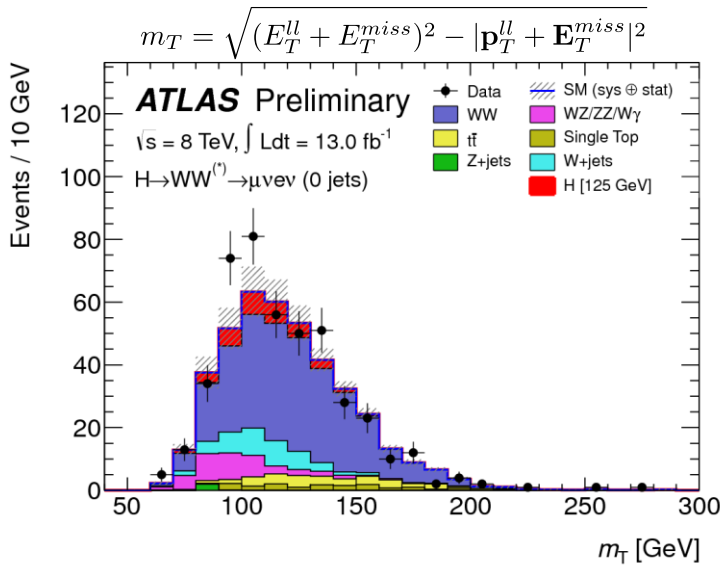


# $H \rightarrow WW^{(*)} \rightarrow l\nu l\nu$

multiplicity of jets for events satisfying the dilepton and  $E_T^{\text{miss rel}}$  selection:



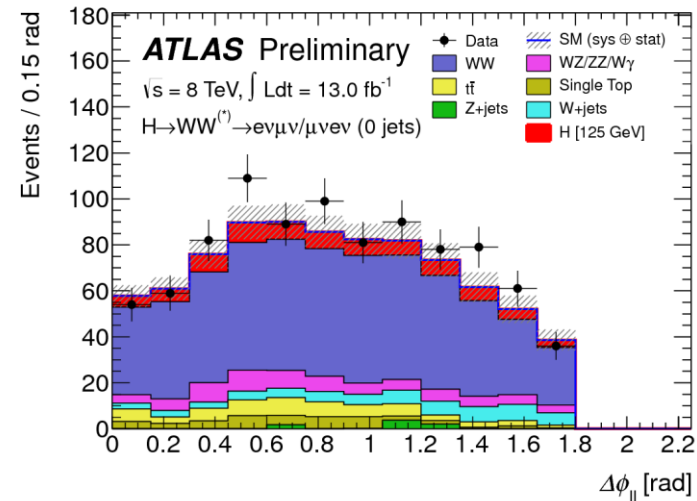
$m_T$  distribution for events satisfying all criteria:



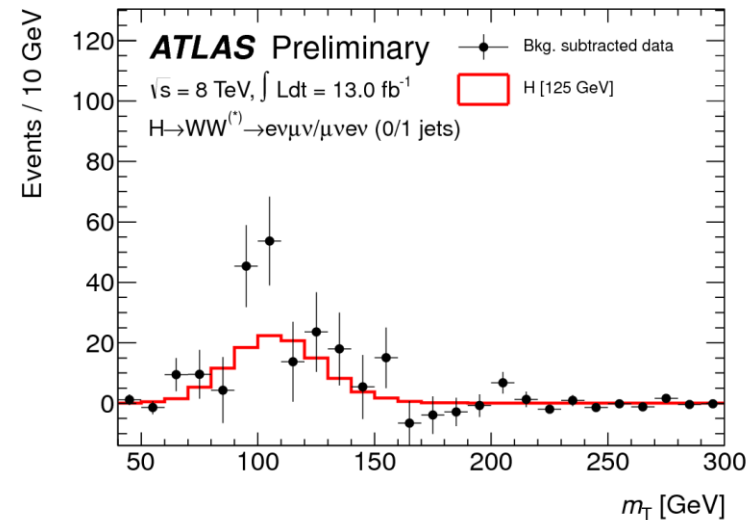
24/01/2013

A. Gabrielli - INFN - Università di Roma  
 "Sapienza"

$\Delta\phi_{||}$  distribution after full event selection:



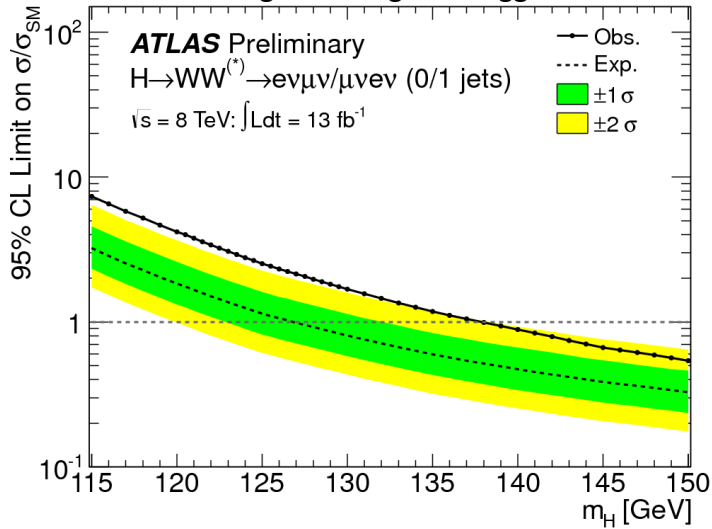
$m_T$  distribution in data with the estimated background subtracted with the predicted signal:



22

# $H \rightarrow WW^{(*)} \rightarrow l\nu l\nu$ : latest results

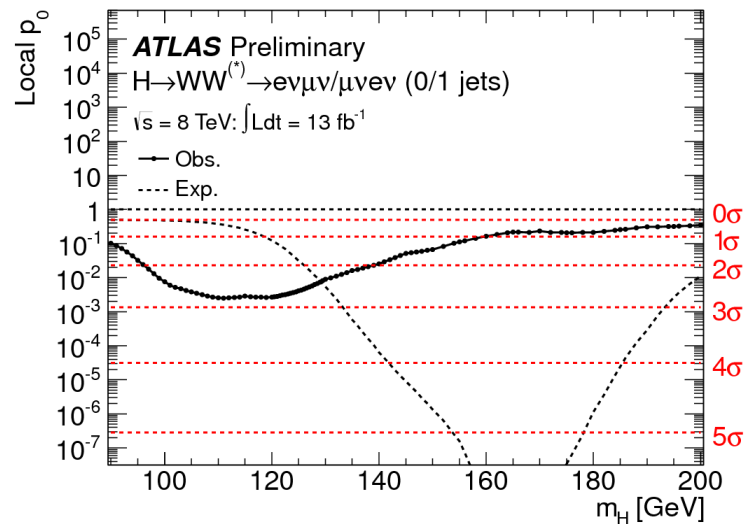
Observed and expected CLs limit on the normalized signal strength vs Higgs mass:



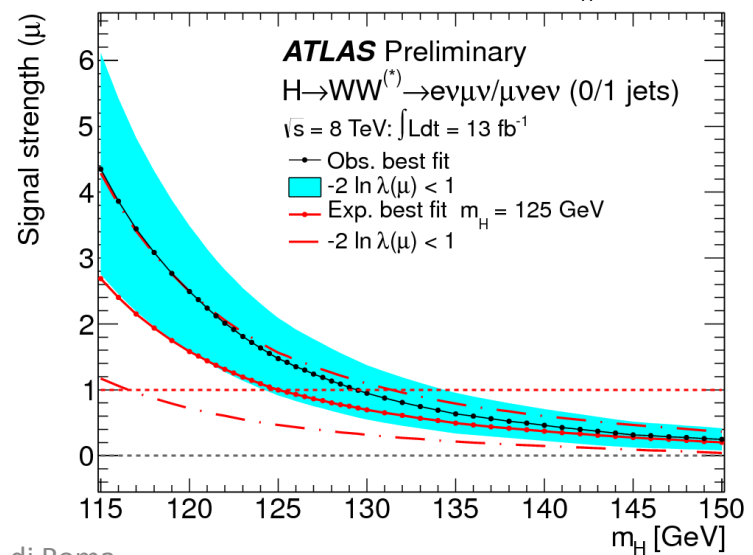
Higgs to WW (HCP 2012):

- Only Different-flavour e/ $\mu$  updated (higher sensitivity);
- Observed  $p_0 \sim 2.8$  standard deviation (exp 3.1) @  $m_H = 125 \text{ GeV c}^{-2}$ ;
- Signal strength  $\mu = 1.5 +/- 0.6$ .

Observed and expected p-value vs Higgs mass:



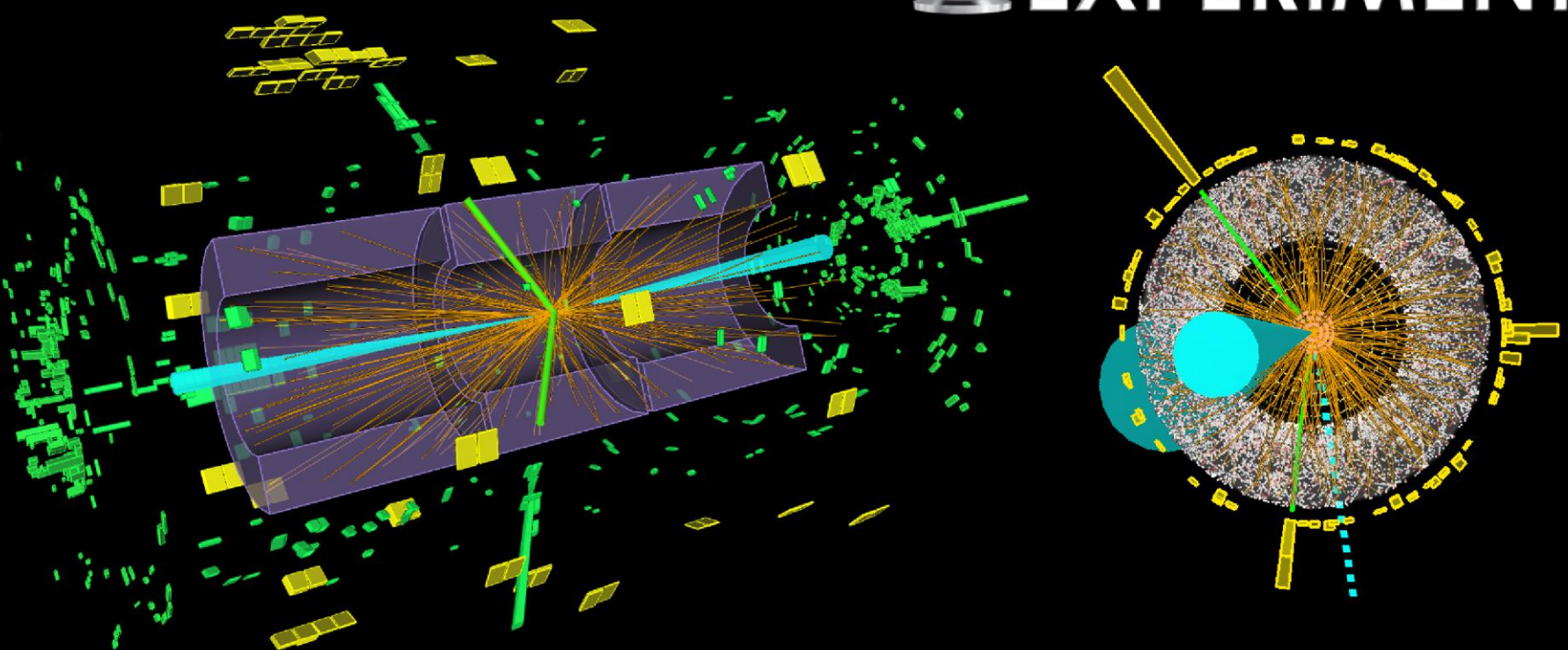
Fitted signal strength parameter vs  $m_H$ :



$H \rightarrow \tau\tau$

Run Number: 209109, Event Number: 86250372

Date: 2012-08-24 07:59:04 UTC

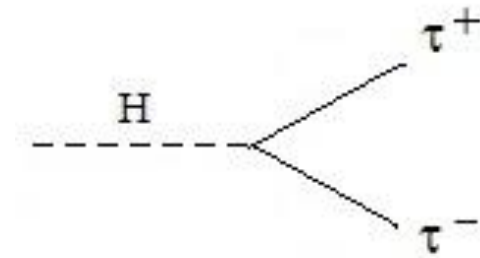


# $H \rightarrow \tau\tau$

## Higgs to $\tau\tau$ :

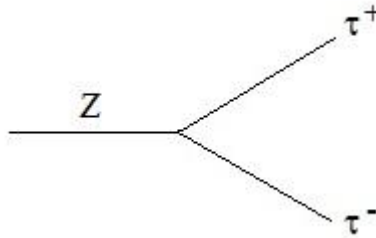
- BR:  $\sim 6 \times 10^{-2}$  (@  $m_H = 125$  GeV  $c^{-2}$ );
- Bkg: Z, Z+jets, top;
- Signal purity (S/B)  $\sim 0.3\%-30\%$ ;
- Many exclusive categories  
 $\tau_{\text{lep}}, \tau_{\text{had}}$ : boosted, 0-1-2 jets (**2 jets for VBF**)...  
 to increase sensitivity;
- Lumi  $4.8 \text{ fb}^{-1}$  @ 7 TeV and  $13 \text{ fb}^{-1}$  @ 8 TeV  
 (HCP 2012).

Signal:

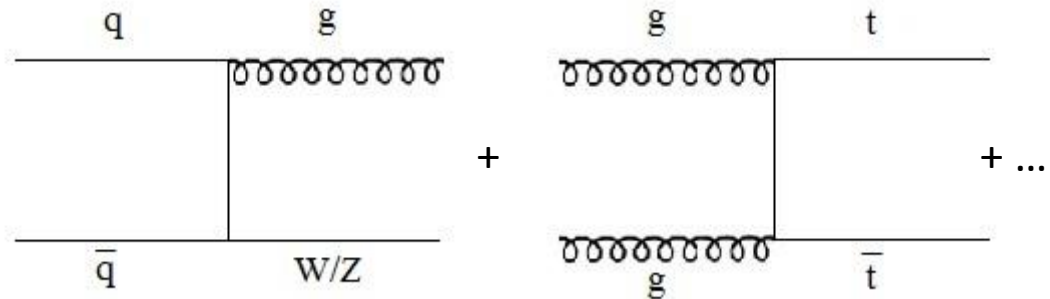


$\tau_{\text{lep}}\tau_{\text{lep}}$	$\tau_{\text{lep}}\tau_{\text{had}}$	$\tau_{\text{had}}\tau_{\text{had}}$
12%	46%	42%

$Z \rightarrow \tau\tau$  from embedding: Start from real  $Z \rightarrow \mu\mu$  events,  
 replace muons with fully-simulated taus with proper  
 polarization and spin correlations:

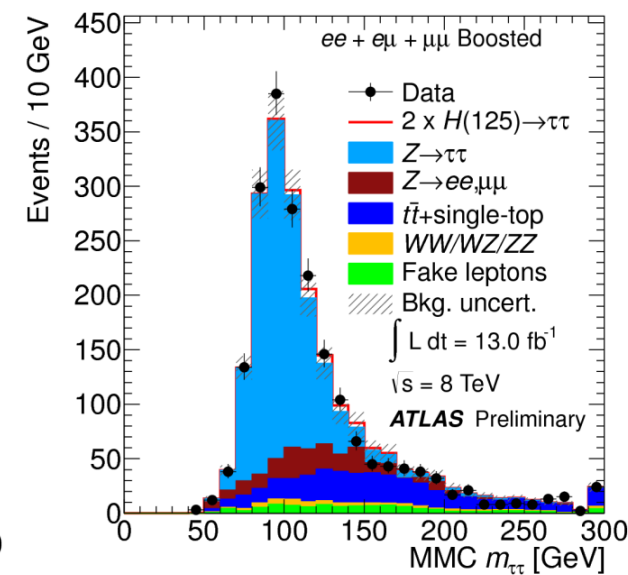
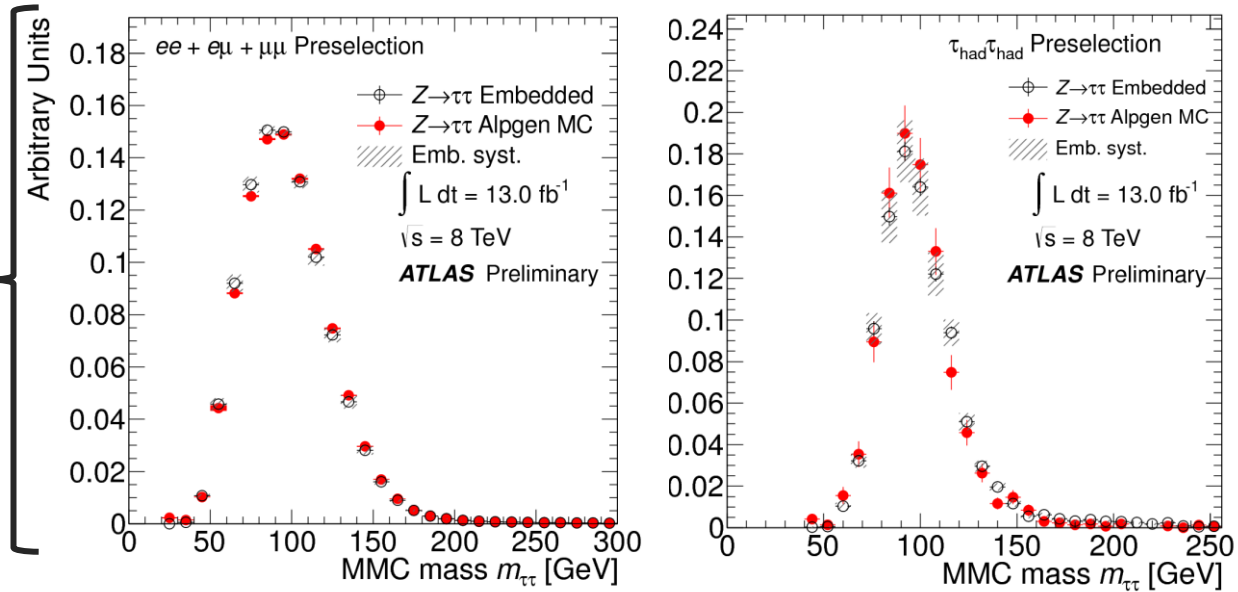


Other backgrounds: W/Z + jet, WW, ZZ, tt... from simulation:



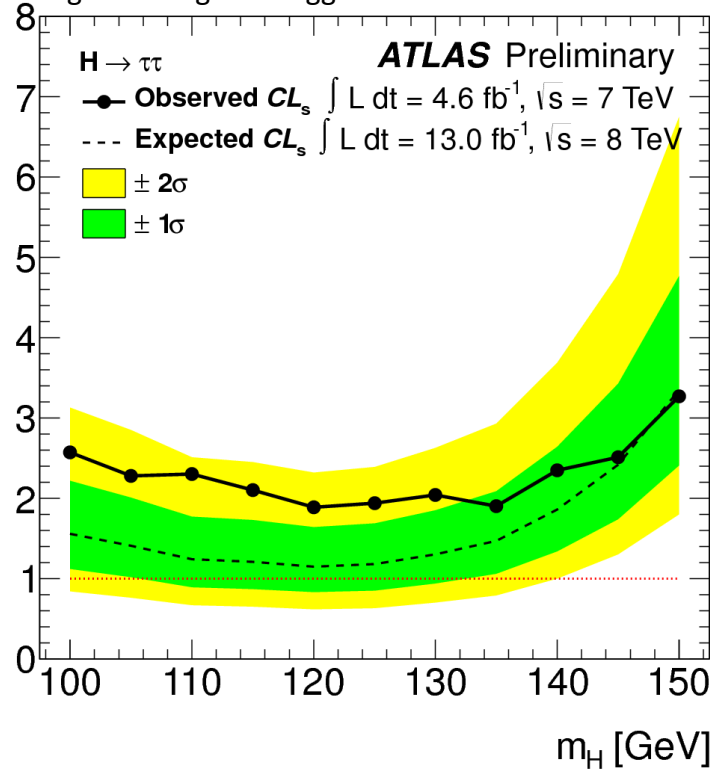
# $H \rightarrow \tau\tau$

MMC mass distributions for the  $\tau$ -embedded  $Z \rightarrow \mu\mu$  data and simulated  $Z \rightarrow \tau\tau$  events:

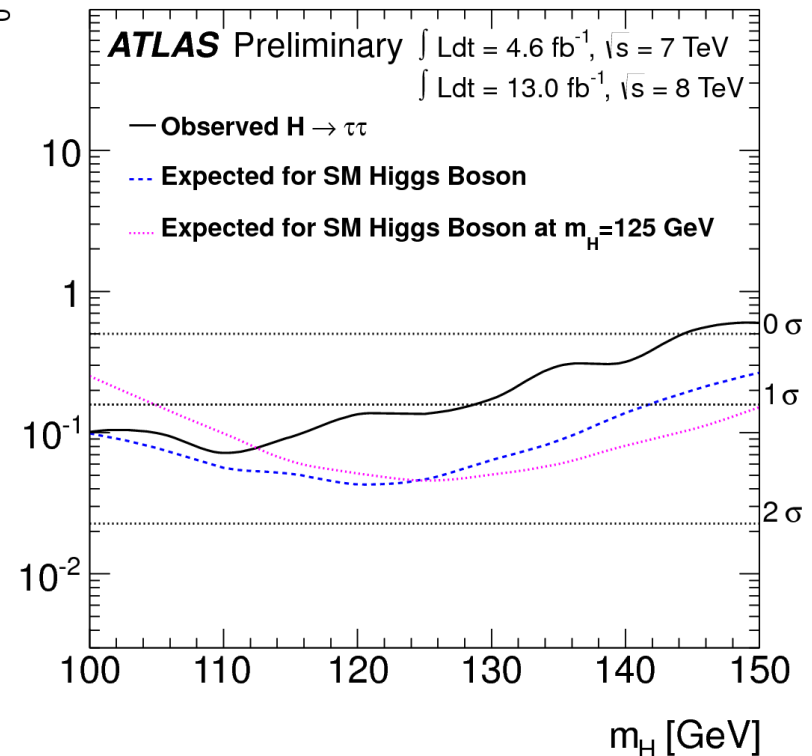


MMC mass distributions of the selected events:

Observed and expected CLs limit on the normalized signal strength vs Higgs mass:



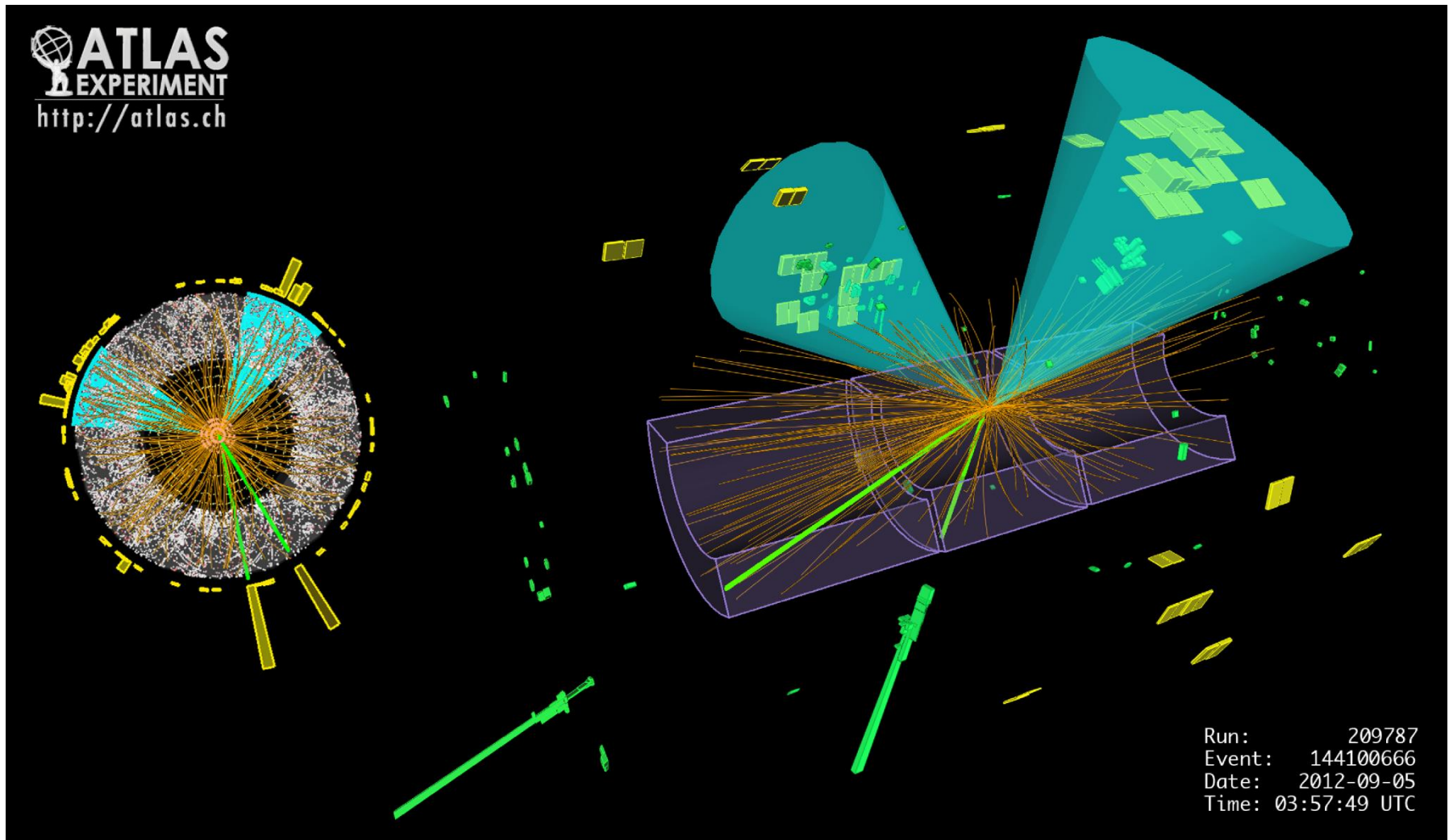
Observed and expected p-value vs Higgs mass:



### Higgs to $\tau\tau$ (HCP 2012):

- 2-3 times SM Higgs boson is excluded at 95% CL:  $\sim 100\text{-}150 \text{ GeV } c^{-2}$ ;
- Observed  $p_0 \sim 1.1$  standard deviation @  $m_H = 125 \text{ GeV } c^{-2}$ ;
- Signal strength  $\mu = 0.7 \pm 0.7$ .

# VH → V+bb

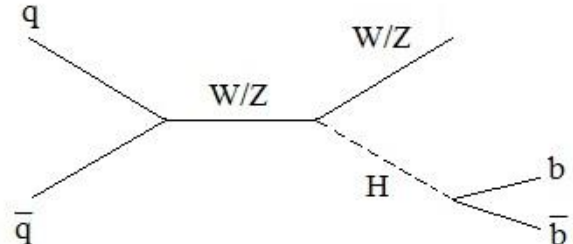


# VH $\rightarrow$ V+bb

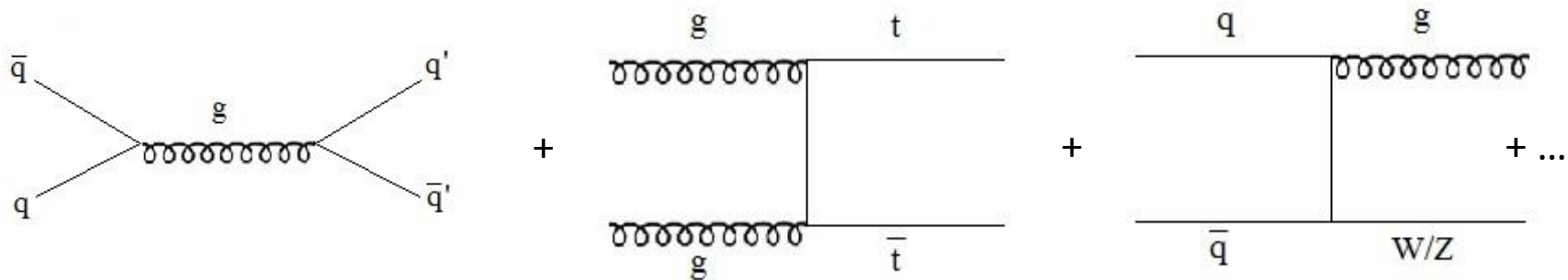
Higgs to bb:

- BR:  $\sim 0.6$  (@  $m_H = 125$  GeV  $c^{-2}$ );
- Production: VH;
- Bkg: Zbb, Wbb, top...;
- Three channels:
  - 0 leptons:  $Z \rightarrow \nu \bar{\nu} + H \rightarrow bb$ ;
  - 1 lepton:  $W \rightarrow l \bar{\nu} + H \rightarrow bb$ ;
  - 2 leptons:  $Z \rightarrow ll + H \rightarrow bb$ ;
- Signal purity (S/B)  $\sim 1\%-10\%$ ;
- Discriminant variables: lep,  $E_t^{\text{miss}}$ ,  $m_{jj}$ ...;
- Lumi  $4.8 \text{ fb}^{-1}$  @ 7 TeV and  $13 \text{ fb}^{-1}$  @ 8 TeV (HCP 2012).

Signal:

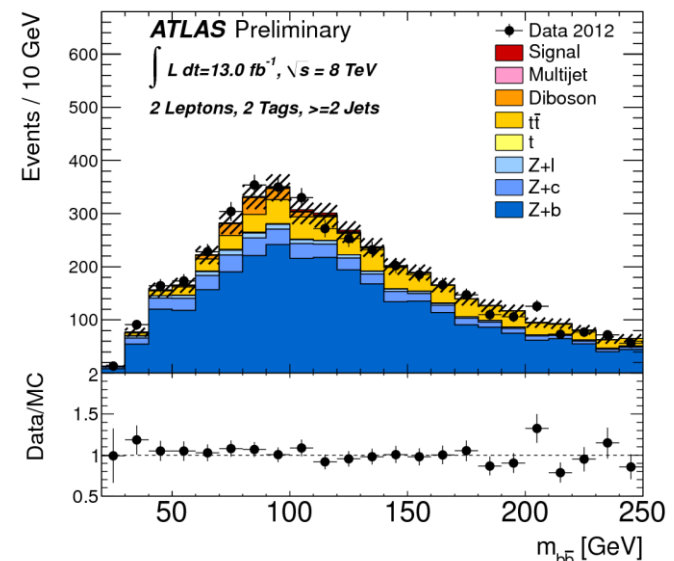
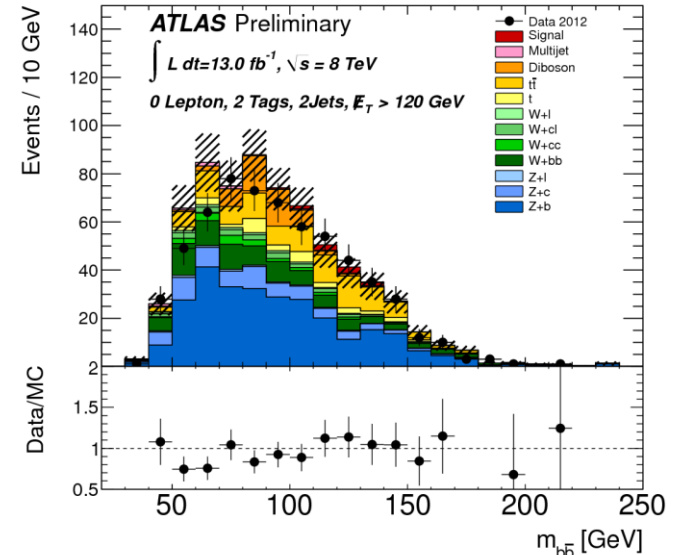
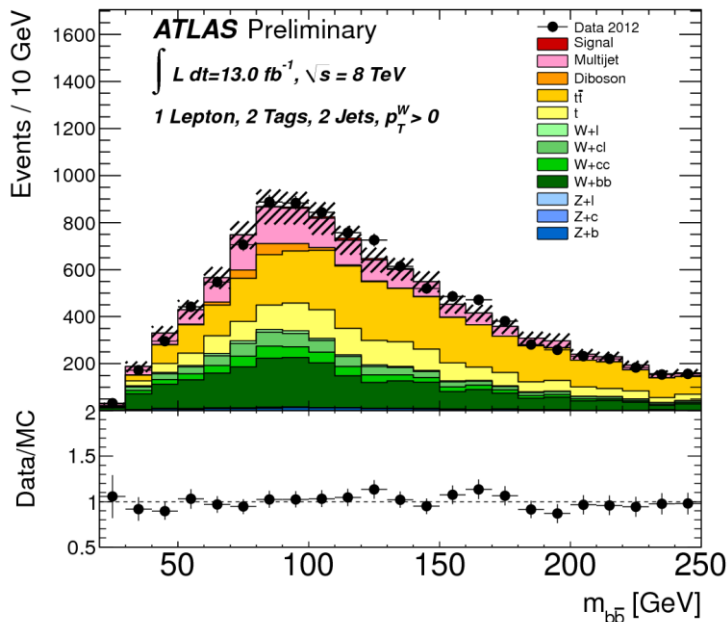


Backgrounds: W/Z + jet, tt... are estimated using a combination of techniques based on the comparison of data and MC predictions. ZZ, WW from simulation and MultiJet only form data:



# VH → V+bb

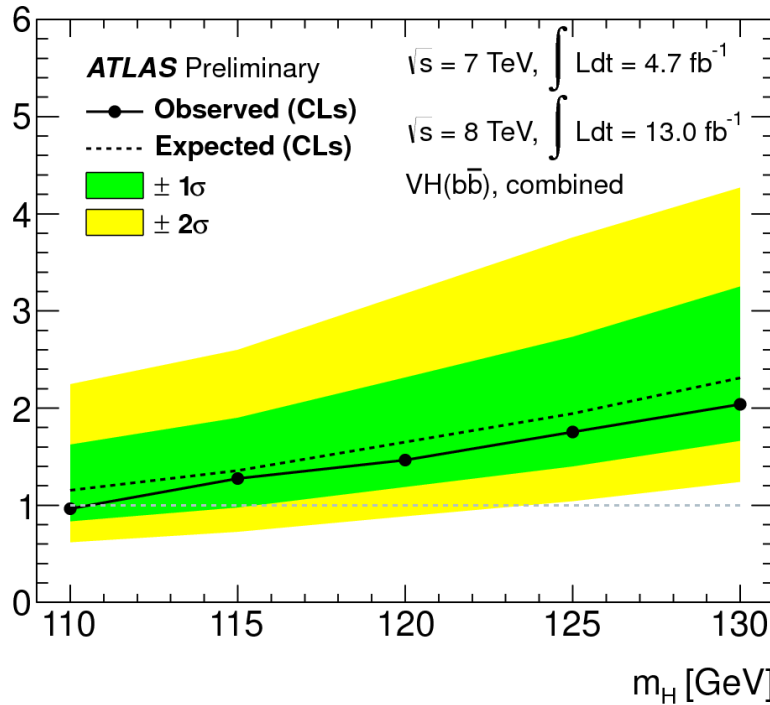
$m_{bb}$  distributions after full event selection for 2 jets and 0-1-2 leptons.



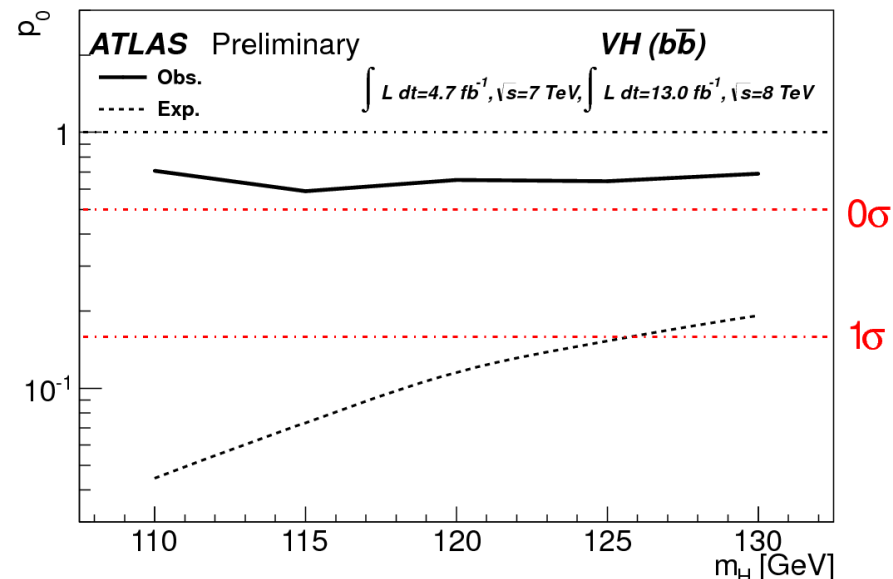
The normalizations of backgrounds are determined by a maximum likelihood fit to control and signal regions.

# VH $\rightarrow$ V+bb

Observed and expected CLs limit on the normalized signal strength vs Higgs mass:



Observed and expected p-value vs Higgs mass:



Higgs to bb (HCP2012):

- The SM Higgs boson is excluded @ 95% CL: 110 GeV c<sup>-2</sup>;
- 2 times SM Higgs boson is excluded at 95% CL: ~ 110-130 GeV c<sup>-2</sup>;
- No significant excess is observed.

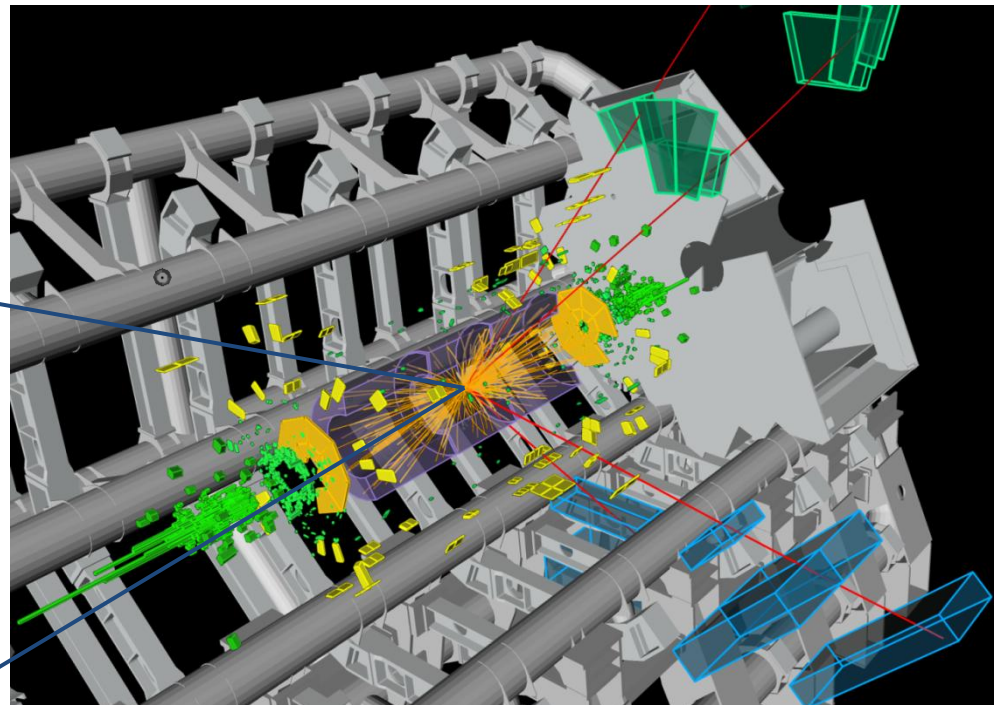
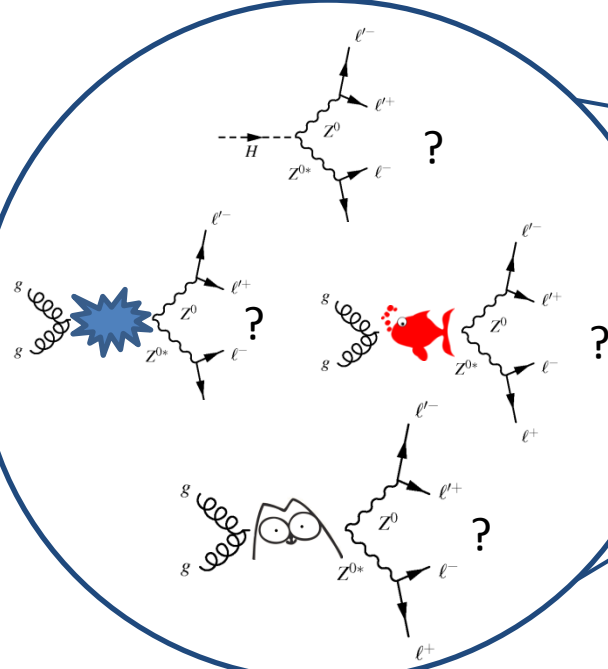
# What is it?

Is it really the Standard Model Higgs boson?

Needed study its properties:

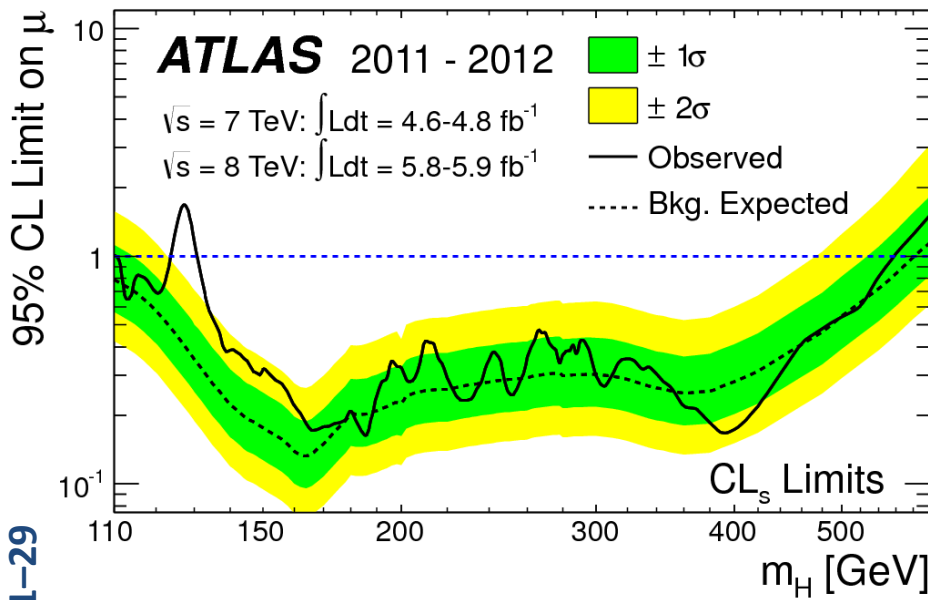
- Mass;
- Couplings;
- Spin/CP.

What is it?

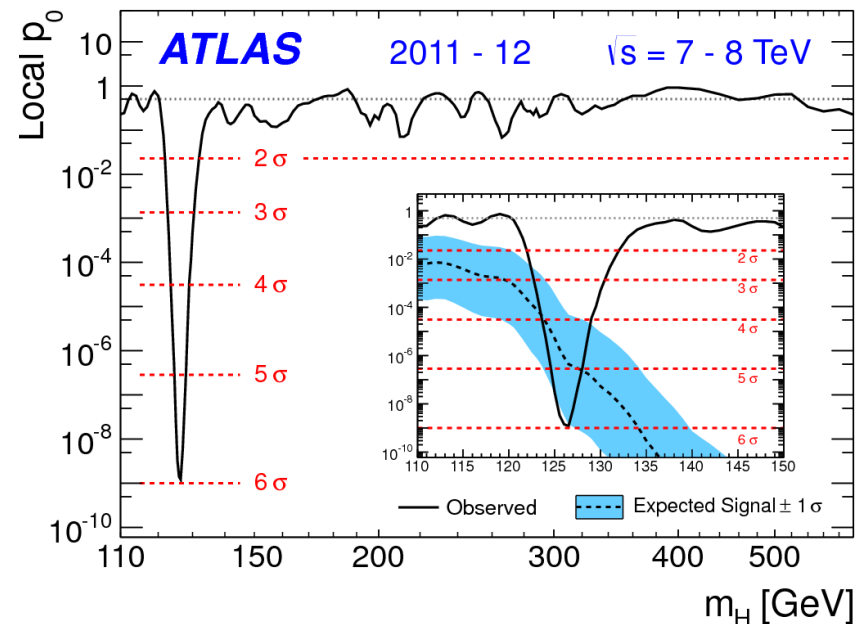


# Higgs combination

Observed and expected CLs limit on the normalized signal strength vs Higgs mass:



Observed and expected p-value vs Higgs mass:



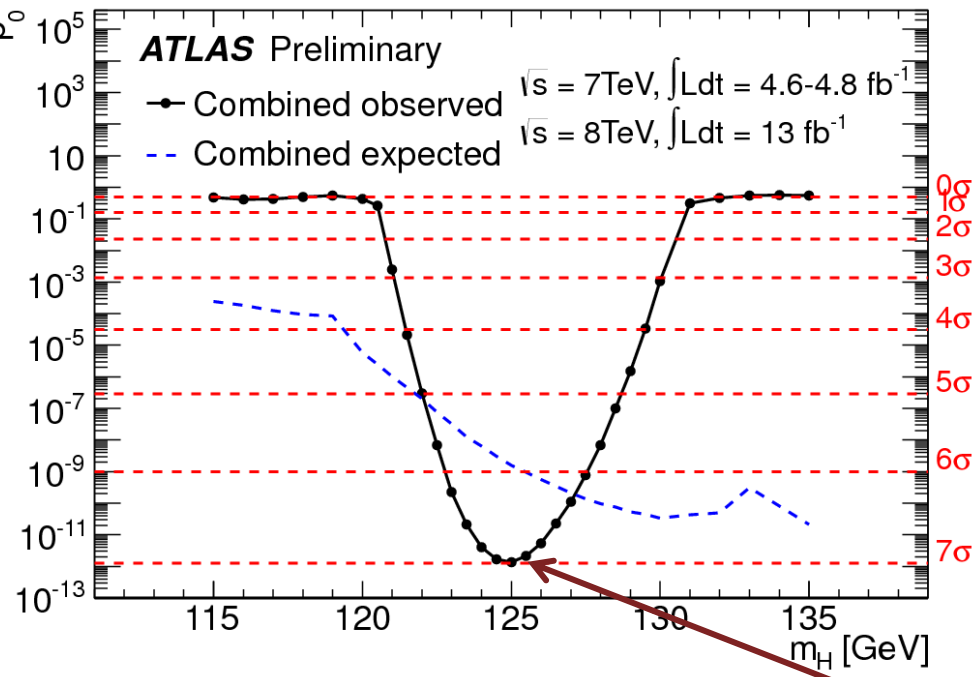
## Higgs combination (July 2012):

- The SM Higgs boson is excluded at 95% CL: [111-122](#) and [131-559](#) GeV  $c^{-2}$  (exp 110-582 GeV  $c^{-2}$ );
- Observed  $p_0 \sim 6.0$  standard deviation (exp 4.9) @  $m_H = 126$  GeV  $c^{-2}$ ;
- Signal strength  $\mu = 1.4 +/- 0.3$ .

# Higgs combination: latest results

ATLAS-CONF-2012-170

Observed and expected p-value vs Higgs mass:

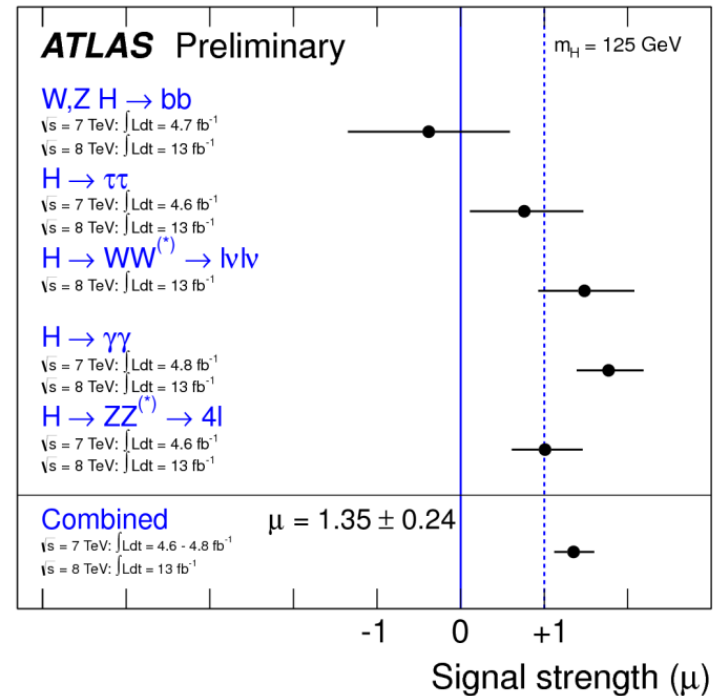


Expected significance : 5.9  $\sigma$

Observed significance: 7.0  $\sigma$

Combined signal strength is:  $\hat{\mu} = 1.35 \pm 0.19(\text{stat}) \pm 0.15(\text{syst})$

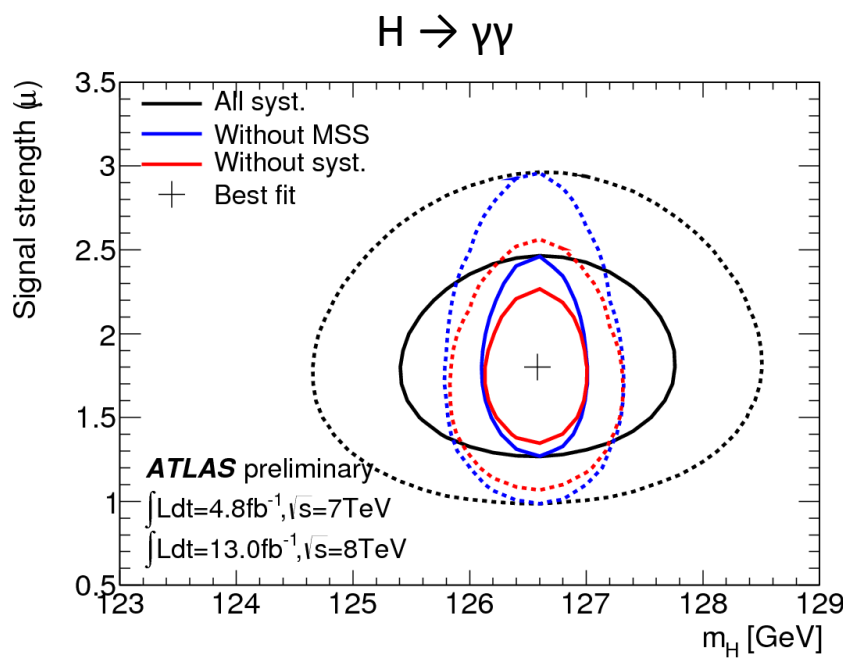
Signal strength for all channels and combined:



Signal is confirmed!!!

# Higgs mass

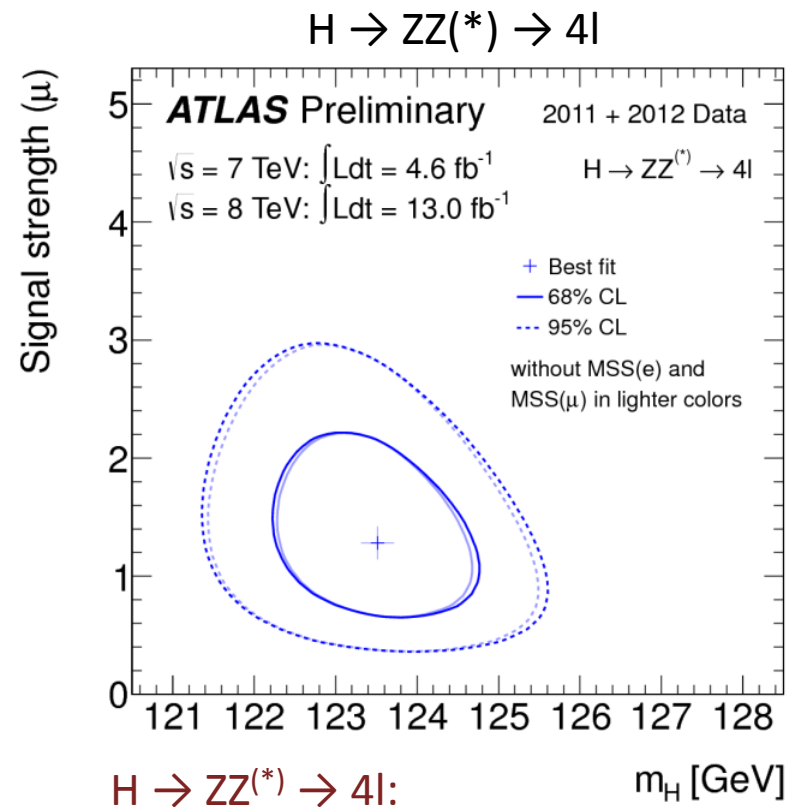
$H \rightarrow \gamma\gamma$  and  $H \rightarrow ZZ^{(*)} \rightarrow 4l$  best-fit values of  $m_H$  and  $\mu$ , and the corresponding 1-2  $\sigma$  contours:



$H \rightarrow \gamma\gamma$ :

Signal strength  $\hat{\mu} = 1.8 \pm 0.3(stat) {}^{+0.29}_{-0.21}(syst)$

Mass  $m_H = 126.6 \pm 0.3(stat) \pm 0.7(syst) \text{ GeV}c^{-2}$

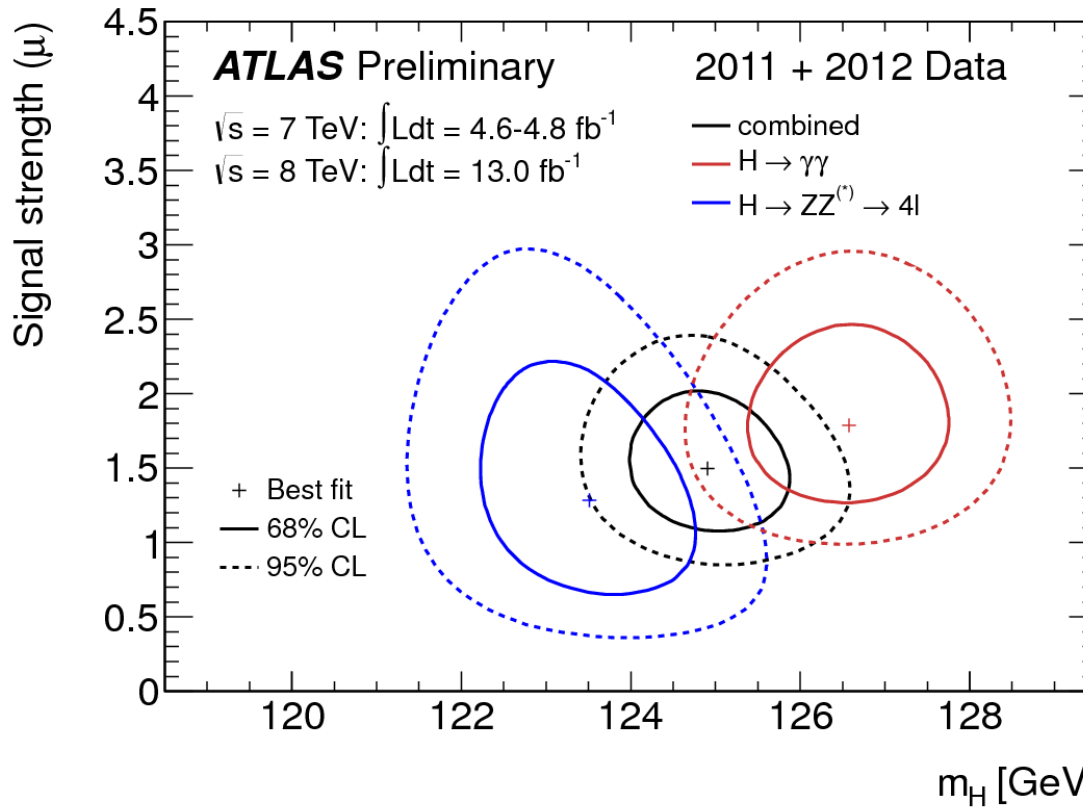


$H \rightarrow ZZ^{(*)} \rightarrow 4l$ :  $m_H$  [GeV]

Signal strength  $\hat{\mu} = 1.3 \pm 0.4$

Mass  $m_H = 123.5 \pm 0.9(stat) {}^{+0.4}_{-0.2} \text{ GeV}c^{-2}$

# Higgs mass



Combined mass measurement is:  $m_H = 125.2 \pm 0.3(stat) \pm 0.6(syst) \text{ GeV} c^{-2}$

Combined signal strength:  $\hat{\mu} = 1.5^{+0.33}_{-0.29}$

Taking all systematics into account the two masses, the compatibility of the two masses is estimated to be at the  $2.7\sigma$  level (A more conservative treatment of scale systematics (rectangular PDFs) leads to a compatibility of  $2.3\sigma$ ).

# Higgs couplings

The framework makes the following assumptions:

- Only modifications of couplings strengths, i.e. of absolute values of couplings, are taken into account: the observed state is assumed to be a CP-even scalar as in the SM.
- The signals observed in the different search channels originate from a single narrow resonance;
- The width of the Higgs boson with a mass of 126 GeV is assumed to be negligible.

Strategy:

Choose a model: More accurate with higher order corrections and external constraints;

Test small deviations from the SM predictions.

$$(\sigma \cdot \text{BR}) (ii \rightarrow H \rightarrow ff) = \frac{\sigma_{ii} \cdot \Gamma_{ff}}{\Gamma_H}$$

*Following prescriptions of LHC Higgs Cross-section Light Mass Subgroup.*

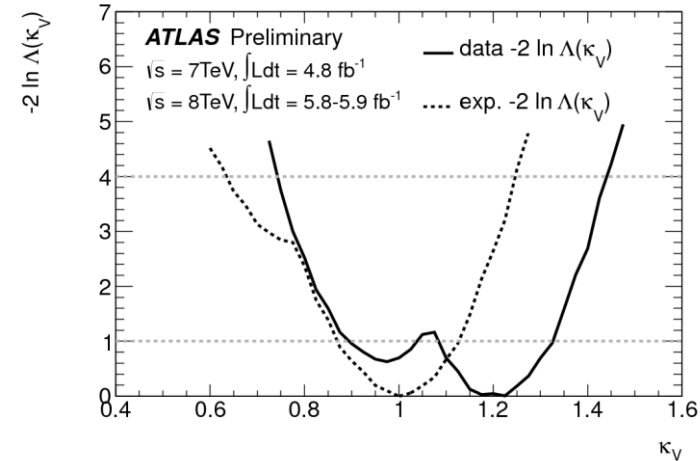
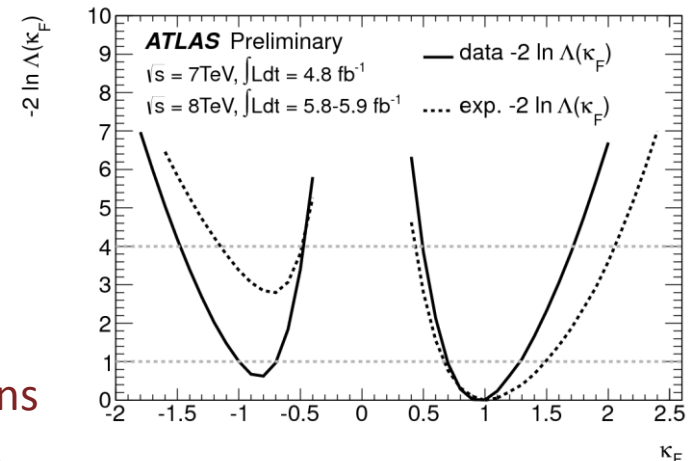
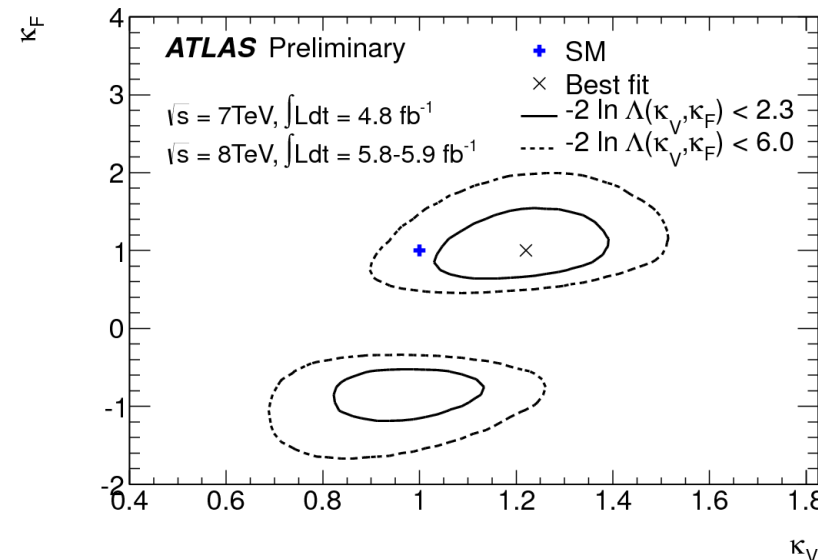
# Higgs couplings

Benchmark model  $\kappa_V - \kappa_F$ .

Some sensitivity to the relative sign of  $\kappa_F$   
gained from the negative interference  
between W and fermion-loop in  $H \rightarrow \gamma\gamma$  decay.

$\kappa_F = \kappa_t = \kappa_b = \kappa_\tau$  Scale factor for all fermions

$\kappa_V = \kappa_W = \kappa_Z$  Scale factor for all vectors



$${\kappa_i}^2 = \frac{\Gamma_{ii}}{\Gamma_{ii}^{SM}}$$

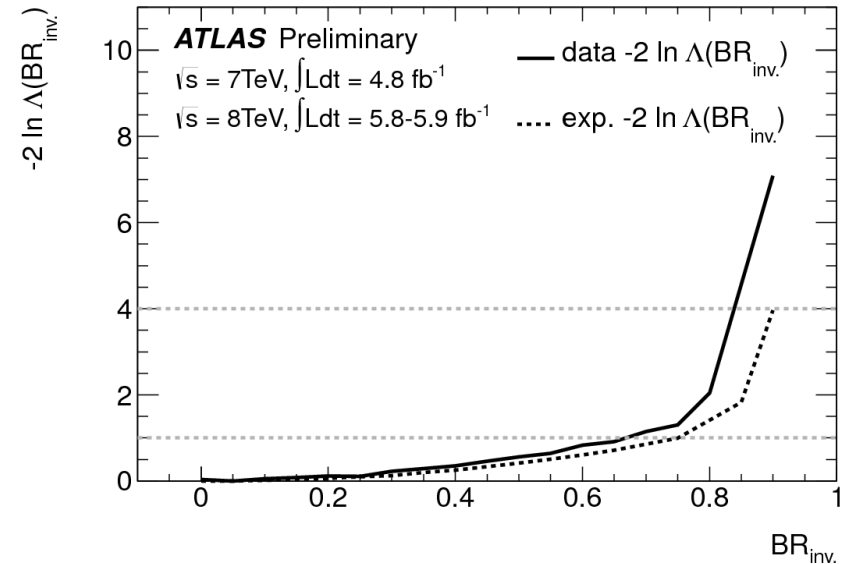
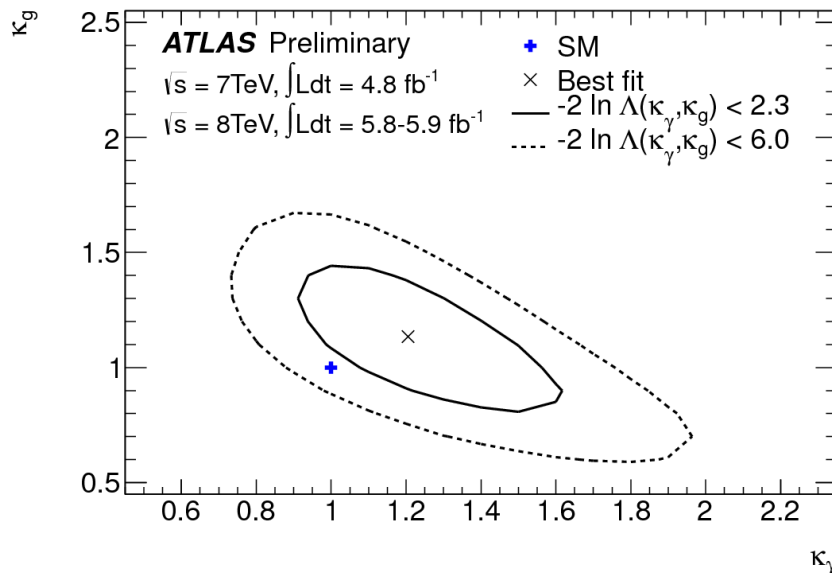
# Higgs couplings

Benchmark model  $k_g$ - $k_\gamma$ .

The potential new particles contributing to the  $H \rightarrow \gamma\gamma$  and  $gg \rightarrow H$  loops, may or may not contribute to the total width of the observed state from direct invisible decays.

$$\kappa_g^2(\kappa_b, \kappa_t, m_H) = \frac{|\kappa_b A_b(m_H) + \kappa_t A_t(m_H)|^2}{|A_b(m_H) + A_t(m_H)|^2} \quad gg \rightarrow H \text{ loop}$$

$$\kappa_\gamma^2(\kappa_b, \kappa_t, \kappa_W, m_H) = \frac{|\kappa_b A'_b(m_H) + \kappa_t A'_t(m_H) + \kappa_W A'_W(m_H)|^2}{|A'_b(m_H) + A'_t(m_H) + A'_W(m_H)|^2} \quad H \rightarrow \gamma\gamma \text{ loop}$$



# Higgs couplings

---

Simplified benchmark models were used to study the correlations of production and decay modes in different final states, and compare them to the predictions for the SM Higgs boson:

- ✓ Couplings to Fermions and Vector Gauge Bosons ( $k_V - k_F$ ,  $k_g - k_\gamma$ ,  $k_{VV} - \lambda_{FV}$ );
- ✓ Probing the custodial symmetry of the W and Z coupling ( $\lambda_{WZ}$ ,  $k_{ZZ}$ ,  $\lambda_{FZ}$ );
- ✓ Probing the up- and down-type fermion symmetry ( $\lambda_{du}$ ,  $k_{uu}$ ,  $\lambda_{vu}$ );
- ✓ Probing the quark and lepton symmetry ( $\lambda_{Vq}$ ,  $k_{qq}$ ,  $\lambda_{lq}$ ).

Within the current statistical uncertainties and assumptions, no significant deviations from the Standard Model couplings are observed.

# Higgs $J^P$ : $H \rightarrow ZZ^{(*)} \rightarrow 4l$

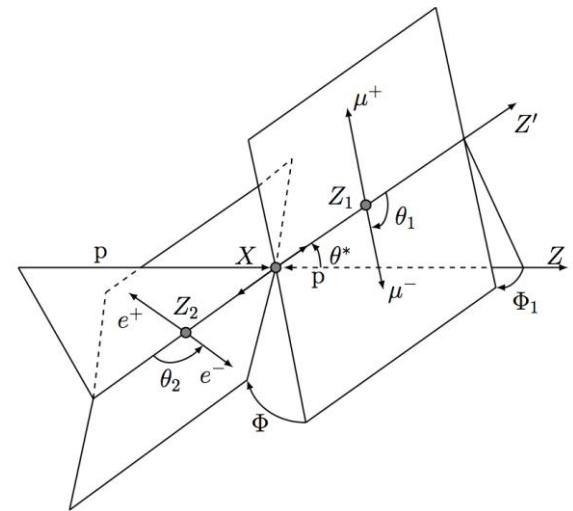
Final state allows measuring  $J^P$ :

- 5 angles ( production, decay );
- $m_{12}, m_{34}$ ;

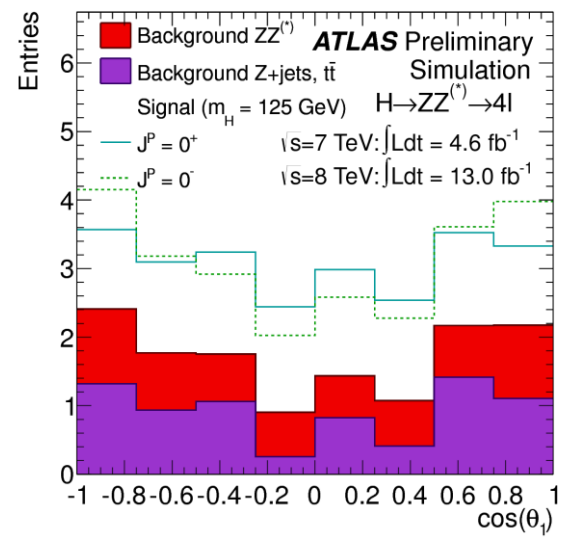
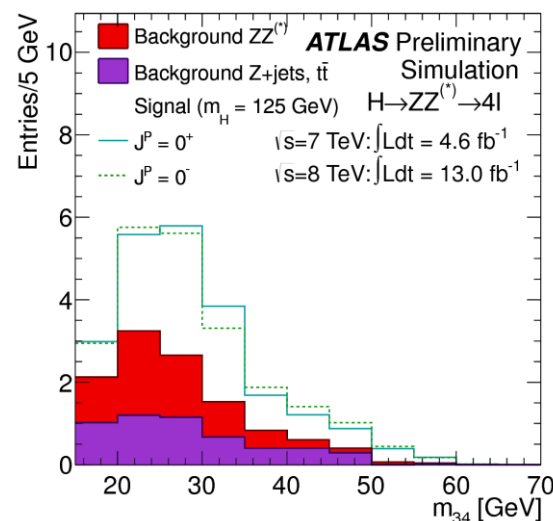
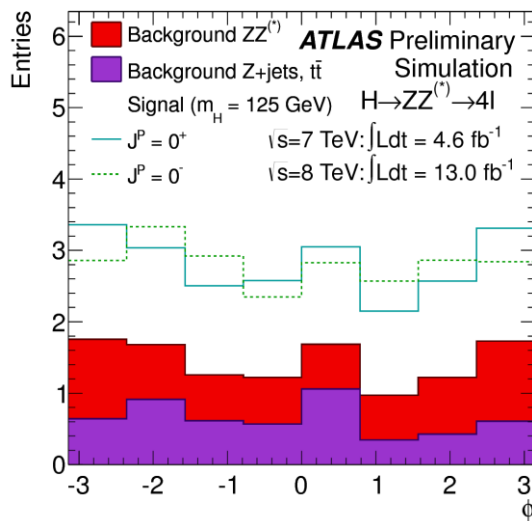
Discriminate  $0^+$  (SM) hypothesis against:  $0^-$ ,  $2^+_m$  (graviton-like tensor with minimal couplings)  $2^-$  (pseudo-tensor).

Two Multi-Variate discriminants used:

- Boosted Decision Tree (BDT);
- Matrix-Element-Likelihood-Analysis ( $J^P$ -MELA).



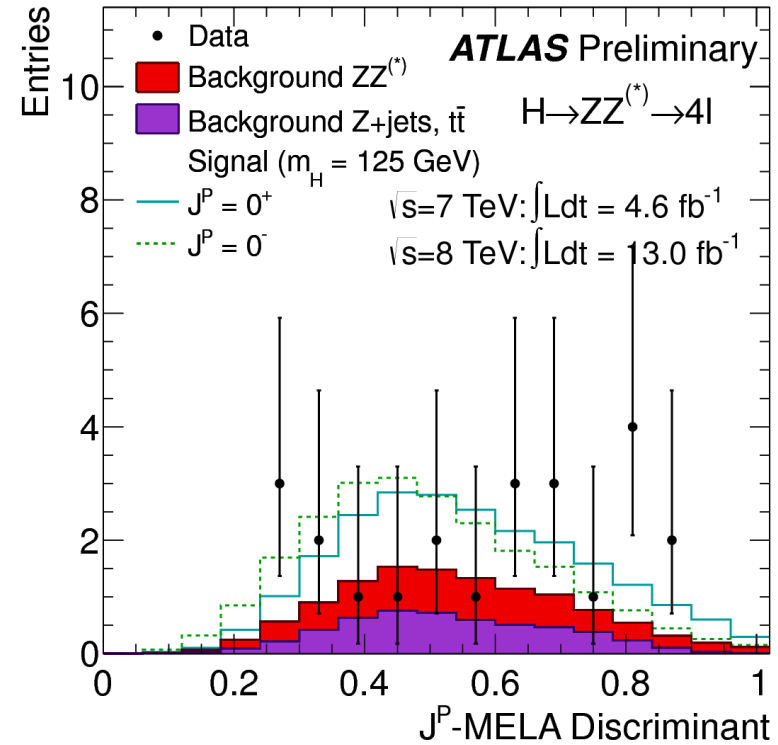
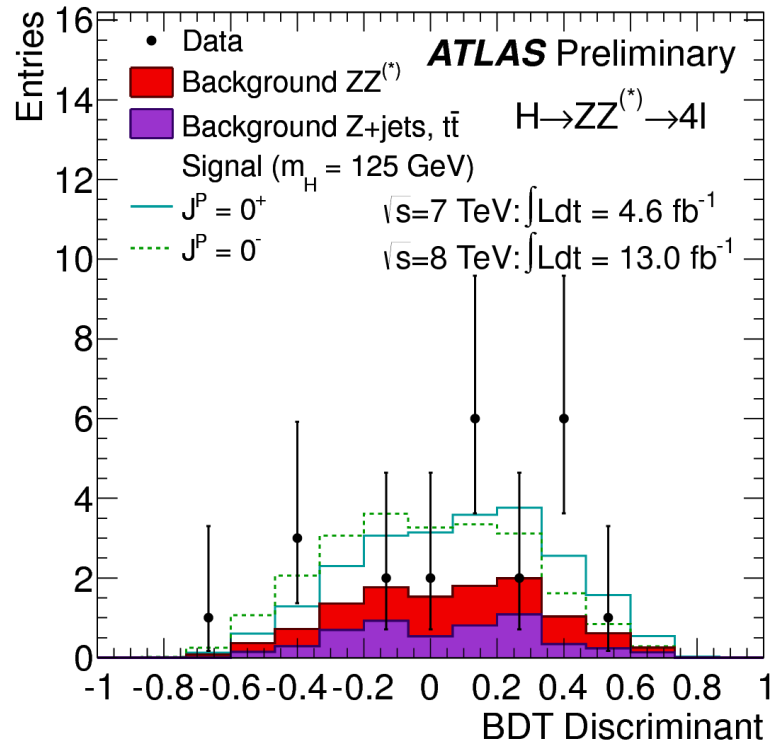
Expected distributions for  $0^+$  and  $0^-$  hypothesis of  $\phi$ ,  $\cos \theta_1$  and  $m_{34}$  for the combined  $\sqrt{s} = 8$  TeV and  $\sqrt{s} = 7$  TeV luminosity:



# Higgs $J^P$ : $H \rightarrow ZZ^{(*)} \rightarrow 4l$

ATLAS-CONF-2012-169

Distributions of the BDT and  $J^P$ -MELA discriminants for data and Monte Carlo expectations for the combined  $\sqrt{s} = 8$  TeV and  $\sqrt{s} = 7$  TeV data sets:

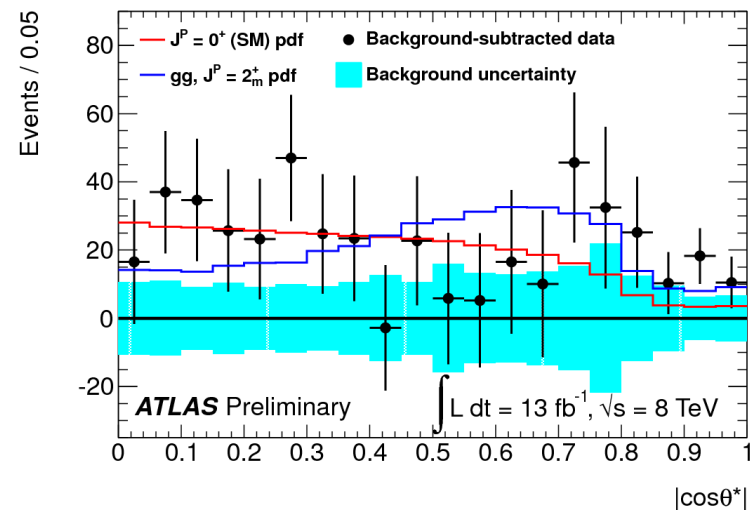
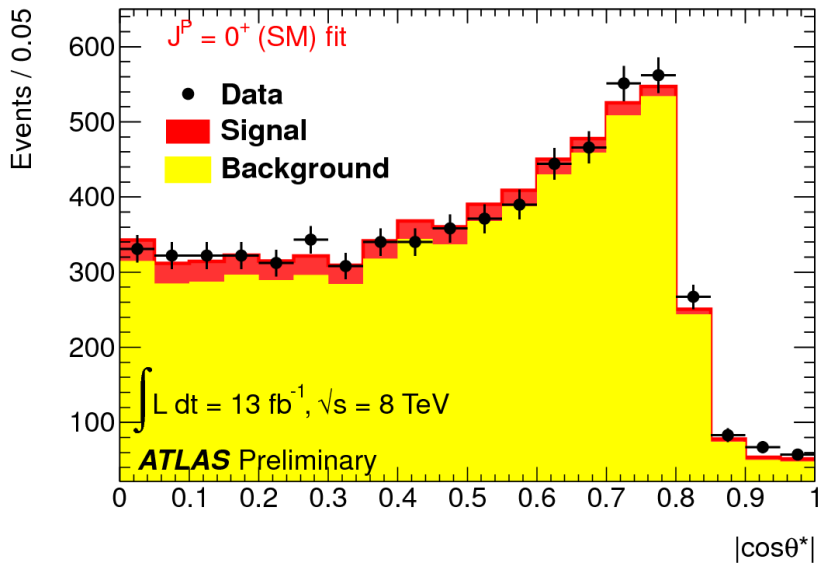
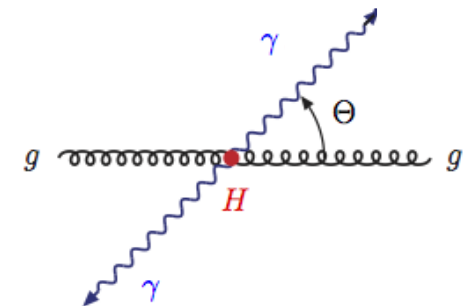


$0^+$  vs  $0^-$ :  $2.3 \sigma$  ( $2.7 \sigma$ ) observed ( $1.7 \sigma$ ,  $1.9 \sigma$  expected);  
 $0^+$  vs  $2^+$ : excluded @ 85% CL.

# Higgs $J^P$ : $H \rightarrow \gamma\gamma$

ATLAS-CONF-2012-168

Sensitive variable is di-photon  $\cos \theta^*$  distribution:



Expected sensitivity: exclusion of the spin  $2^+$  hypothesis @ the 97% CL;  
 Observed exclusion of spin  $2^+$  hypothesis @the 91% CL.

# Conclusions

---

- ✓ Excellent performance of LHC and of the ATLAS detector allowed to strengthen the observation of the new boson;
- ✓ The discovery is fully confirmed on all the most sensitive channel;
- ✓ First measurements of its coupling properties and its mass;
- ✓ All properties measured until now are consistent with a SM Higgs;
- ✓ The analyses are now moving from searches to measurement: more results to come using the full set of  $\sim 21 \text{ fb}^{-1}$  collected in 2012.

# References

---

Higgs to gamma gamma:

arXiv:1207.7214 [hep-ex], ATLAS-CONF-2012-168

Higgs to four leptons:

arXiv:1207.7214 [hep-ex], ATLAS-CONF-2012-169

Higgs to WW:

arXiv:1207.7214 [hep-ex], ATLAS-CONF-2012-158

Higgs to tautau:

ATLAS-CONF-2012-160

Higgs to bb

ATLAS-CONF-2012-161

Higgs properties:

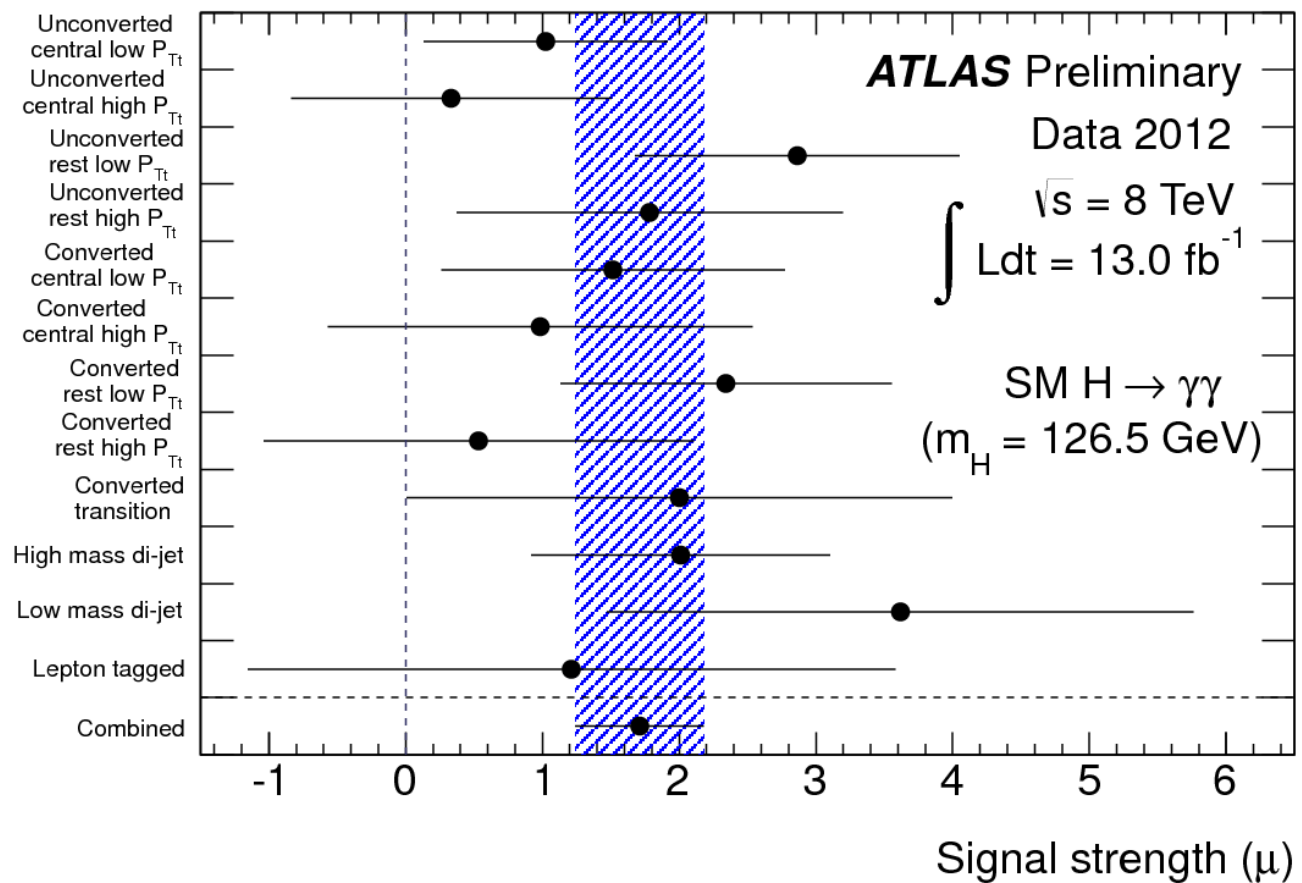
arXiv:1207.7214 [hep-ex], ATLAS-CONF-2012-168, ATLAS-CONF-2012-127, ATLAS-CONF-2012-169, ATLAS-CONF-2012-170, arXiv:1209.0040 [hep-ph]



Table 1: Number of events in the data ( $N_D$ ) and expected number of expected signal events ( $N_S$ ) for  $m_H = 126.5$  GeV from the  $H \rightarrow \gamma\gamma$  analysis, for each category in the mass range 100-160 GeV, based on SM predictions. The mass resolution Full Width at Half Maximum (FWHM) is also given. Numbers for the 7 TeV analysis can be found in Ref. [7]. The statistical uncertainties on  $N_S$  and FWHM are less than 1%. The breakdown of expected signal events in the  $gg \rightarrow H$ , VBF, WH, ZH, ttH processes is detailed. For more details, see the text.

$\sqrt{s}$	8 TeV							
Category	$N_D$	$N_S$	$gg \rightarrow H$ [%]	VBF [%]	WH [%]	ZH [%]	$ttH$ [%]	FWHM [GeV]
Unconv. central, low $p_{Tt}$	6797	32	93	4.2	1.4	0.9	0.2	3.45
Unconv. central, high $p_{Tt}$	319	4.7	76	15.2	3.9	2.9	1.7	3.22
Unconv. rest, low $p_{Tt}$	26802	69	93	4.2	1.7	1.1	0.2	3.75
Unconv. rest, high $p_{Tt}$	1538	9.7	76	15.1	4.5	3.3	1.2	3.59
Conv. central, low $p_{Tt}$	4480	21	93	4.2	1.4	0.9	0.2	3.86
Conv. central, high $p_{Tt}$	199	3.1	77	14.5	4.1	2.8	1.7	3.51
Conv. rest, low $p_{Tt}$	24107	60	93	4.1	1.7	1.1	0.2	4.32
Conv. rest, high $p_{Tt}$	1324	8.3	75	15.1	4.9	3.4	1.3	4.00
Conv. transition	10891	28	90	5.6	2.3	1.5	0.3	5.57
High Mass two-jet	345	7.6	31	68.2	0.3	0.2	0.1	3.65
Low Mass two-jet	477	4.7	60	5.1	20.7	12.1	1.6	3.45
One-lepton	151	2.0	3.2	0.4	62.5	15.8	18.0	3.85
All categories (inclusive)	77430	249	88	7.4	2.8	1.6	0.5	3.87

Best fit value for the signal strength in the different categories and combined:



The  $p_{Tt}$  of the diphoton system is defined as the transverse component of the diphoton momentum, when projected on the axis given by the difference of the photon momenta

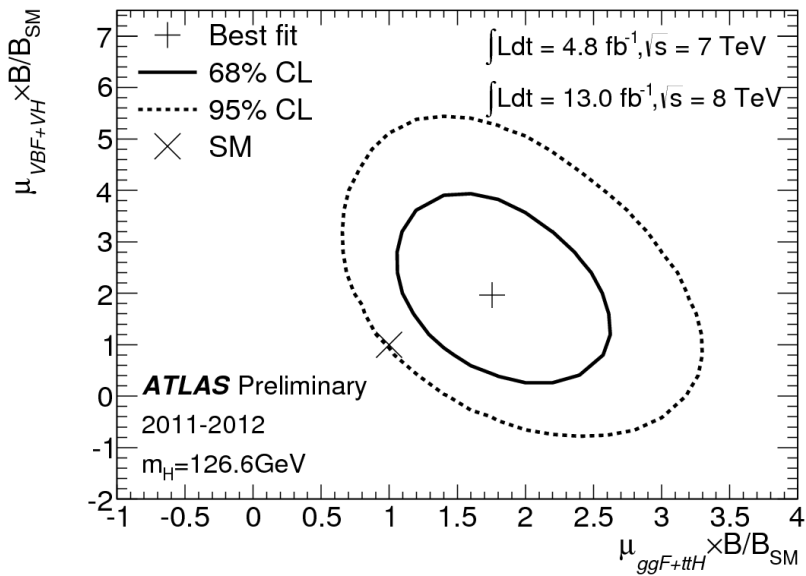
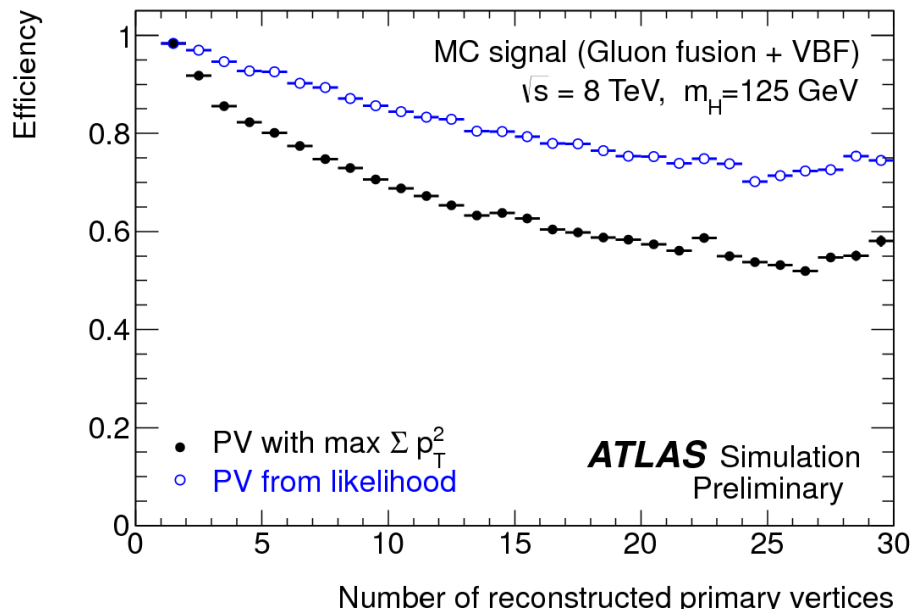
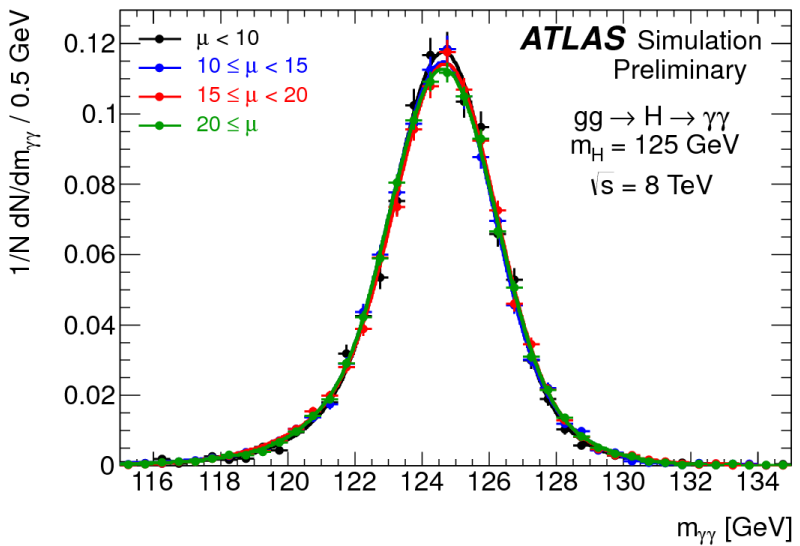
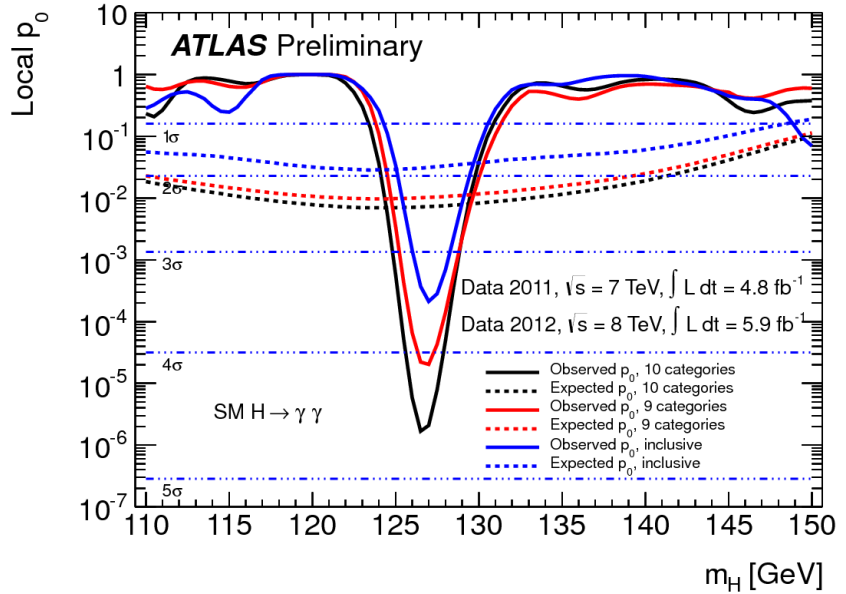
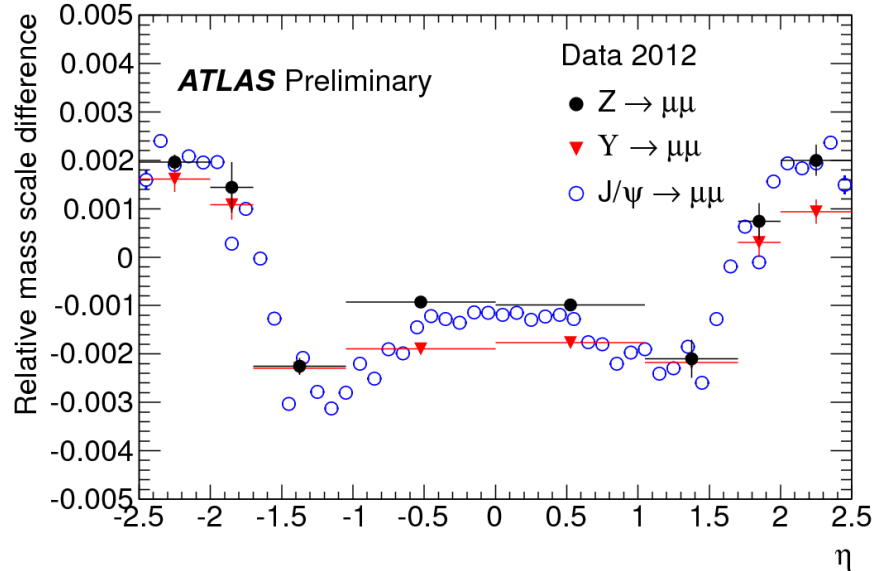
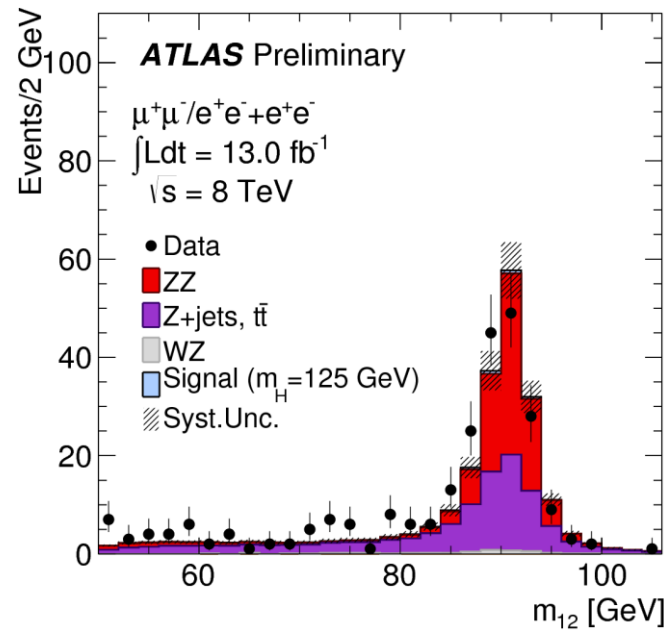
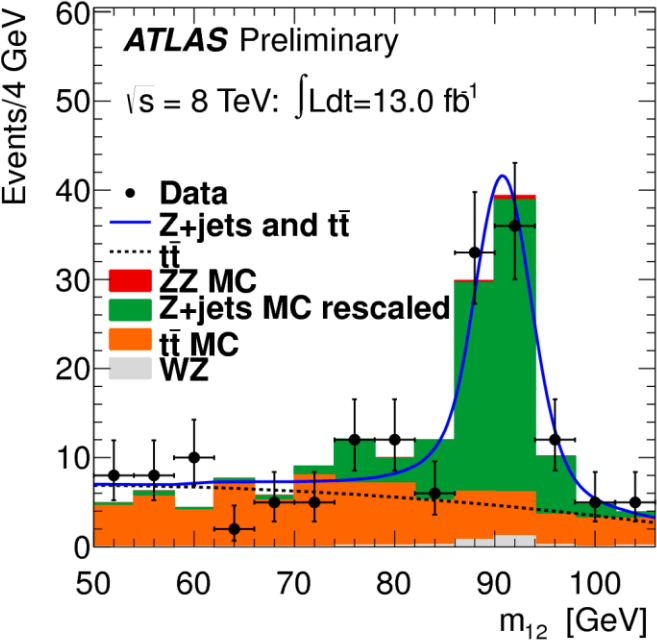
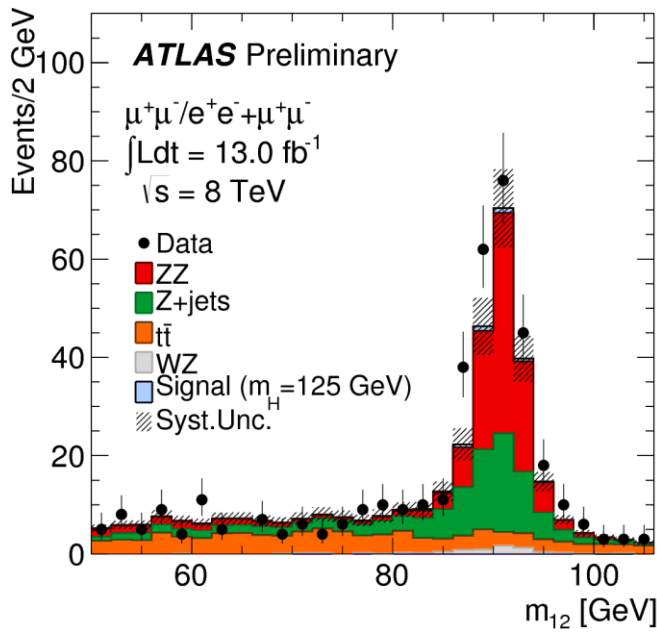
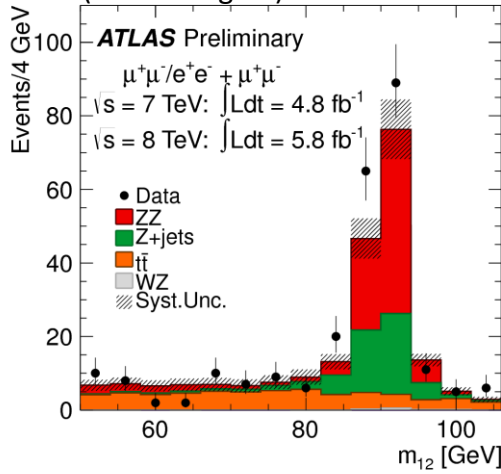


Table 6: The numbers of expected signal and background events together with the number of observed events, in a window of  $\pm 5$  GeV around 125 GeV for  $13.0 \text{ fb}^{-1}$  at  $\sqrt{s} = 8 \text{ TeV}$  and  $4.6 \text{ fb}^{-1}$  at  $\sqrt{s} = 7 \text{ TeV}$  as well as for their combination.

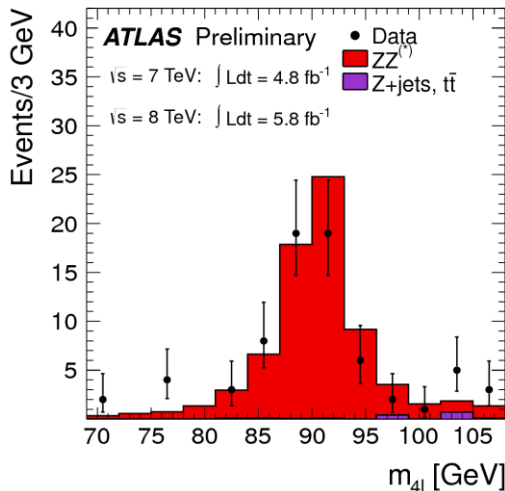
$\sqrt{s} = 8 \text{ TeV}$				
	Signal ( $m_H=125 \text{ GeV}$ )	$ZZ^{(*)}$	$Z + \text{jets}, t\bar{t}$	Observed
$4\mu$	$3.1 \pm 0.4$	$1.55 \pm 0.07$	$0.31 \pm 0.09$	6
$2\mu 2e$	$1.4 \pm 0.2$	$0.56 \pm 0.04$	$0.78 \pm 0.16$	1
$2e 2\mu$	$1.9 \pm 0.3$	$0.80 \pm 0.04$	$0.26 \pm 0.07$	3
$4e$	$1.5 \pm 0.2$	$0.77 \pm 0.08$	$1.20 \pm 0.19$	4
total	$7.9 \pm 1.1$	$3.7 \pm 0.2$	$2.6 \pm 0.3$	14
$\sqrt{s} = 7 \text{ TeV}$				
$4\mu$	$0.88 \pm 0.11$	$0.48 \pm 0.02$	$0.05 \pm 0.02$	2
$2\mu 2e$	$0.32 \pm 0.05$	$0.14 \pm 0.01$	$0.43 \pm 0.09$	1
$2e 2\mu$	$0.48 \pm 0.06$	$0.22 \pm 0.01$	$0.04 \pm 0.02$	1
$4e$	$0.28 \pm 0.04$	$0.17 \pm 0.02$	$0.52 \pm 0.13$	0
total	$2.0 \pm 0.3$	$1.0 \pm 0.1$	$1.0 \pm 0.2$	4
$\sqrt{s} = 8 \text{ TeV} \text{ and } \sqrt{s} = 7 \text{ TeV}$				
$4\mu$	$4.0 \pm 0.5$	$2.03 \pm 0.09$	$0.36 \pm 0.09$	8
$2\mu 2e$	$1.7 \pm 0.2$	$0.70 \pm 0.05$	$1.21 \pm 0.18$	2
$2e 2\mu$	$2.4 \pm 0.3$	$1.02 \pm 0.05$	$0.30 \pm 0.07$	4
$4e$	$1.8 \pm 0.3$	$0.94 \pm 0.09$	$1.72 \pm 0.23$	4
total	$9.9 \pm 1.3$	$4.7 \pm 0.3$	$3.6 \pm 0.3$	18



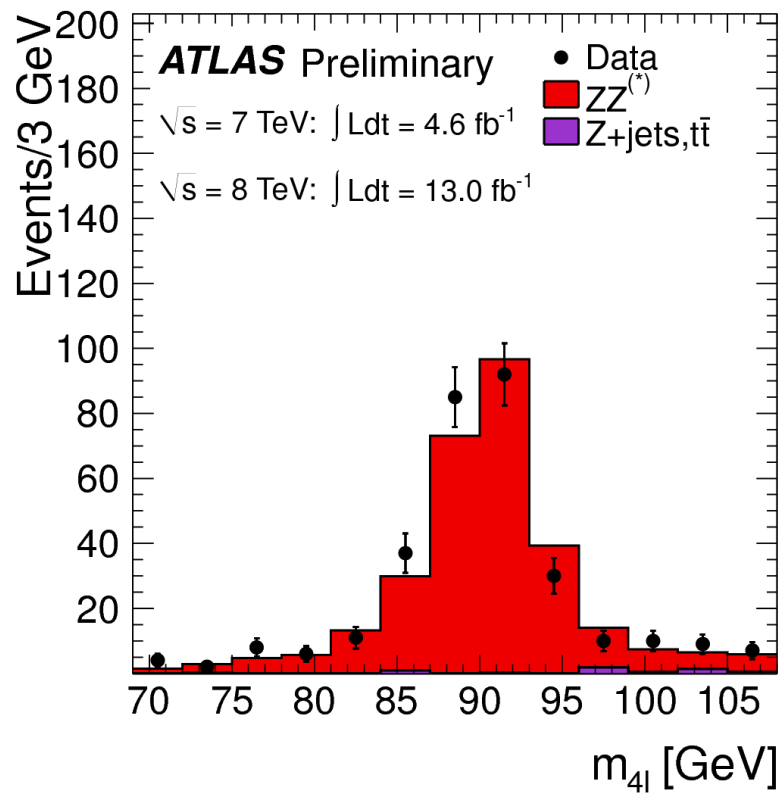
$m_{12}$  distribution for the combined  $\sqrt{s} = 7$  TeV and  $\sqrt{s} = 8$  TeV data (control region):

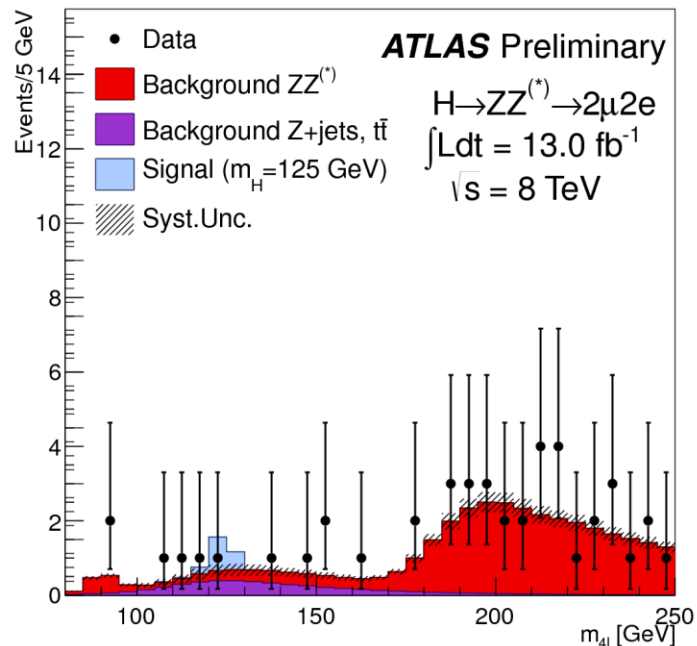
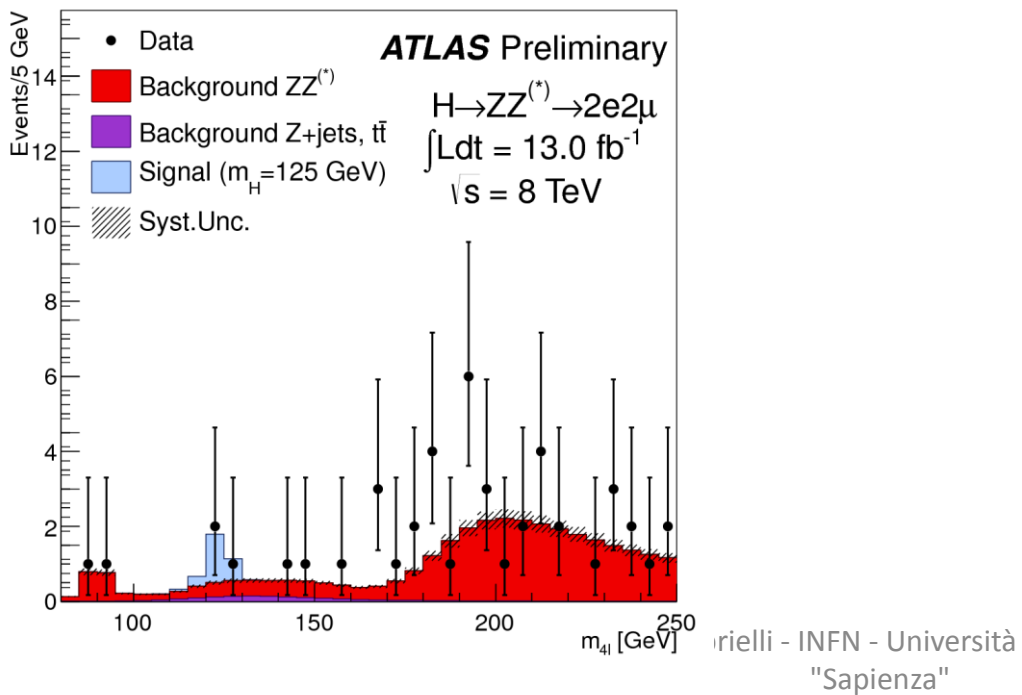
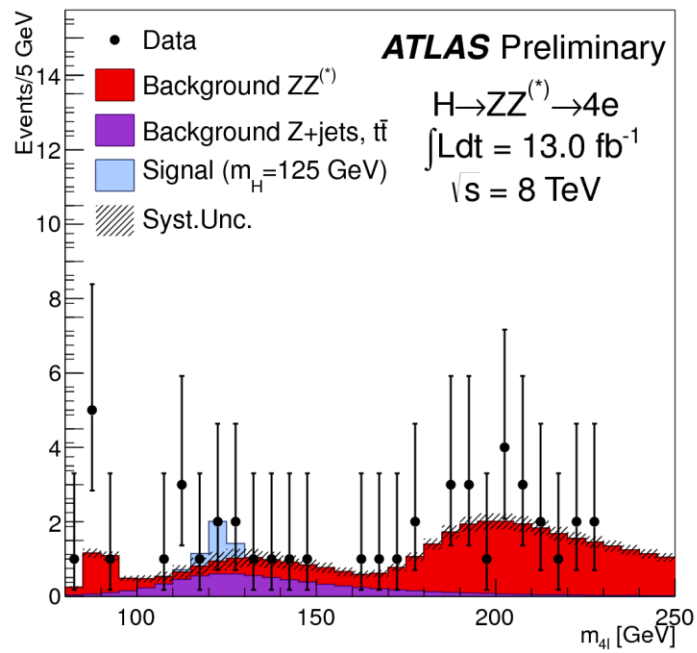
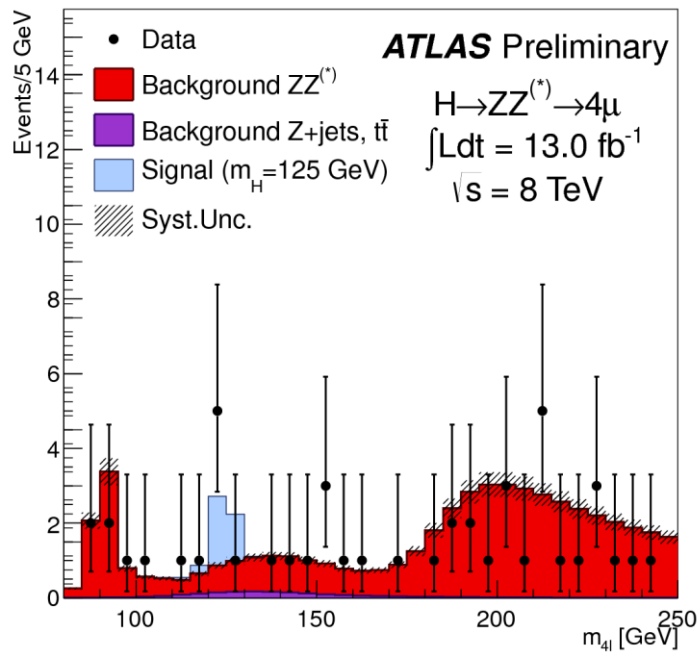


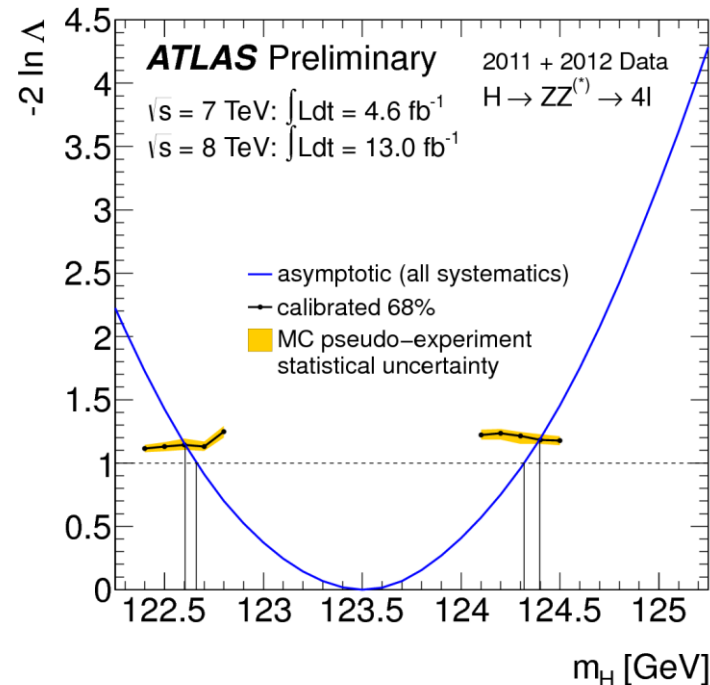
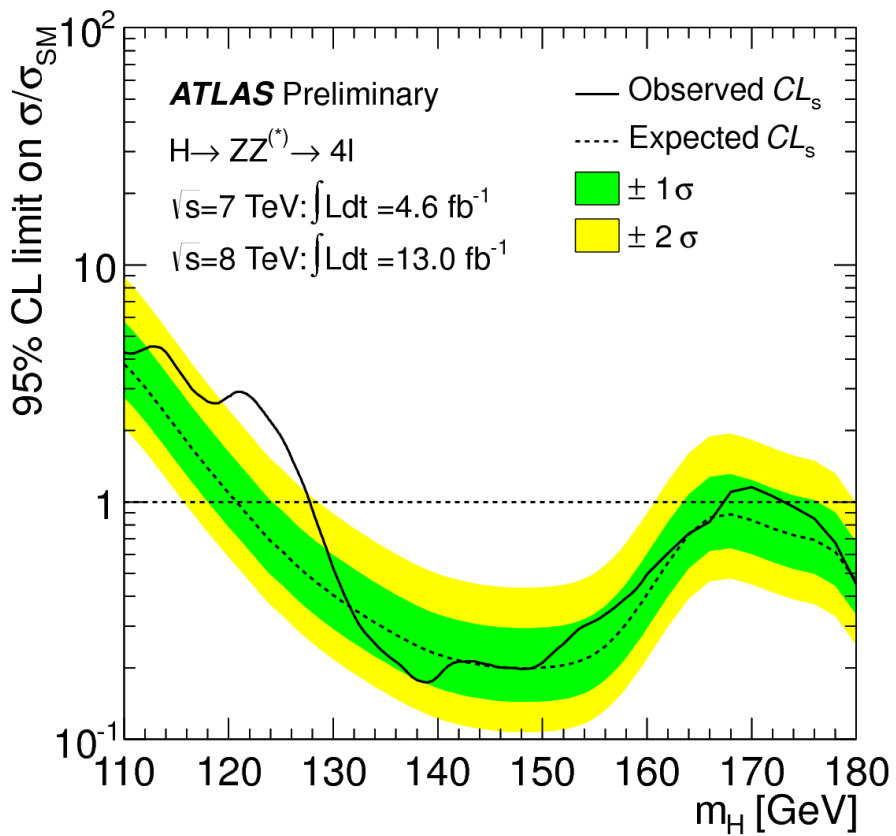
$m_{4l}$  distribution at Z peak for the combined  $\sqrt{s} = 7$  TeV and  $\sqrt{s} = 8$  TeV data (loose selection):

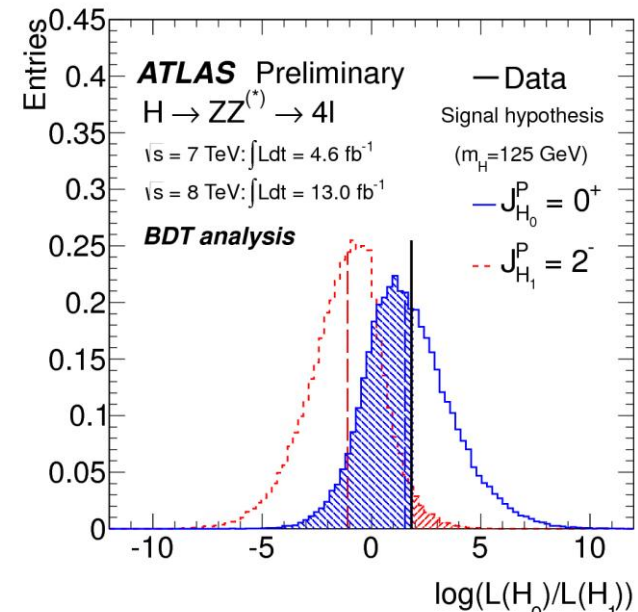
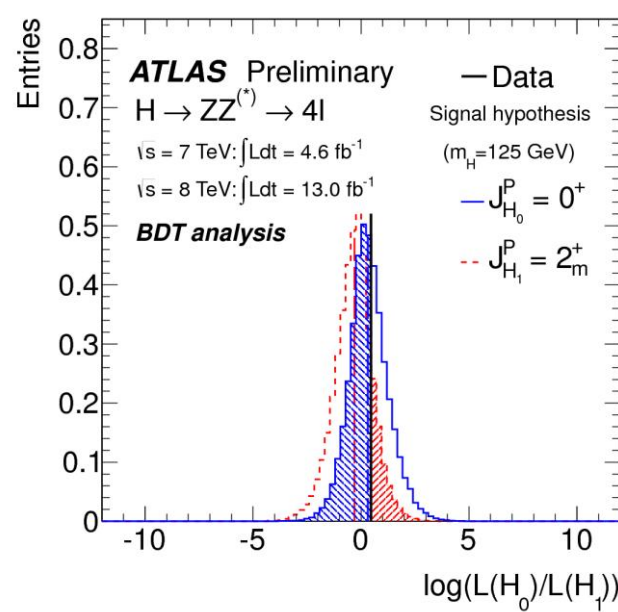
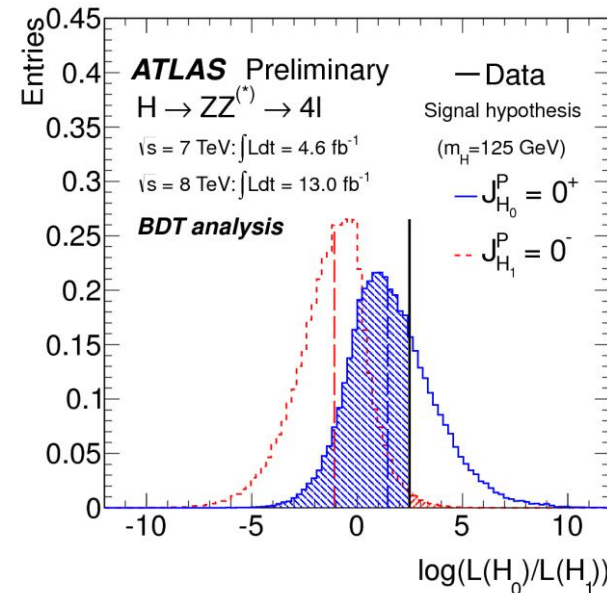


$m_{4l}$  distribution at Z peak for the combined  $\sqrt{s} = 7$  TeV and  $\sqrt{s} = 8$  TeV data (loose selection):







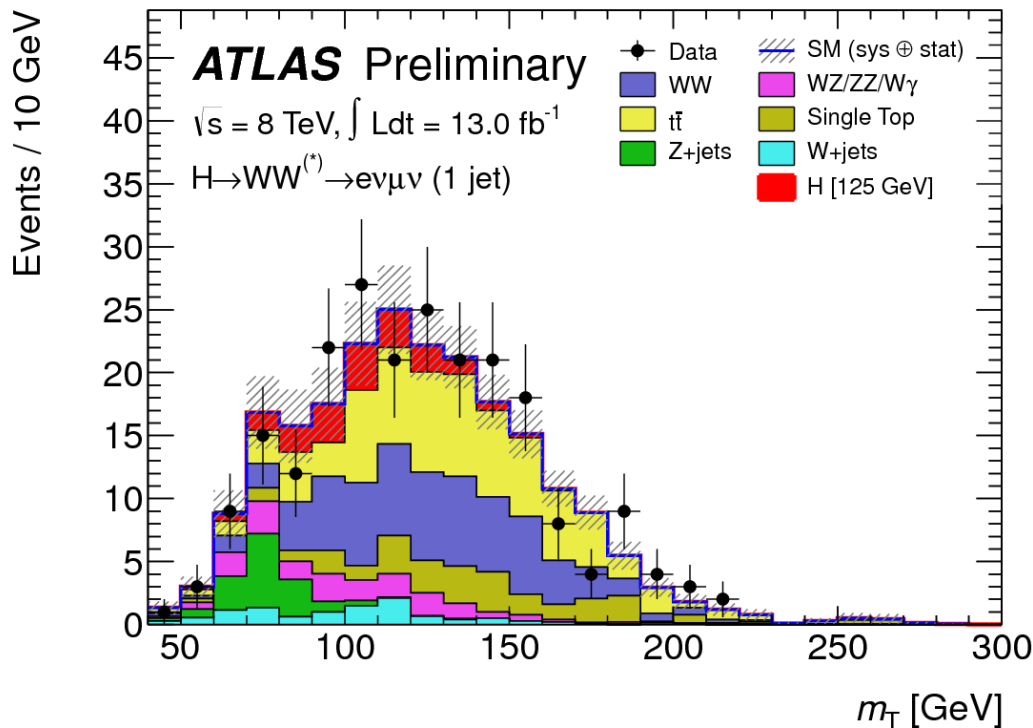
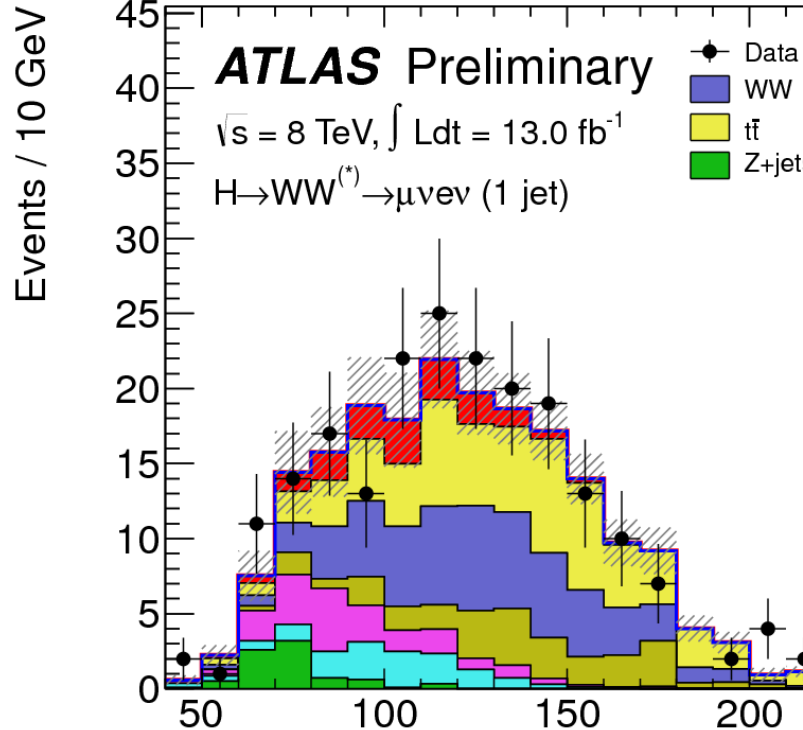


### Tested $J^P$ hypotheses for an assumed $0^+$

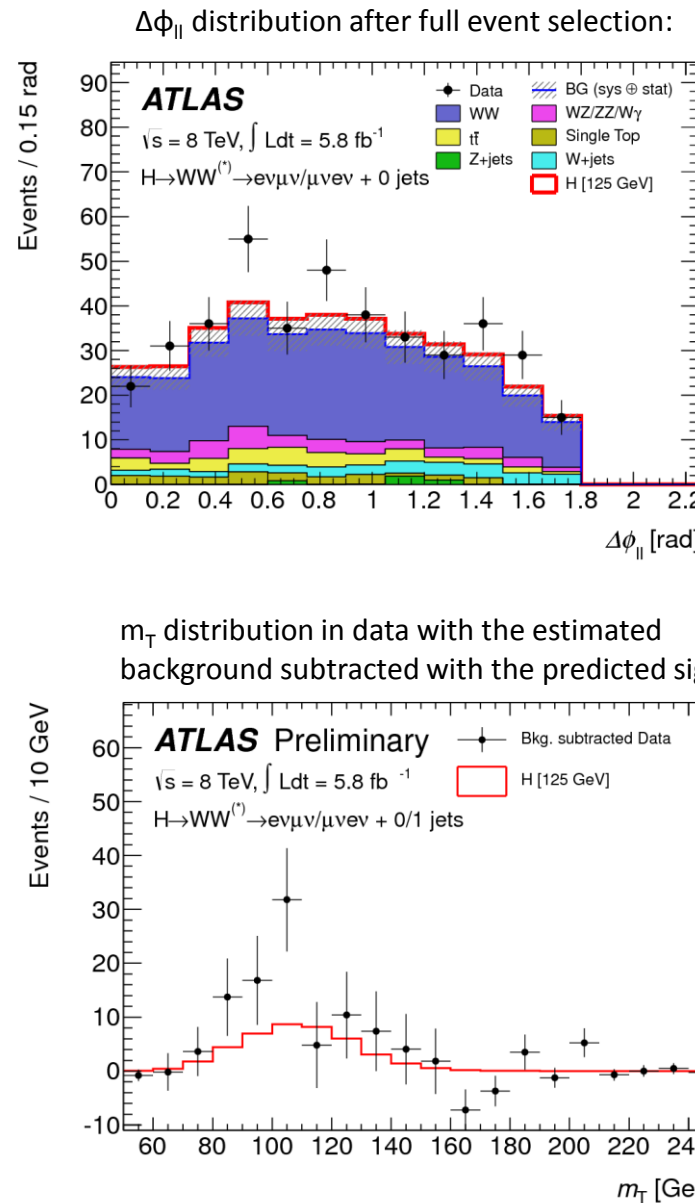
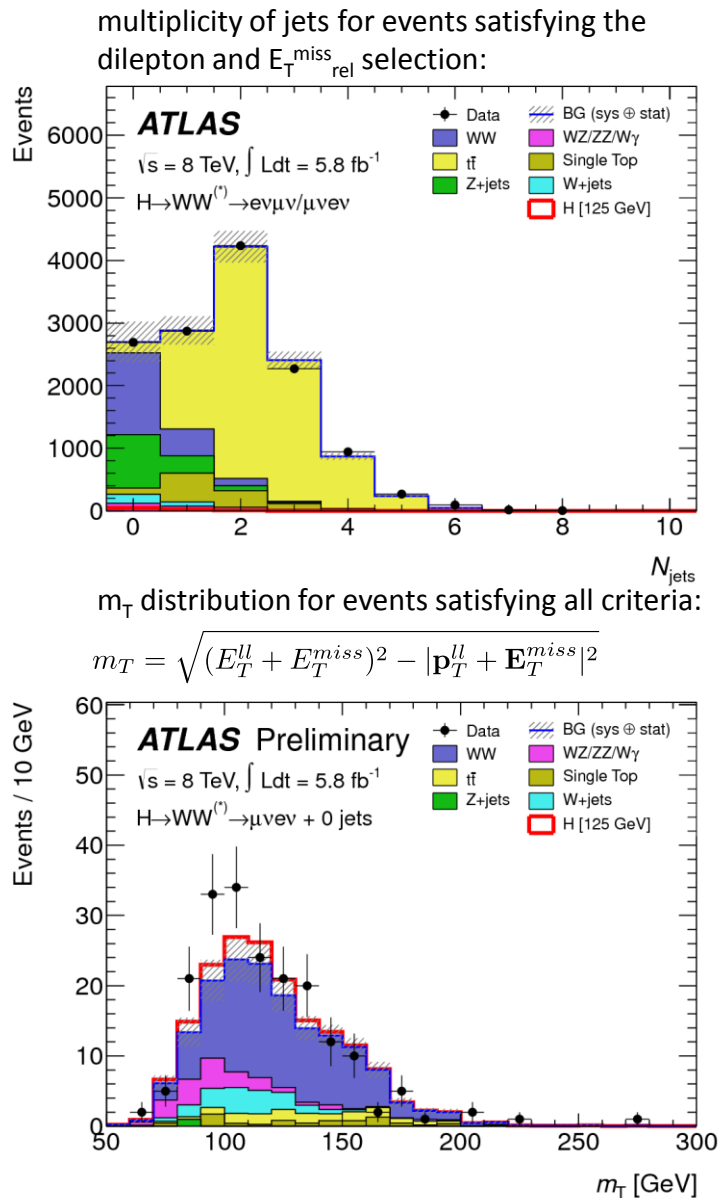
	$0^-$			$2_m^+$			$2^-$		
	expected	observed	obs $0^+$	expected	observed	obs $0^+$	expected	observed	obs $0^+$
<b>BDT analysis</b>									
$p_0$ -value	0.041	0.011	0.69	0.20	0.16	0.57	0.046	0.029	0.56
$\sigma$	1.7	2.3	-0.50	0.84	0.99	-0.18	1.7	1.9	-0.15
<b><math>J^P</math>-MELA analysis</b>									
$p_0$ -value	0.031	0.0028	0.76	0.18	0.17	0.53	0.04	0.025	0.56
$\sigma$	1.9	2.7	-0.72	0.91	0.97	-0.08	1.7	2.0	-0.15

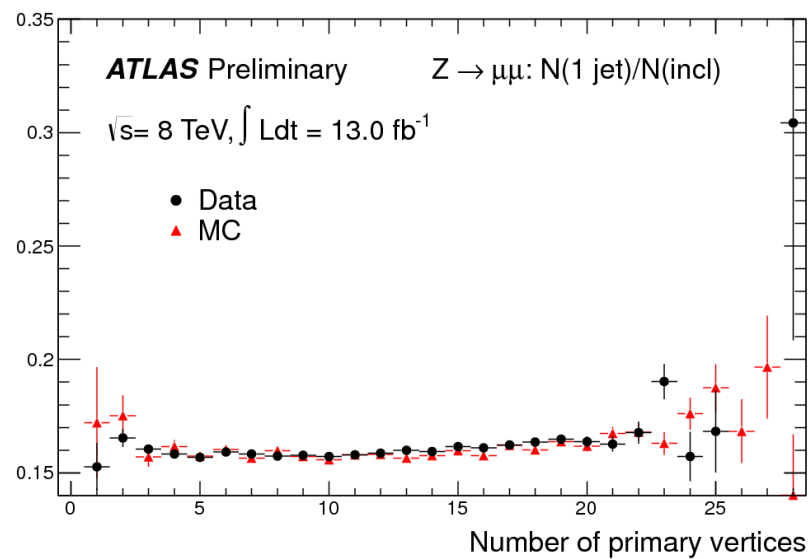
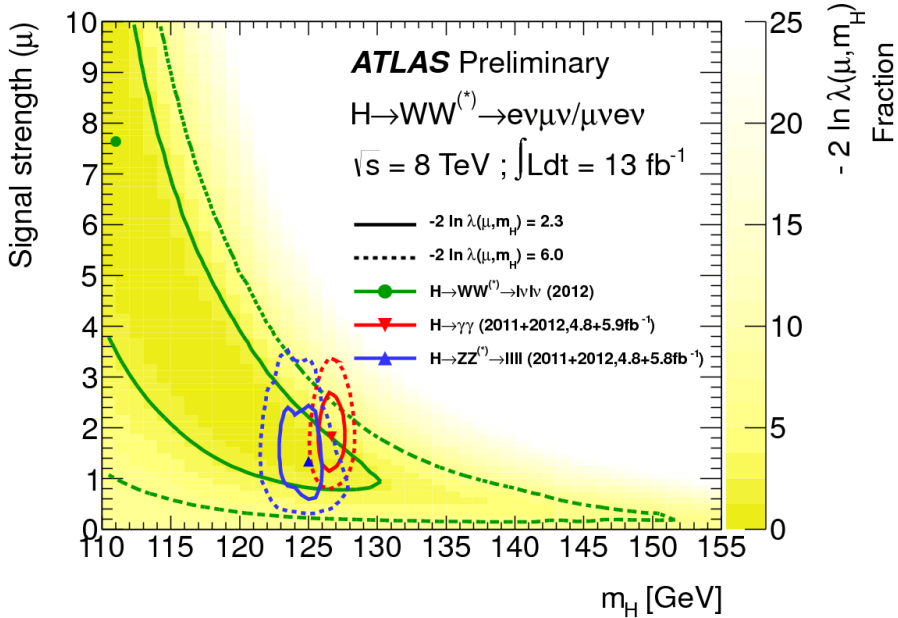
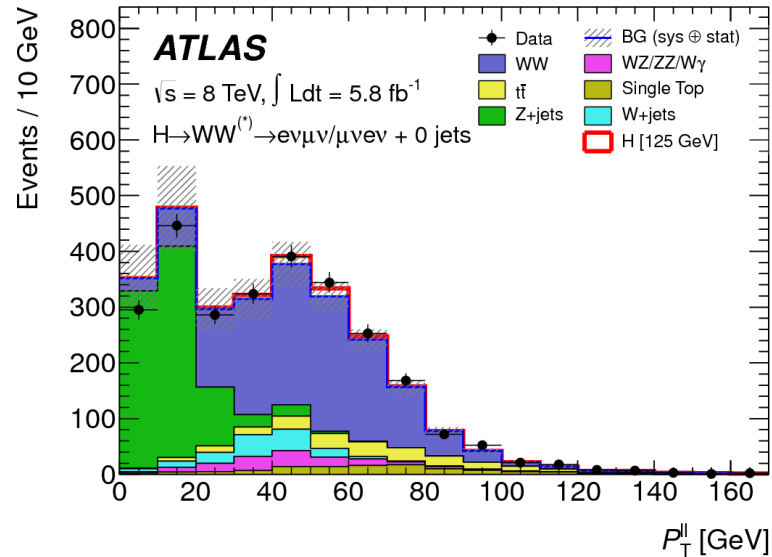
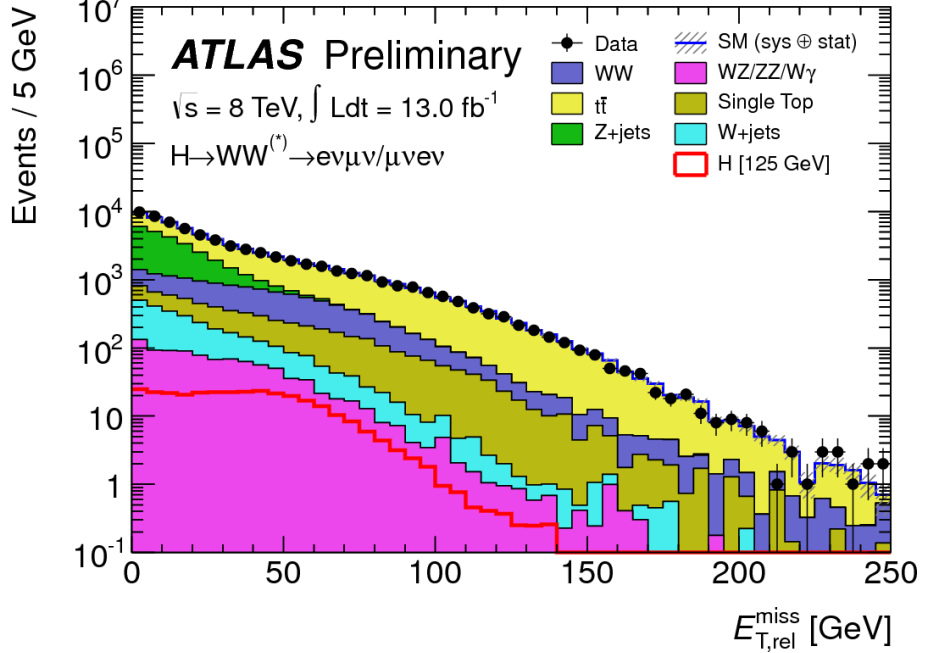
Table 4: The expected numbers of signal and background events after the requirements listed in the first column, as well as the observed numbers of events, are shown for the different signal regions (upper table) and the main control regions (middle table). The signal is shown for  $m_H = 125$  GeV. The  $W + \text{jets}$  background is estimated entirely from data, whereas MC predictions normalised to data in control regions are used for the  $WW$ ,  $t\bar{t}$ ,  $tW/tb/tqb$  and  $Z/\gamma^* \rightarrow \tau\tau$  processes in all the stages of the selection. Contributions from other diboson background sources are taken entirely from MC predictions. For the middle table, the  $W + \text{jets}$  contribution is also estimated entirely from data, however no normalisation factors are applied, except that the top normalisation factor is applied for the top background estimate in the  $WW$  control regions. The lower table lists the numbers of expected and observed events after the  $\Delta\phi_{\ell\ell}$  cut, for both 0-jet and 1-jet events and separately depending on the flavour of the leading lepton. Only statistical uncertainties associated with the numbers of events in the MC samples are shown.

Cutflow evolution in the different signal regions									
$H + 0\text{-jet}$	Signal	$WW$	$WZ/ZZ/W\gamma$	$t\bar{t}$	$tW/tb/tqb$	$Z/\gamma^* + \text{jets}$	$W + \text{jets}$	Total Bkg.	Obs.
Jet veto	$110 \pm 1$	$3004 \pm 12$	$242 \pm 8$	$387 \pm 8$	$215 \pm 8$	$1575 \pm 20$	$340 \pm 5$	$5762 \pm 28$	5960
$\Delta\phi_{\ell\ell, E_T^{\text{miss}}} > \pi/2$	$108 \pm 1$	$2941 \pm 12$	$232 \pm 8$	$361 \pm 8$	$206 \pm 8$	$1201 \pm 21$	$305 \pm 5$	$5246 \pm 28$	5230
$p_{T,\ell\ell} > 30$ GeV	$99 \pm 1$	$2442 \pm 11$	$188 \pm 7$	$330 \pm 7$	$193 \pm 8$	$57 \pm 8$	$222 \pm 3$	$3433 \pm 19$	3630
$m_{\ell\ell} < 50$ GeV	$78.6 \pm 0.8$	$579 \pm 5$	$69 \pm 4$	$55 \pm 3$	$34 \pm 3$	$11 \pm 4$	$65 \pm 2$	$814 \pm 9$	947
$\Delta\phi_{\ell\ell} < 1.8$	$75.6 \pm 0.8$	$555 \pm 5$	$68 \pm 4$	$54 \pm 3$	$34 \pm 3$	$8 \pm 4$	$56 \pm 2$	$774 \pm 9$	917
$H + 1\text{-jet}$	Signal	$WW$	$WZ/ZZ/W\gamma$	$t\bar{t}$	$tW/tb/tqb$	$Z/\gamma^* + \text{jets}$	$W + \text{jets}$	Total Bkg.	Obs.
One jet	$59.5 \pm 0.8$	$850 \pm 5$	$158 \pm 7$	$3451 \pm 24$	$1037 \pm 17$	$505 \pm 9$	$155 \pm 5$	$6155 \pm 33$	6264
$b$ -jet veto	$50.4 \pm 0.7$	$728 \pm 5$	$128 \pm 5$	$862 \pm 13$	$283 \pm 10$	$429 \pm 8$	$126 \pm 4$	$2555 \pm 20$	2655
$Z \rightarrow \tau\tau$ veto	$50.1 \pm 0.7$	$708 \pm 5$	$122 \pm 5$	$823 \pm 12$	$268 \pm 9$	$368 \pm 8$	$122 \pm 4$	$2411 \pm 19$	2511
$m_{\ell\ell} < 50$ GeV	$37.7 \pm 0.6$	$130 \pm 2$	$39 \pm 2$	$142 \pm 5$	$55 \pm 4$	$99 \pm 3$	$30 \pm 2$	$495 \pm 8$	548
$\Delta\phi_{\ell\ell} < 1.8$	$34.9 \pm 0.6$	$118 \pm 2$	$35 \pm 2$	$134 \pm 5$	$52 \pm 4$	$22 \pm 2$	$24 \pm 1$	$386 \pm 8$	433



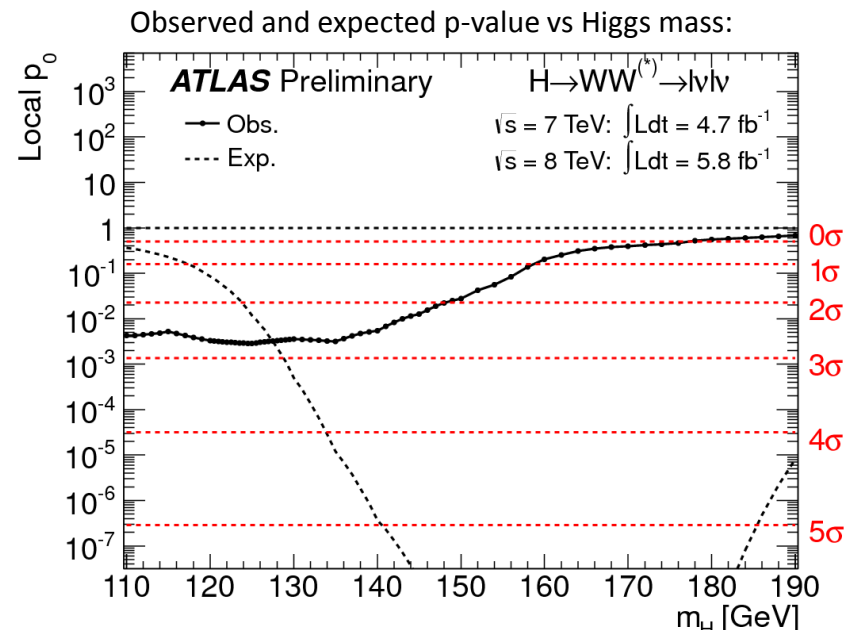
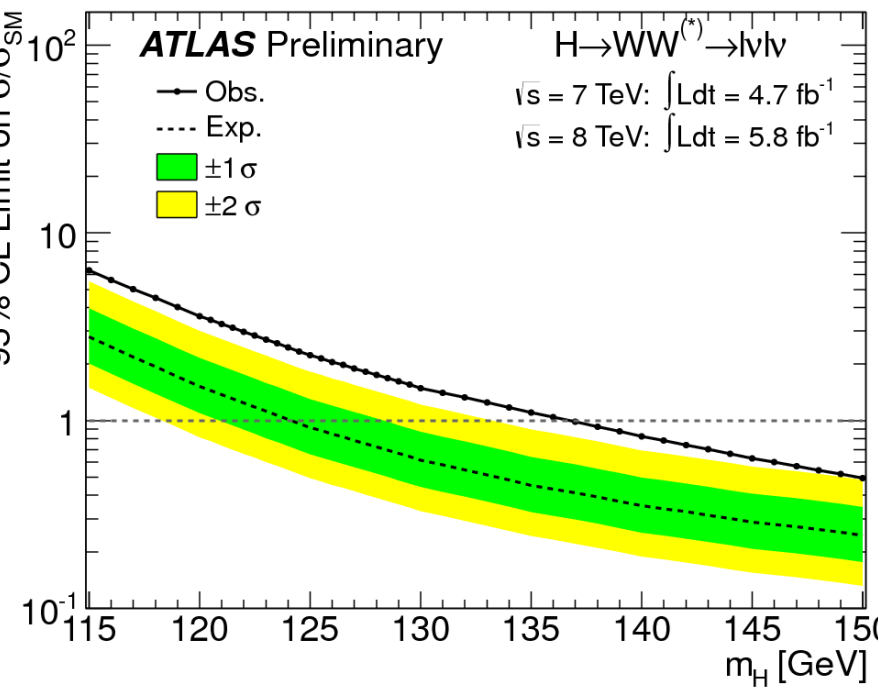
# $H \rightarrow WW^{(*)} \rightarrow l\nu l\nu$





# $H \rightarrow WW^{(*)} \rightarrow l\nu l\nu$

Observed and expected CLs limit on the normalized signal strength vs Higgs mass:



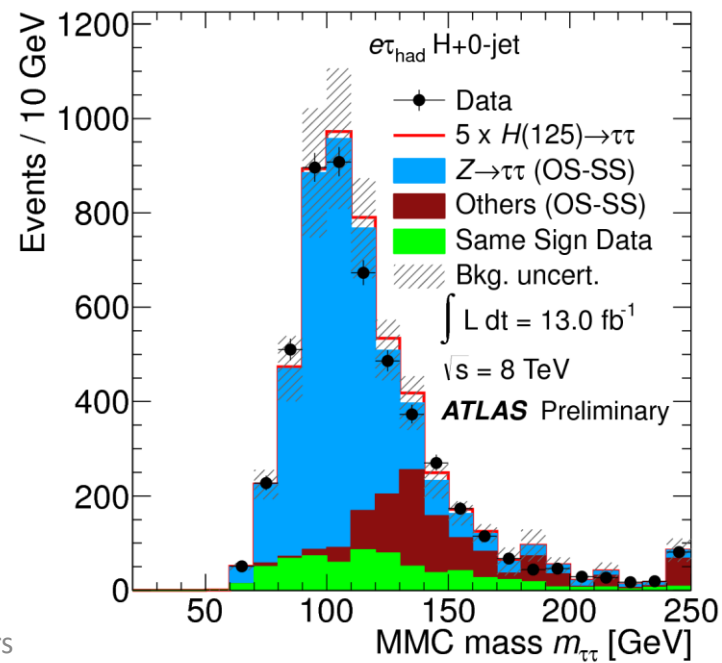
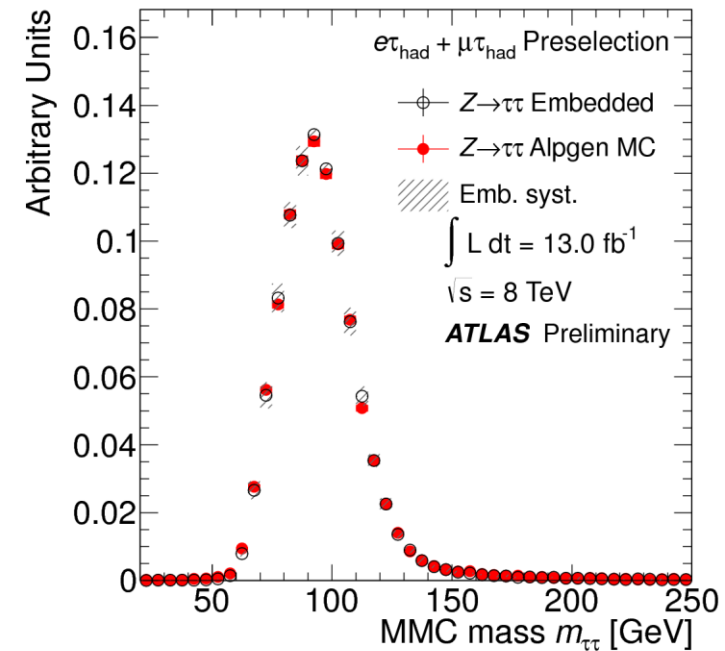
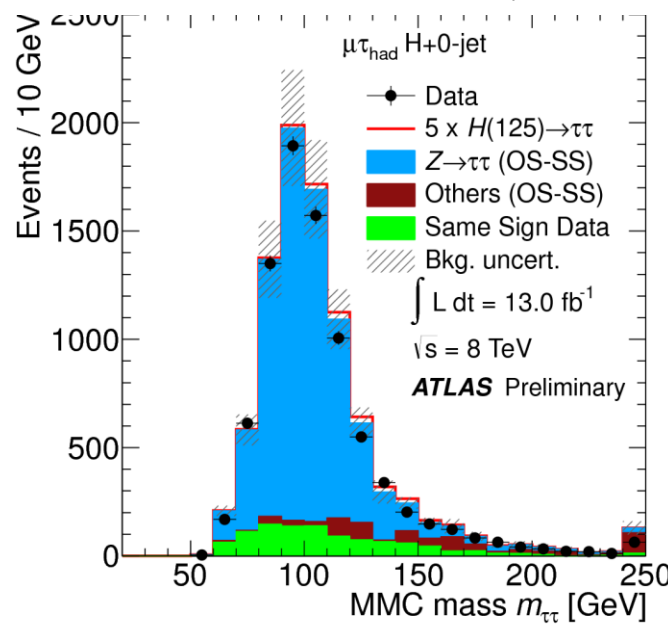
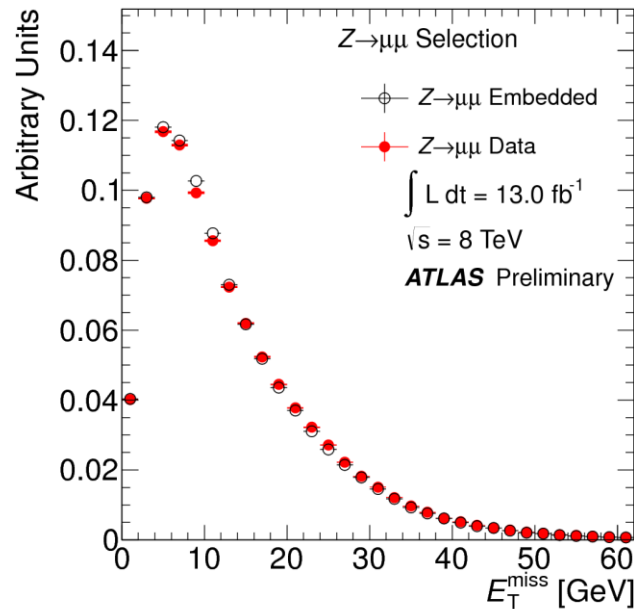
## Higgs to WW (July 2012):

- The SM Higgs boson is excluded at 95% CL: 137-261  $\text{GeV c}^{-2}$  (exp 124-233  $\text{GeV c}^{-2}$ );
- Observed  $p_0 \sim 2.8$  standard deviation (exp 2.3) @  $m_H = 125 \text{ GeV c}^{-2}$ ;
- Signal strength  $\mu = 1.3 \pm 0.5$ .

Table 3: Event requirements applied in the different categories of the  $H \rightarrow \tau_{\text{lep}}\tau_{\text{had}}$  analysis. Requirements marked with a triangle ( $\triangleright$ ) are categorization requirements, meaning that if an event fails that requirement it is still considered for the remaining categories. Requirements marked with a bullet ( $\bullet$ ) are only applied to events passing all categorization requirements in a category; events failing such requirements are discarded.

7 TeV		8 TeV	
VBF Category	Boosted Category	VBF Category	Boosted Category
$\triangleright p_T^{\tau_{\text{had-vis}}} > 30 \text{ GeV}$	—	$\triangleright p_T^{\tau_{\text{had-vis}}} > 30 \text{ GeV}$	$\triangleright p_T^{\tau_{\text{had-vis}}} > 30 \text{ GeV}$
$\triangleright E_T^{\text{miss}} > 20 \text{ GeV}$	$\triangleright E_T^{\text{miss}} > 20 \text{ GeV}$	$\triangleright E_T^{\text{miss}} > 20 \text{ GeV}$	$\triangleright E_T^{\text{miss}} > 20 \text{ GeV}$
$\triangleright \geq 2 \text{ jets}$	$\triangleright p_T^H > 100 \text{ GeV}$	$\triangleright \geq 2 \text{ jets}$	$\triangleright p_T^H > 100 \text{ GeV}$
$\triangleright p_T^{j1}, p_T^{j2} > 40 \text{ GeV}$	$\triangleright 0 < x_1 < 1$	$\triangleright p_T^{j1} > 40, p_T^{j2} > 30 \text{ GeV}$	$\triangleright 0 < x_1 < 1$
$\triangleright \Delta\eta_{jj} > 3.0$	$\triangleright 0.2 < x_2 < 1.2$	$\triangleright \Delta\eta_{jj} > 3.0$	$\triangleright 0.2 < x_2 < 1.2$
$\triangleright m_{jj} > 500 \text{ GeV}$	$\triangleright \text{Fails VBF}$	$\triangleright m_{jj} > 500 \text{ GeV}$	$\triangleright \text{Fails VBF}$
$\triangleright \text{centrality req.}$	—	$\triangleright \text{centrality req.}$	—
$\triangleright \eta_{j1} \times \eta_{j2} < 0$	—	$\triangleright \eta_{j1} \times \eta_{j2} < 0$	—
$\triangleright p_T^{\text{Total}} < 40 \text{ GeV}$	—	$\triangleright p_T^{\text{Total}} < 30 \text{ GeV}$	—
—	—	$\triangleright p_T^\ell > 26 \text{ GeV}$	—
$\bullet m_T < 50 \text{ GeV}$	$\bullet m_T < 50 \text{ GeV}$	$\bullet m_T < 50 \text{ GeV}$	$\bullet m_T < 50 \text{ GeV}$
$\bullet \Delta(\Delta R) < 0.8$	$\bullet \Delta(\Delta R) < 0.8$	$\bullet \Delta(\Delta R) < 0.8$	$\bullet \Delta(\Delta R) < 0.8$
$\bullet \sum \Delta\phi < 3.5$	$\bullet \sum \Delta\phi < 1.6$	$\bullet \sum \Delta\phi < 2.8$	—
—	—	$\bullet b\text{-tagged jet veto}$	$\bullet b\text{-tagged jet veto}$
1 Jet Category	0 Jet Category	1 Jet Category	0 Jet Category
$\triangleright \geq 1 \text{ jet}, p_T > 25 \text{ GeV}$	$\triangleright 0 \text{ jets } p_T > 25 \text{ GeV}$	$\triangleright \geq 1 \text{ jet}, p_T > 30 \text{ GeV}$	$\triangleright 0 \text{ jets } p_T > 30 \text{ GeV}$
$\triangleright E_T^{\text{miss}} > 20 \text{ GeV}$	$\triangleright E_T^{\text{miss}} > 20 \text{ GeV}$	$\triangleright E_T^{\text{miss}} > 20 \text{ GeV}$	$\triangleright E_T^{\text{miss}} > 20 \text{ GeV}$
$\triangleright \text{Fails VBF, Boosted}$	$\triangleright \text{Fails Boosted}$	$\triangleright \text{Fails VBF, Boosted}$	$\triangleright \text{Fails Boosted}$
$\bullet m_T < 50 \text{ GeV}$	$\bullet m_T < 30 \text{ GeV}$	$\bullet m_T < 50 \text{ GeV}$	$\bullet m_T < 30 \text{ GeV}$
$\bullet \Delta(\Delta R) < 0.6$	$\bullet \Delta(\Delta R) < 0.5$	$\bullet \Delta(\Delta R) < 0.6$	$\bullet \Delta(\Delta R) < 0.5$
$\bullet \sum \Delta\phi < 3.5$	$\bullet \sum \Delta\phi < 3.5$	$\bullet \sum \Delta\phi < 3.5$	$\bullet \sum \Delta\phi < 3.5$
—	$\bullet p_T^\ell - p_T^\tau < 0$	—	$\bullet p_T^\ell - p_T^\tau < 0$

$E_T^{\text{miss}}$  distributions for the  $Z \rightarrow \mu\mu$  data before and after muon embedding:



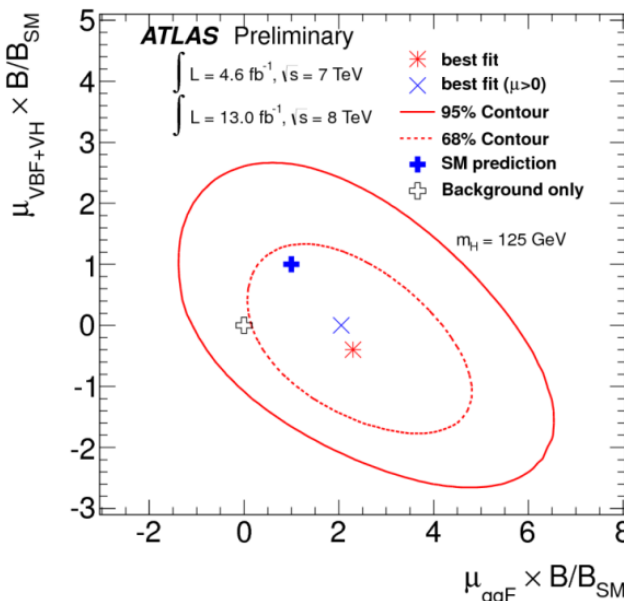
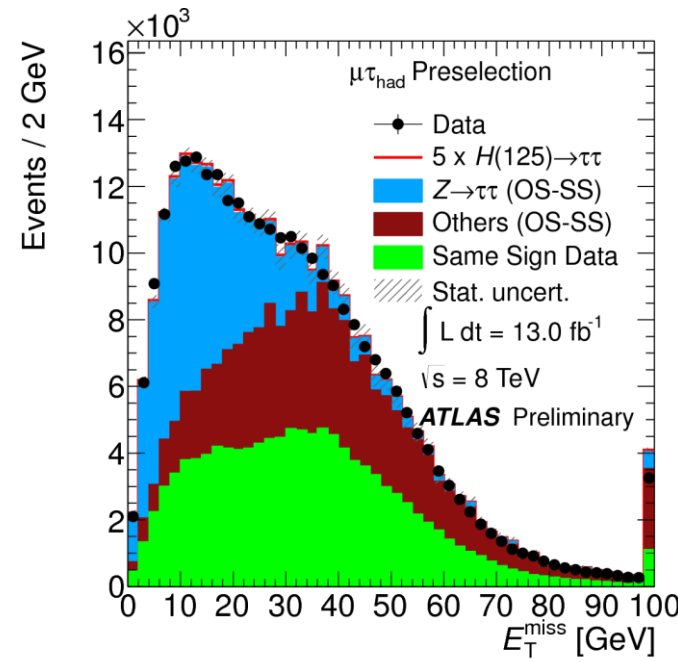
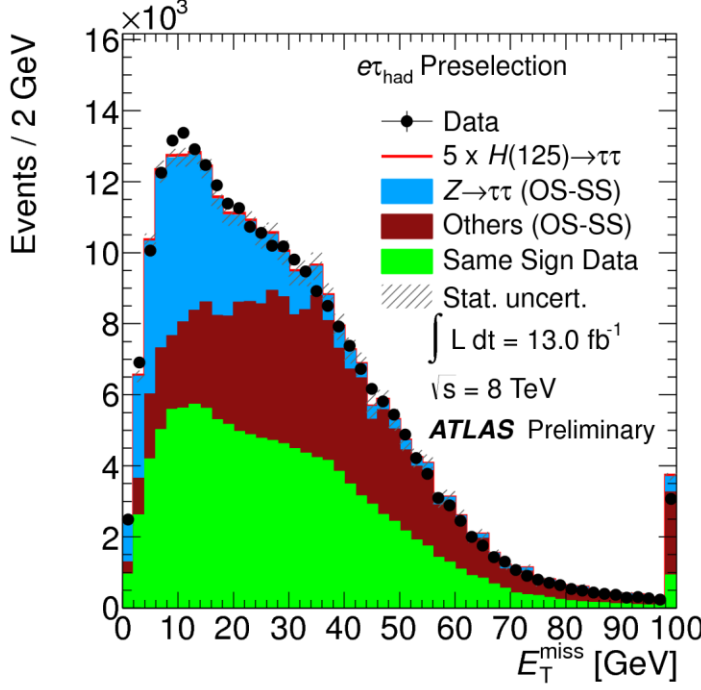
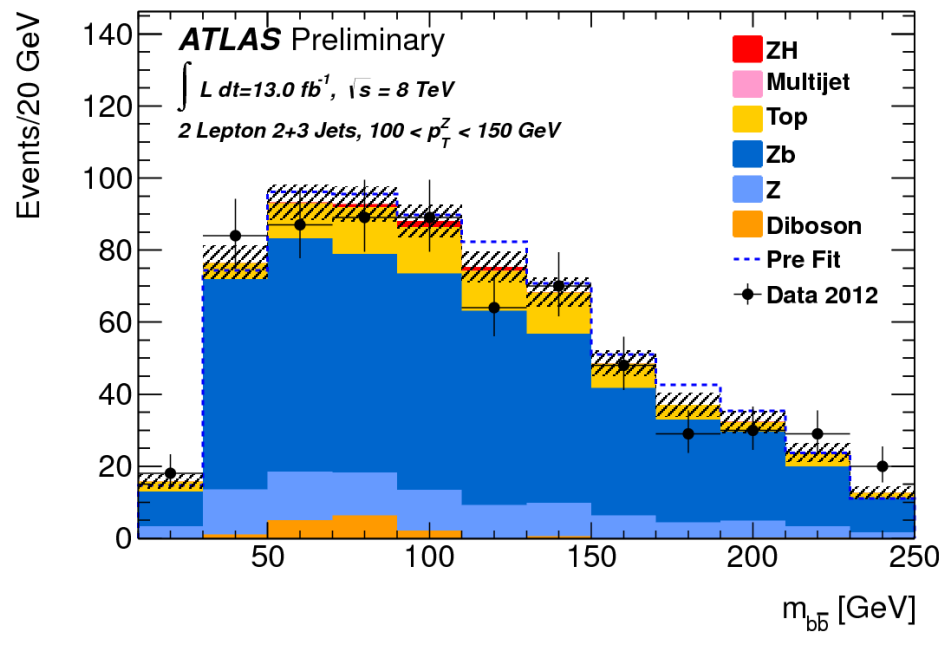
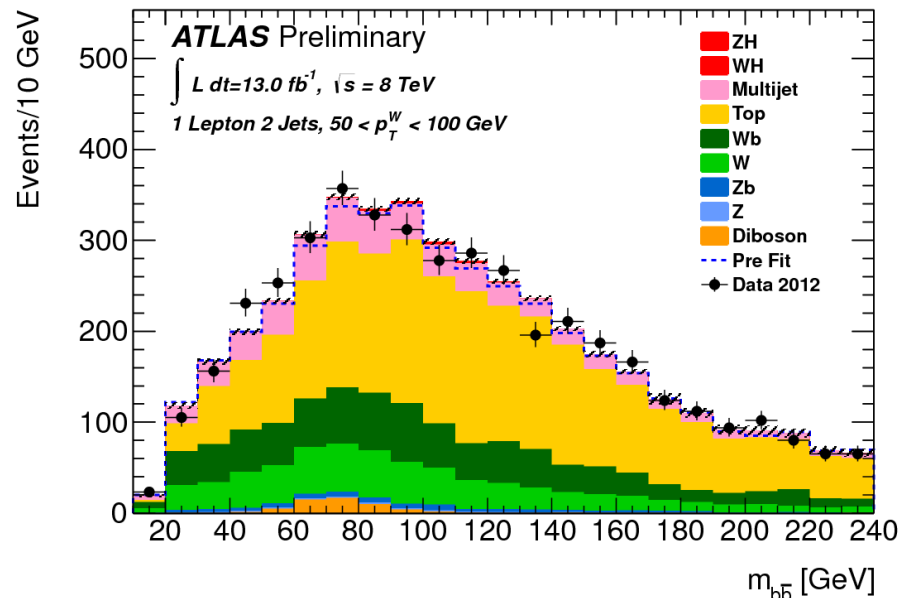
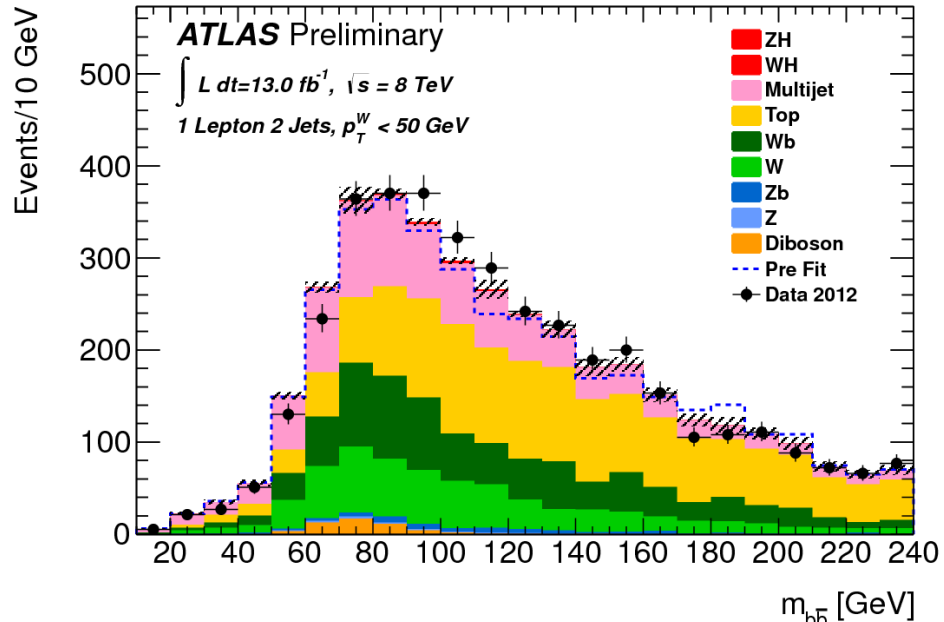
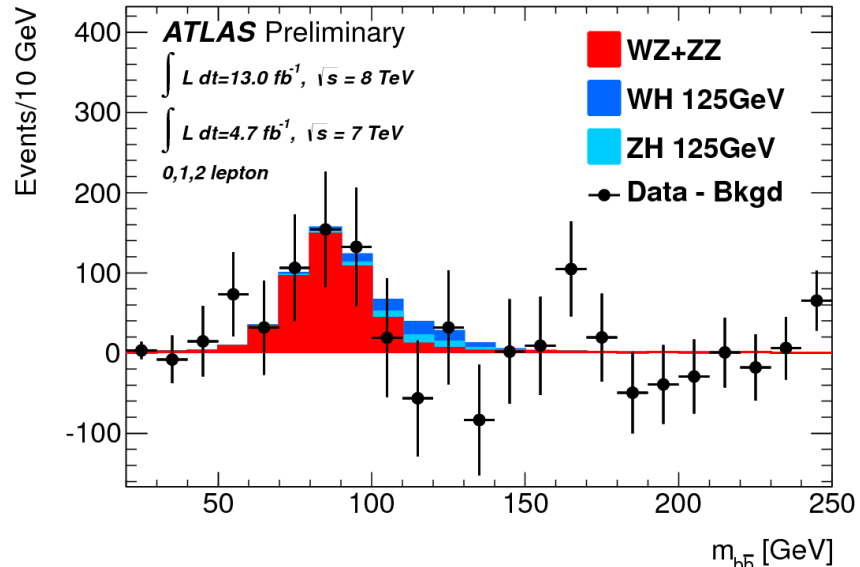


Table 6: The expected numbers of signal and background events for the  $\sqrt{s} = 8$  TeV data after the profile likelihood fit, as well as the observed number of events, are shown. The expected number of signal events are shown for  $WH$  and  $ZH$  production separately for  $m_H = 125$  GeV. The quoted error on the total background represents one standard deviation of the profiled nuisance parameters incorporating both the systematic and statistical uncertainties.

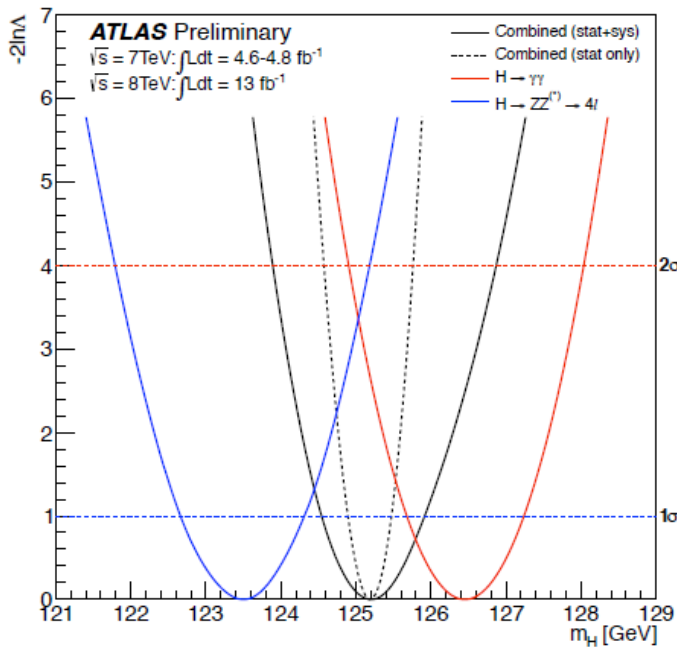
Bin	0-lepton, 2 jet			0-lepton, 3 jet			1-lepton						2-lepton			
	$E_T^{\text{miss}}$ [GeV]			$p_T^W$ [GeV]						$p_T^Z$ [GeV]						
$ZH$	120-160	160-200	>200	120-160	160-200	>200	0-50	50-100	100-150	150-200	>200	0-50	50-100	100-150	150-200	>200
$WH$	2.9	2.1	2.6	0.8	0.8	1.1	0.3	0.4	0.1	0.0	0.0	4.7	6.8	4.0	1.5	1.4
Top	89	25	8	92	25	10	1440	2276	1120	147	43	230	310	84	3	0
$W + c, \text{light}$	30	10	5	9	3	2	580	585	209	36	17	0	0	0	0	0
$W + b$	35	13	13	8	3	2	770	778	288	77	64	0	0	0	0	0
$Z + c, \text{light}$	35	14	14	8	5	8	17	17	4	1	0	201	230	91	12	15
$Z + b$	144	51	43	41	22	16	50	63	13	5	1	1010	1180	469	75	51
Diboson	23	11	10	4	4	3	53	59	23	13	7	37	39	16	6	4
Multijet	3	1	1	1	1	0	890	522	68	14	3	12	3	0	0	0
Total Bkg.	361	127	98	164	63	42	3810	4310	1730	297	138	1500	1770	665	97	72
	$\pm 29$	$\pm 11$	$\pm 12$	$\pm 13$	$\pm 8$	$\pm 5$	$\pm 150$	$\pm 86$	$\pm 90$	$\pm 27$	$\pm 14$	$\pm 90$	$\pm 110$	$\pm 47$	$\pm 12$	$\pm 12$
Data	342	131	90	175	65	32	3821	4301	1697	297	132	1485	1773	657	100	69



# $H \rightarrow \gamma\gamma$ and $H \rightarrow ZZ^* \rightarrow 4l$ masses

Mass scale and resolution uncertainties  
cross checked in great detail for both channels  
( more details in the backup )

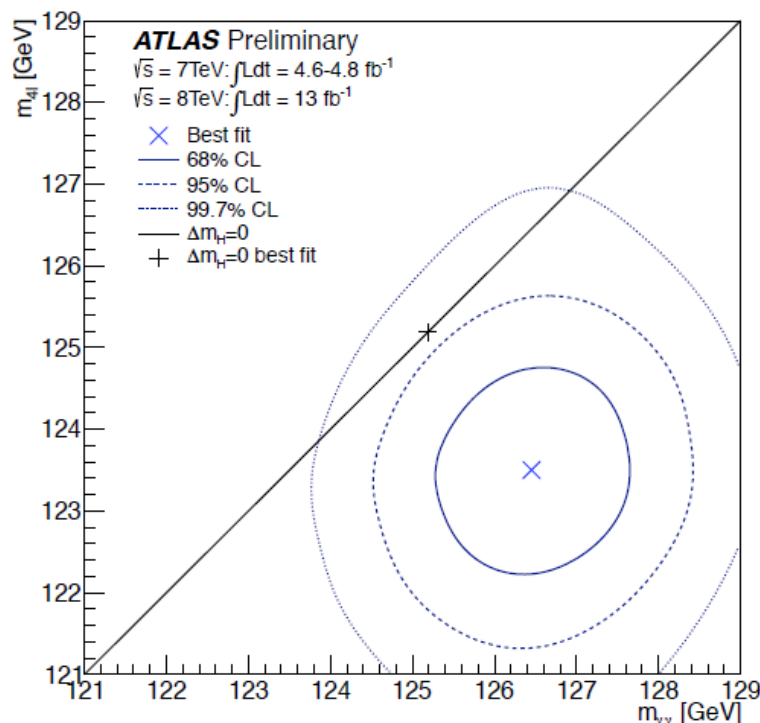
- $\gamma\gamma$  error dominated by systematics,  
mainly photon energy scale  
( total syst. 0.5%, stat error is 0.3% )
- $H \rightarrow ZZ^* \rightarrow 4l$ : error dominated by statistics,  
most of the sensitivity is coming from the  $4\mu$   
channel ( total syst is 0.3%, stat error is 0.7% )



Measurements consistency is  
evaluated via a likelihood function of the  
mass difference, when fitting a common mass

The difference corresponds to  $2.7 \sigma$

A more conservative treatment of scale  
systematics ( rectangular PDFs ) leads  
to  $2.3 \sigma$



## $H \rightarrow \gamma\gamma$ mass systematic uncertainties

Absolute energy scale	0.3%
Uncertainties on upstream material simulation	0.3%
Pre-sampler energy scale	0.1%
Non-linearity of EM calo electronics	0.15%
Conversion fraction	0.1%
Relative calibration of first and second sampling	0.2%
Lateral leakage corrections	0.1%
Resolution	0.15%

+other smaller effects

Total systematic error is 0.55% (0.7 GeV)

4l mass measurement  
dominated by the 4 $\mu$  channel

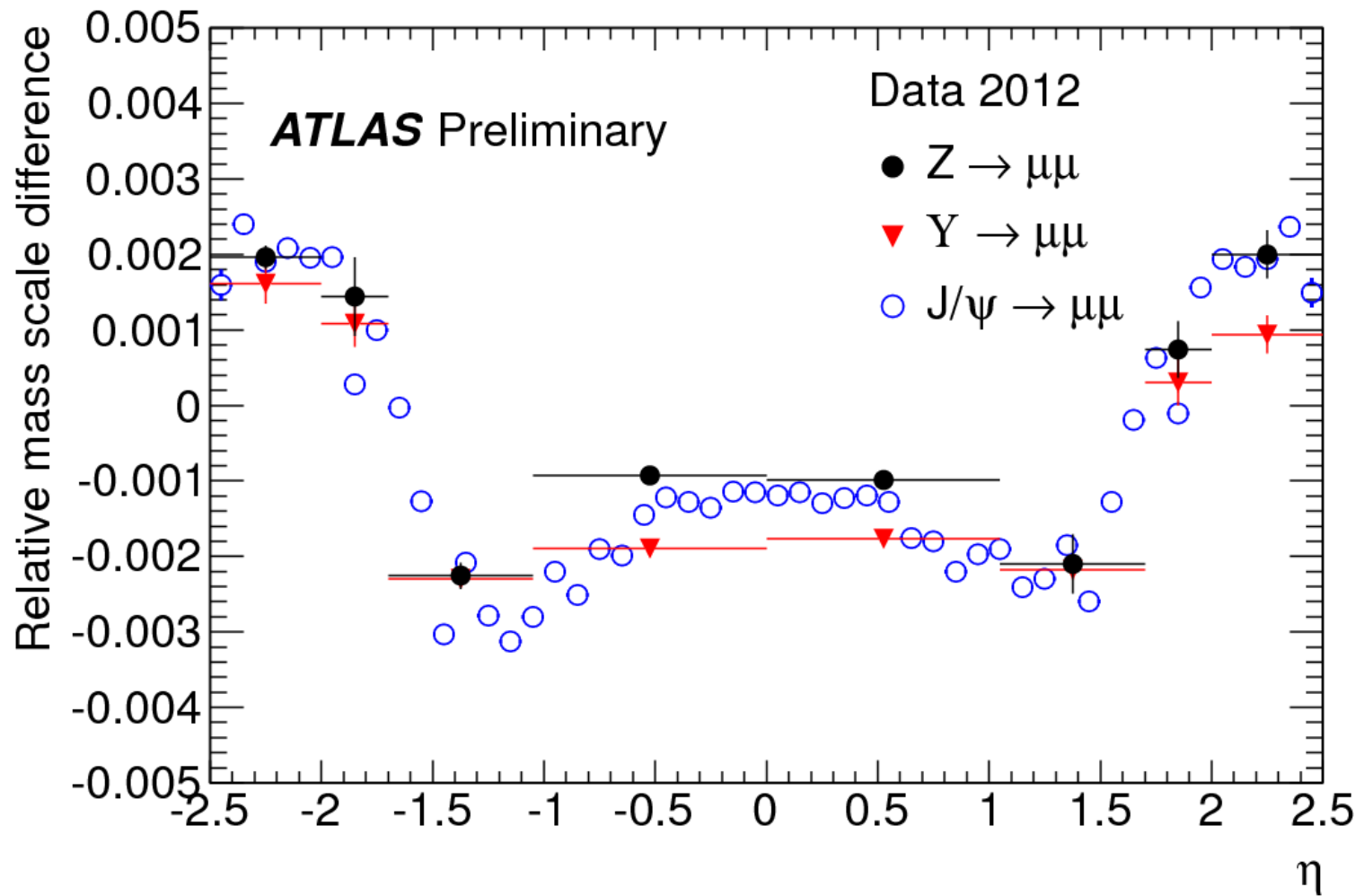
Muon momentum scale	0.2%
Electron energy scale (4e)	0.4%
Low $E_T$ electrons	0.1%

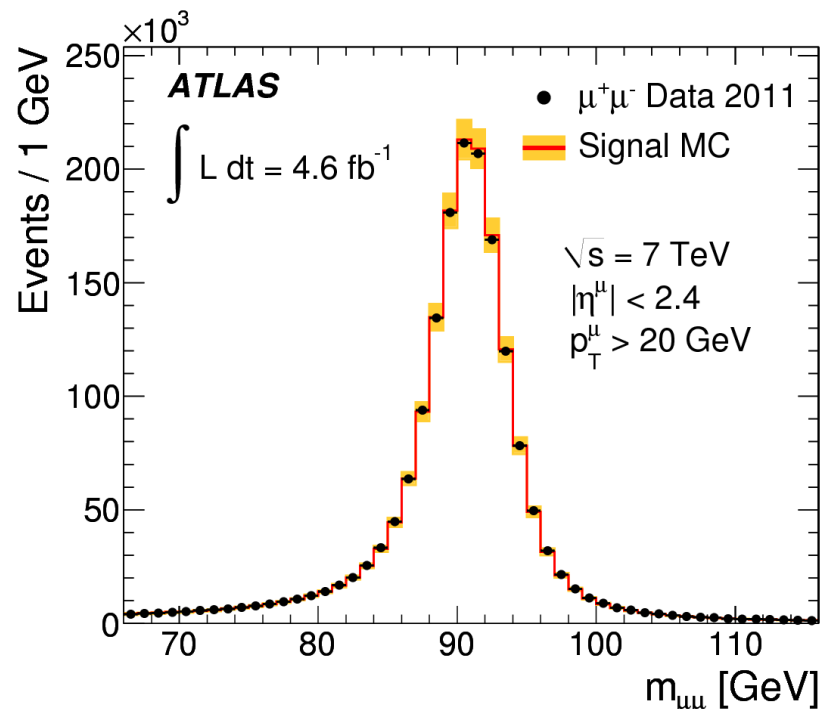
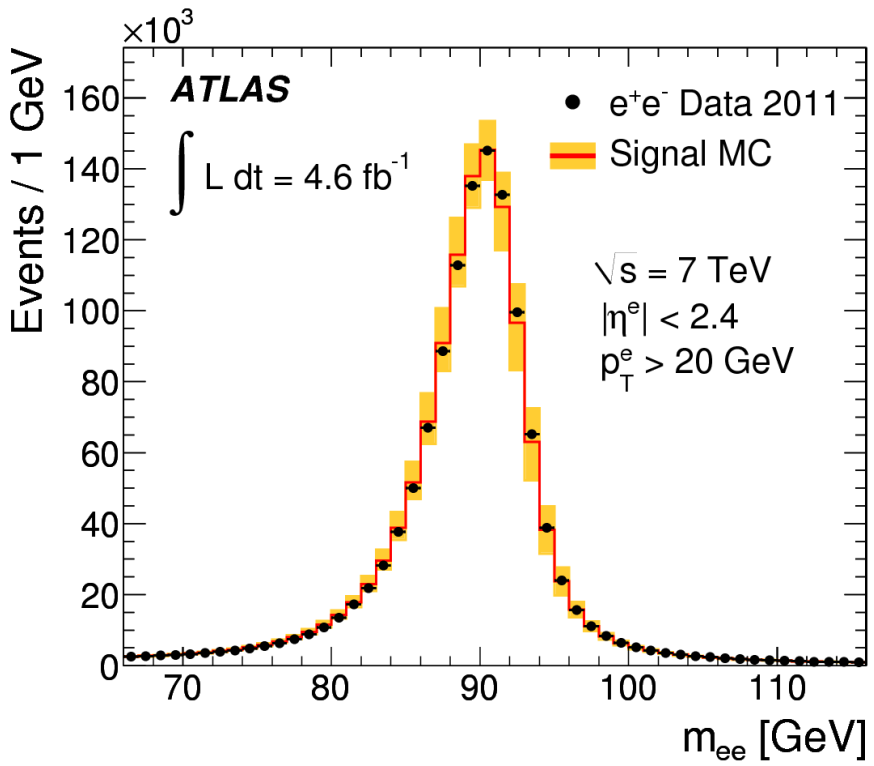
Possible local detector biases checked  
event by event

FSR contribution negligible

ID and MS measurements also checked  
separately

Relative global mass scale difference between the measured resonance mass and the PDG value





### Production modes

$$\frac{\sigma_{ggH}}{\sigma_{ggH}^{SM}} = \begin{cases} \kappa_b^2 & (\kappa_b, \kappa_t, m_H) \\ \kappa_g^2 & \end{cases} \quad (3)$$

$$\frac{\sigma_{VBF}}{\sigma_{VBF}^{SM}} = \kappa_{VBF}^2(\kappa_W, \kappa_Z, m_H) \quad (4)$$

$$\frac{\sigma_{WH}}{\sigma_{WH}^{SM}} = \kappa_W^2 \quad (5)$$

$$\frac{\sigma_{ZH}}{\sigma_{ZH}^{SM}} = \kappa_Z^2 \quad (6)$$

$$\frac{\sigma_{t\bar{t}H}}{\sigma_{t\bar{t}H}^{SM}} = \kappa_t^2 \quad (7)$$

### Detectable decay modes

$$\frac{\Gamma_{WW^{(*)}}}{\Gamma_{WW^{(*)}}^{SM}} = \kappa_W^2$$

$$\frac{\Gamma_{ZZ^{(*)}}}{\Gamma_{ZZ^{(*)}}^{SM}} = \kappa_Z^2$$

$$\frac{\Gamma_{b\bar{b}}}{\Gamma_{b\bar{b}}^{SM}} = \kappa_b^2$$

$$\frac{\Gamma_{\tau^-\tau^+}}{\Gamma_{\tau^-\tau^+}^{SM}} = \kappa_\tau^2$$

$$\frac{\Gamma_{\gamma\gamma}}{\Gamma_{\gamma\gamma}^{SM}} = \begin{cases} \kappa_\gamma^2(\kappa_b, \kappa_t, \kappa_\tau, \kappa_W, m_H) \\ \kappa_\gamma^2 \end{cases}$$

$$\frac{\Gamma_{Z\gamma}}{\Gamma_{Z\gamma}^{SM}} = \begin{cases} \kappa_{(Z\gamma)}^2(\kappa_b, \kappa_t, \kappa_\tau, \kappa_W, m_H) \\ \kappa_{(Z\gamma)}^2 \end{cases}$$

### Currently undetectable decay modes

$$\frac{\Gamma_{t\bar{t}}}{\Gamma_{t\bar{t}}^{SM}} = \kappa_t^2$$

$$\frac{\Gamma_{gg}}{\Gamma_{gg}^{SM}} : \text{ see Section 3.1.2}$$

$$\frac{\Gamma_{c\bar{c}}}{\Gamma_{c\bar{c}}^{SM}} = \kappa_t^2$$

$$\frac{\Gamma_{s\bar{s}}}{\Gamma_{s\bar{s}}^{SM}} = \kappa_b^2$$

$$\frac{\Gamma_{\mu^-\mu^+}}{\Gamma_{\mu^-\mu^+}^{SM}} = \kappa_\tau^2$$

### Total width

$$\frac{\Gamma_H}{\Gamma_H^{SM}} = \begin{cases} \kappa_H^2(\kappa_i, m_H) \\ \kappa_H^2 \end{cases}$$

### Boson and fermion scaling assuming no invisible or undetectable widths

Free parameters:  $\kappa_V (= \kappa_W = \kappa_Z)$ ,  $\kappa_F (= \kappa_t = \kappa_b = \kappa_\tau)$ .

	$H \rightarrow \gamma\gamma$	$H \rightarrow ZZ^{(*)}$	$H \rightarrow WW^{(*)}$	$H \rightarrow b\bar{b}$	$H \rightarrow \tau^-\tau^+$
ggH	$\frac{\kappa_f^2 \cdot \kappa_\gamma^2 (\kappa_f, \kappa_f, \kappa_f, \kappa_V)}{\kappa_H^2 (\kappa_i)}$				
tH		$\frac{\kappa_f^2 \cdot \kappa_V^2}{\kappa_H^2 (\kappa_i)}$			$\frac{\kappa_f^2 \cdot \kappa_f^2}{\kappa_H^2 (\kappa_i)}$
VBF	$\frac{\kappa_V^2 \cdot \kappa_\gamma^2 (\kappa_f, \kappa_f, \kappa_f, \kappa_V)}{\kappa_H^2 (\kappa_i)}$		$\frac{\kappa_V^2 \cdot \kappa_V^2}{\kappa_H^2 (\kappa_i)}$		$\frac{\kappa_V^2 \cdot \kappa_f^2}{\kappa_H^2 (\kappa_i)}$
WH					
ZH					

### Boson and fermion scaling without assumptions on the total width

Free parameters:  $\kappa_{VV} (= \kappa_V \cdot \kappa_V / \kappa_H)$ ,  $\lambda_{fV} (= \kappa_f / \kappa_V)$ .

	$H \rightarrow \gamma\gamma$	$H \rightarrow ZZ^{(*)}$	$H \rightarrow WW^{(*)}$	$H \rightarrow b\bar{b}$	$H \rightarrow \tau^-\tau^+$
ggH					
tH	$\kappa_{VV}^2 \cdot \lambda_{fV}^2 \cdot \kappa_\gamma^2 (\lambda_{fV}, \lambda_{fV}, \lambda_{fV}, 1)$		$\kappa_{VV}^2 \cdot \lambda_{fV}^2$		$\kappa_{VV}^2 \cdot \lambda_{fV}^2 \cdot \lambda_{fV}^2$
VBF					
WH	$\kappa_{VV}^2 \cdot \kappa_\gamma^2 (\lambda_{fV}, \lambda_{fV}, \lambda_{fV}, 1)$		$\kappa_{VV}^2$		$\kappa_{VV}^2 \cdot \lambda_{fV}^2$
ZH					

$$\kappa_i^2 = \Gamma_{ii}/\Gamma_{ii}^{\text{SM}}$$

### Probing custodial symmetry assuming no invisible or undetectable widths

Free parameters:  $\kappa_Z, \lambda_{WZ} (= \kappa_W / \kappa_Z)$ ,  $\kappa_F (= \kappa_t = \kappa_b = \kappa_\tau)$ .

	$H \rightarrow \gamma\gamma$	$H \rightarrow ZZ^{(*)}$	$H \rightarrow WW^{(*)}$	$H \rightarrow b\bar{b}$	$H \rightarrow \tau^-\tau^+$
ggH	$\frac{\kappa_f^2 \cdot \kappa_\gamma^2 (\kappa_f, \kappa_f, \kappa_f, \kappa_Z \lambda_{WZ})}{\kappa_H^2 (\kappa_i)}$		$\frac{\kappa_f^2 \cdot \kappa_Z^2}{\kappa_H^2 (\kappa_i)}$	$\frac{\kappa_f^2 \cdot (\kappa_Z \lambda_{WZ})^2}{\kappa_H^2 (\kappa_i)}$	$\frac{\kappa_f^2 \cdot \kappa_f^2}{\kappa_H^2 (\kappa_i)}$
tH					
VBF	$\frac{\kappa_{VBF}^2 (\kappa_Z, \kappa_Z \lambda_{WZ}) \cdot \kappa_\gamma^2 (\kappa_f, \kappa_f, \kappa_f, \kappa_Z \lambda_{WZ})}{\kappa_H^2 (\kappa_i)}$	$\frac{\kappa_{VBF}^2 (\kappa_Z, \kappa_Z \lambda_{WZ}) \cdot \kappa_Z^2}{\kappa_H^2 (\kappa_i)}$	$\frac{\kappa_{VBF}^2 (\kappa_Z, \kappa_Z \lambda_{WZ}) \cdot (\kappa_Z \lambda_{WZ})^2}{\kappa_H^2 (\kappa_i)}$	$\frac{\kappa_{VBF}^2 (\kappa_Z, \kappa_Z \lambda_{WZ}) \cdot \kappa_f^2}{\kappa_H^2 (\kappa_i)}$	
WH	$\frac{(\kappa_Z \lambda_{WZ})^2 \cdot \kappa_f^2 (\kappa_f, \kappa_f, \kappa_f, \kappa_Z \lambda_{WZ})}{\kappa_H^2 (\kappa_i)}$	$\frac{(\kappa_Z \lambda_{WZ})^2 \cdot \kappa_Z^2}{\kappa_H^2 (\kappa_i)}$	$\frac{(\kappa_Z \lambda_{WZ})^2 \cdot (\kappa_Z \lambda_{WZ})^2}{\kappa_H^2 (\kappa_i)}$	$\frac{(\kappa_Z \lambda_{WZ})^2 \cdot \kappa_f^2}{\kappa_H^2 (\kappa_i)}$	
ZH	$\frac{\kappa_Z^2 \cdot \kappa_\gamma^2 (\kappa_f, \kappa_f, \kappa_f, \kappa_Z \lambda_{WZ})}{\kappa_H^2 (\kappa_i)}$	$\frac{\kappa_Z^2 \cdot \kappa_Z^2}{\kappa_H^2 (\kappa_i)}$	$\frac{\kappa_Z^2 \cdot (\kappa_Z \lambda_{WZ})^2}{\kappa_H^2 (\kappa_i)}$	$\frac{\kappa_Z^2 \cdot \kappa_f^2}{\kappa_H^2 (\kappa_i)}$	

### Probing custodial symmetry without assumptions on the total width

Free parameters:  $\kappa_{ZZ} (= \kappa_Z \cdot \kappa_Z / \kappa_H)$ ,  $\lambda_{WZ} (= \kappa_W / \kappa_Z)$ ,  $\lambda_{FZ} (= \kappa_f / \kappa_Z)$ .

	$H \rightarrow \gamma\gamma$	$H \rightarrow ZZ^{(*)}$	$H \rightarrow WW^{(*)}$	$H \rightarrow b\bar{b}$	$H \rightarrow \tau^-\tau^+$
ggH					
tH	$\kappa_{ZZ}^2 \lambda_{FZ}^2 \cdot \kappa_\gamma^2 (\lambda_{FZ}, \lambda_{FZ}, \lambda_{FZ}, \lambda_{WZ})$	$\kappa_{ZZ}^2 \lambda_{FZ}^2$	$\kappa_{ZZ}^2 \lambda_{FZ}^2 \cdot \lambda_{WZ}^2$		$\kappa_{ZZ}^2 \lambda_{FZ}^2 \cdot \lambda_{FZ}^2$
VBF	$\kappa_{ZZ}^2 \kappa_{VBF}^2 (1, \lambda_{WZ}^2) \cdot \kappa_\gamma^2 (\lambda_{FZ}, \lambda_{FZ}, \lambda_{FZ}, \lambda_{WZ})$	$\kappa_{ZZ}^2 \kappa_{VBF}^2 (1, \lambda_{WZ}^2)$	$\kappa_{ZZ}^2 \kappa_{VBF}^2 (1, \lambda_{WZ}^2) \cdot \lambda_{WZ}^2$	$\kappa_{ZZ}^2 \kappa_{VBF}^2 (1, \lambda_{WZ}^2) \cdot \lambda_{FZ}^2$	
WH	$\kappa_{ZZ}^2 \lambda_{WZ}^2 \cdot \kappa_\gamma^2 (\lambda_{FZ}, \lambda_{FZ}, \lambda_{FZ}, \lambda_{WZ})$	$\kappa_{ZZ}^2 \cdot \lambda_{WZ}^2$	$\kappa_{ZZ}^2 \lambda_{WZ}^2 \cdot \lambda_{WZ}^2$	$\kappa_{ZZ}^2 \lambda_{WZ}^2 \cdot \lambda_{FZ}^2$	
ZH	$\kappa_{ZZ}^2 \cdot \kappa_\gamma^2 (\lambda_{FZ}, \lambda_{FZ}, \lambda_{FZ}, \lambda_{WZ})$	$\kappa_{ZZ}^2$	$\kappa_{ZZ}^2 \cdot \lambda_{WZ}^2$	$\kappa_{ZZ}^2 \cdot \lambda_{FZ}^2$	

$$\kappa_i^2 = \Gamma_{ii}/\Gamma_{ii}^{\text{SM}}$$

Table 5: A benchmark parametrization where custodial symmetry is probed through the  $\lambda_{WZ}$  parameter.

Probing up-type and down-type fermion symmetry assuming no invisible or undetectable widths					
Free parameters: $\kappa_V (= \kappa_Z = \kappa_W)$ , $\lambda_{du} (= \kappa_d / \kappa_u)$ , $\kappa_t (= \kappa_t)$ .					
	H $\rightarrow \gamma\gamma$	H $\rightarrow ZZ^{(*)}$	H $\rightarrow WW^{(*)}$	H $\rightarrow b\bar{b}$	H $\rightarrow \tau^-\tau^+$
ggH	$\frac{\kappa_g^2(\kappa_u \lambda_{du}, \kappa_u) \cdot \kappa_\gamma^2(\kappa_u \lambda_{du}, \kappa_u, \kappa_u \lambda_{du}, \kappa_V)}{\kappa_H^2(\kappa_i)}$	$\frac{\kappa_g^2(\kappa_u \lambda_{du}, \kappa_u) \cdot \kappa_V^2}{\kappa_H^2(\kappa_i)}$	$\frac{\kappa_g^2(\kappa_u \lambda_{du}, \kappa_u) \cdot (\kappa_u \lambda_{du})^2}{\kappa_H^2(\kappa_i)}$		
t $\bar{t}$ H	$\frac{\kappa_u^2 \cdot \kappa_\gamma^2(\kappa_u \lambda_{du}, \kappa_u, \kappa_u \lambda_{du}, \kappa_V)}{\kappa_H^2(\kappa_i)}$	$\frac{\kappa_u^2 \cdot \kappa_V^2}{\kappa_H^2(\kappa_i)}$	$\frac{\kappa_u^2 \cdot (\kappa_u \lambda_{du})^2}{\kappa_H^2(\kappa_i)}$		
VBF WH ZH	$\frac{\kappa_V^2 \cdot \kappa_\gamma^2(\kappa_u \lambda_{du}, \kappa_u, \kappa_u \lambda_{du}, \kappa_V)}{\kappa_H^2(\kappa_i)}$	$\frac{\kappa_V^2 \cdot \kappa_V^2}{\kappa_H^2(\kappa_i)}$	$\frac{\kappa_V^2 \cdot (\kappa_u \lambda_{du})^2}{\kappa_H^2(\kappa_i)}$		

#### Probing up-type and down-type fermion symmetry without assumptions on the total width

Free parameters:  $\kappa_{uu} (= \kappa_u \cdot \kappa_u / \kappa_H)$ ,  $\lambda_{du} (= \kappa_d / \kappa_u)$ ,  $\lambda_{Vu} (= \kappa_V / \kappa_u)$ .

	H $\rightarrow \gamma\gamma$	H $\rightarrow ZZ^{(*)}$	H $\rightarrow WW^{(*)}$	H $\rightarrow b\bar{b}$	H $\rightarrow \tau^-\tau^+$
ggH	$\kappa_{uu}^2 \kappa_g^2(\lambda_{du}, 1) \cdot \kappa_\gamma^2(\lambda_{du}, 1, \lambda_{du}, \lambda_{Vu})$	$\kappa_{uu}^2 \kappa_g^2(\lambda_{du}, 1) \cdot \lambda_{Vu}^2$	$\kappa_{uu}^2 \kappa_g^2(\lambda_{du}, 1) \cdot \lambda_{du}^2$		
t $\bar{t}$ H	$\kappa_{uu}^2 \cdot \kappa_\gamma^2(\lambda_{du}, 1, \lambda_{du}, \lambda_{Vu})$	$\kappa_{uu}^2 \cdot \lambda_{Vu}^2$	$\kappa_{uu}^2 \cdot \lambda_{du}^2$		
VBF WH ZH	$\kappa_{uu}^2 \lambda_{Vu}^2 \cdot \kappa_\gamma^2(\lambda_{du}, 1, \lambda_{du}, \lambda_{Vu})$	$\kappa_{uu}^2 \lambda_{Vu}^2 \cdot \lambda_{Vu}^2$	$\kappa_{uu}^2 \lambda_{Vu}^2 \cdot \lambda_{du}^2$		

$$\kappa_i^2 = \Gamma_{ii}/\Gamma_{ii}^{\text{SM}}, \kappa_d = \kappa_b = \kappa_t$$

**Table 6:** A benchmark parametrization where the up-type and down-type symmetry of fermions is probed through the  $\lambda_{du}$  parameter.

#### Probing quark and lepton fermion symmetry assuming no invisible or undetectable widths

Free parameters:  $\kappa_V (= \kappa_Z = \kappa_W)$ ,  $\lambda_{lq} (= \kappa_l / \kappa_q)$ ,  $\kappa_t (= \kappa_t = \kappa_b)$ .

	H $\rightarrow \gamma\gamma$	H $\rightarrow ZZ^{(*)}$	H $\rightarrow WW^{(*)}$	H $\rightarrow b\bar{b}$	H $\rightarrow \tau^-\tau^+$
ggH	$\frac{\kappa_q^2 \cdot \kappa_\gamma^2(\kappa_q, \kappa_q, \kappa_q \lambda_{lq}, \kappa_V)}{\kappa_H^2(\kappa_i)}$	$\frac{\kappa_q^2 \cdot \kappa_V^2}{\kappa_H^2(\kappa_i)}$	$\frac{\kappa_q^2 \cdot (\kappa_q \lambda_{lq})^2}{\kappa_H^2(\kappa_i)}$		
t $\bar{t}$ H					
VBF WH ZH	$\frac{\kappa_V^2 \cdot \kappa_\gamma^2(\kappa_q, \kappa_q, \kappa_q \lambda_{lq}, \kappa_V)}{\kappa_H^2(\kappa_i)}$	$\frac{\kappa_V^2 \cdot \kappa_V^2}{\kappa_H^2(\kappa_i)}$	$\frac{\kappa_V^2 \cdot (\kappa_q \lambda_{lq})^2}{\kappa_H^2(\kappa_i)}$		

#### Probing quark and lepton fermion symmetry without assumptions on the total width

Free parameters:  $\kappa_{qq} (= \kappa_q \cdot \kappa_q / \kappa_H)$ ,  $\lambda_{lq} (= \kappa_l / \kappa_q)$ ,  $\lambda_{Vq} (= \kappa_V / \kappa_q)$ .

	H $\rightarrow \gamma\gamma$	H $\rightarrow ZZ^{(*)}$	H $\rightarrow WW^{(*)}$	H $\rightarrow b\bar{b}$	H $\rightarrow \tau^-\tau^+$
ggH	$\kappa_{qq}^2 \cdot \kappa_\gamma^2(1, 1, \lambda_{lq}, \lambda_{Vq})$	$\kappa_{qq}^2 \cdot \lambda_{Vq}^2$	$\kappa_{qq}^2$	$\kappa_{qq}^2 \cdot \lambda_{lq}^2$	
t $\bar{t}$ H					
VBF WH ZH	$\kappa_{qq}^2 \lambda_{Vq}^2 \cdot \kappa_\gamma^2(1, 1, \lambda_{lq}, \lambda_{Vq})$	$\kappa_{qq}^2 \lambda_{Vq}^2 \cdot \lambda_{Vq}^2$	$\kappa_{qq}^2 \cdot \lambda_{Vq}^2$	$\kappa_{qq}^2 \lambda_{Vq}^2 \cdot \lambda_{lq}^2$	

$$\kappa_i^2 = \Gamma_{ii}/\Gamma_{ii}^{\text{SM}}, \kappa_t = \kappa_\tau$$

**Table 7:** A benchmark parametrization where the quark and lepton symmetry of fermions is probed through the  $\lambda_{lq}$  parameter.

Probing loop structure assuming no invisible or undetectable widths					
Free parameters: $\kappa_g, \kappa_\gamma$ .					
	H $\rightarrow \gamma\gamma$	H $\rightarrow ZZ^{(*)}$	H $\rightarrow WW^{(*)}$	H $\rightarrow b\bar{b}$	H $\rightarrow \tau^-\tau^+$
ggH	$\frac{\kappa_g^2 \cdot \kappa_\gamma^2}{\kappa_H^2(\kappa_i)}$			$\frac{\kappa_g^2}{\kappa_H^2(\kappa_i)}$	
tH					
VBF	$\frac{\kappa_\gamma^2}{\kappa_H^2(\kappa_i)}$			$\frac{1}{\kappa_H^2(\kappa_i)}$	
WH					
ZH					

#### Probing loop structure allowing for invisible or undetectable widths

Free parameters:  $\kappa_g, \kappa_\gamma, BR_{inv.,undet.}$ .

	H $\rightarrow \gamma\gamma$	H $\rightarrow ZZ^{(*)}$	H $\rightarrow WW^{(*)}$	H $\rightarrow b\bar{b}$	H $\rightarrow \tau^-\tau^+$
ggH	$\frac{\kappa_g^2 \cdot \kappa_\gamma^2}{\kappa_H^2(\kappa_i)/(1-BR_{inv.,undet.})}$		$\frac{\kappa_g^2}{\kappa_H^2(\kappa_i)/(1-BR_{inv.,undet.})}$		
tH					
VBF	$\frac{\kappa_\gamma^2}{\kappa_H^2(\kappa_i)/(1-BR_{inv.,undet.})}$			$\frac{1}{\kappa_H^2(\kappa_i)/(1-BR_{inv.,undet.})}$	
WH					
ZH					

$$\kappa_i^2 = \Gamma_{ii}/\Gamma_{ii}^{\text{SM}}$$

**Table 8:** A benchmark parametrization where effective vertex couplings are allowed to float through the  $\kappa_g$  and  $\kappa_\gamma$  parameters. Instead of absorbing  $\kappa_H$ , explicit allowance is made for a contribution from invisible or undetectable widths via the  $BR_{inv.,undet.}$  parameter.

#### Probing loops while allowing other couplings to float assuming no invisible or undetectable widths

Free parameters:  $\kappa_g, \kappa_\gamma, \kappa_V (= \kappa_W = \kappa_Z), \kappa_f (= \kappa_t = \kappa_b = \kappa_\tau)$ .

	H $\rightarrow \gamma\gamma$	H $\rightarrow ZZ^{(*)}$	H $\rightarrow WW^{(*)}$	H $\rightarrow b\bar{b}$	H $\rightarrow \tau^-\tau^+$
ggH	$\frac{\kappa_g^2 \cdot \kappa_\gamma^2}{\kappa_H^2(\kappa_i)}$		$\frac{\kappa_g^2 \cdot \kappa_V^2}{\kappa_H^2(\kappa_i)}$		$\frac{\kappa_g^2 \cdot \kappa_f^2}{\kappa_H^2(\kappa_i)}$
tH	$\frac{\kappa_f^2 \cdot \kappa_\gamma^2}{\kappa_H^2(\kappa_i)}$		$\frac{\kappa_f^2 \cdot \kappa_V^2}{\kappa_H^2(\kappa_i)}$		$\frac{\kappa_f^2 \cdot \kappa_f^2}{\kappa_H^2(\kappa_i)}$
VBF	$\frac{\kappa_V^2 \cdot \kappa_\gamma^2}{\kappa_H^2(\kappa_i)}$		$\frac{\kappa_V^2 \cdot \kappa_V^2}{\kappa_H^2(\kappa_i)}$		$\frac{\kappa_V^2 \cdot \kappa_f^2}{\kappa_H^2(\kappa_i)}$
WH					
ZH					

#### Probing loops while allowing other couplings to float allowing for invisible or undetectable widths

Free parameters:  $\kappa_{gV} (= \kappa_g \cdot \kappa_V/\kappa_H), \lambda_{Vg} (= \kappa_V/\kappa_g), \lambda_{tV} (= \kappa_t/\kappa_V), \lambda_{fV} (= \kappa_f/\kappa_V)$ .

	H $\rightarrow \gamma\gamma$	H $\rightarrow ZZ^{(*)}$	H $\rightarrow WW^{(*)}$	H $\rightarrow b\bar{b}$	H $\rightarrow \tau^-\tau^+$
ggH	$\kappa_{gV}^2 \cdot \lambda_{tV}^2$		$\kappa_{gV}^2$		$\kappa_{gV}^2 \cdot \lambda_{fV}^2$
tH	$\kappa_{gV}^2 \lambda_{Vg}^2 \lambda_{tV}^2 \cdot \lambda_{tV}^2$		$\kappa_{gV}^2 \lambda_{Vg}^2 \lambda_{fV}^2$		$\kappa_{gV}^2 \lambda_{Vg}^2 \lambda_{tV}^2 \cdot \lambda_{fV}^2$
VBF	$\kappa_{gV}^2 \lambda_{Vg}^2 \cdot \lambda_{tV}^2$		$\kappa_{gV}^2 \lambda_{Vg}^2$		$\kappa_{gV}^2 \lambda_{Vg}^2 \cdot \lambda_{fV}^2$
WH					
ZH					

$$\kappa_i^2 = \Gamma_{ii}/\Gamma_{ii}^{\text{SM}}, \kappa_V = \kappa_W = \kappa_Z, \kappa_t = \kappa_b = \kappa_\tau$$

**Table 9:** A benchmark parametrization where effective vertex couplings are allowed to float through the  $\kappa_g$  and  $\kappa_\gamma$  parameters and the gauge and fermion couplings through the unified parameters  $\kappa_V$  and  $\kappa_f$ .